

**Effect of different surfactant structures on the brine-crude oil and brine-alkane interface in different aqueous environments.**

By Kristian Vikholm Greenway



Master thesis

Department of Chemistry

Faculty of Mathematics and Natural Science

University of Bergen

June 2017



## **Acknowledgement**

First, I would like to thank my supervisors Kristine Spildo and Ketil Djurhuus for all their help and guidance, both during experimental work at the laboratory, as well as during the process of writing this thesis. I would also like to thank Jonas Solbakken for always being available, and willing to answer all more or less stupid questions. In addition, a huge thanks to Christer Llano Andresen for being great company during long hours in the laboratory.

Great thanks also to all my fellow students at the office for creating a welcoming and relaxed atmosphere, where all questions, thoughts and comments can be shared with constructive feedback.

Finally, thanks to my mom, dad, brother and Tåndsja for their support and patience in both ups and downs during the making of this thesis.

Thank you,

Kristian Vikholm Greenway.



## **Abstract**

In producing oil fields, both the production rate and ultimate recovery from the field can be enhanced by injection of chemicals into the reservoir formation. To optimise the commercial benefits, it is important to understand the interactions between the injected chemicals and the reservoir fluids. This understanding is crucial for selecting the most appropriate chemical additive for a given reservoir.

This thesis investigates the interactions between oil and a brine which contains surfactant. Surfactants are chemical additives which improve oil flow from and through the reservoir by reducing the interfacial tension between the brine and the oil. The effects of three surfactants, all with different structures, were studied in relation to two crude oils and two alkanes. The three surfactants studied are Sodium Dodecyl Sulphate, Sodium Dodecylbenzene sulphonate and Aerosol OT. This work investigated the systems' response across a range of variables: concentration of surfactant and brine composition in terms of ion valence, brine salinity, pH and temperature. The interfacial tension (IFT) between the fluids, was measured using both the spinning drop- and the pendant drop method, as well as by measuring the system's geometry and absorption of UV-light.

The results did prove that the most effective surfactant was the one which had the most similar solubility in both the aqueous- and the oil phase. The IFT decreased with increasing salinity for all systems, until reaching a minimum, after which the IFT conversely began to increase with salinity. In tests varying the pH of the brine, the crudes exhibited their lowest IFT's in a more alkaline environment, since acidic species in the oil were ionized, giving them a hydrophilic character. Changes in ion valence by addition of  $\text{Ca}^{2+}$  also decreased the IFT for the crudes as the divalent ions created in-situ surfactants with certain compounds in the crudes. Increases in temperature increased the IFT for all systems as surfactant solubility in the bulk phase increased.



## Abbreviations and Symbols

### Abbreviations

ACN	Alkane Carbon Number
AOT	Dioctyl sulfosuccinate
cf.	confer
COB	Crude Oil/Brine
CPP	Critical Packing Parameter
e.g	For example
EACN	Equivalent Alkane Carbon Number
EDL	Electrical Double Layer
EOR	Enhanced Oil Recovery
et. al.	with others
HLB	Hydrophilic-Lipophilic-Balance
i.e.	in other words
IFT	Interfacial tension
LS	Lower Salinity
ME	Microemulsion
NSO	Nitrogen, Sulphur and Oxygen
O/W	Oil in Water
OOIP	Oil Originally In Place
OS	Optimal Salinity
PIT	Phase Inversion Temperature
SCOB	Surfactant/Crude Oil/Brine
SDBS	Sodium DodecylBenzene Sulfonate
SDS	Sodium Dodecyl Sulfonate
SOB	Surfactant/Oil/Brine
ST	Surface Tension

TAN	Total Acid Number
TBN	Total Base Number
US	Upper Salinity
W/O	Water in Oil
WOR	Water/Oil Ratio

### Symbols (unit)

A	absorption ( $\text{W}/\text{m}^2 / \text{W}/\text{m}^2$ )
$a_h$	area of a surfactants headgroup
b	length of sample (cm)
c	concentration of sample (mol/L)
g	gravity constant ( $\text{m}/\text{s}^2$ )
$l_t$	length of a surfactants hydrocarbon chain (m)
M	molar concentration (mol/L)
$N_c$	capillary number (dimensionless)
P	pressure (bar)
r	radii of droplet (m)
$R_i$	Principal radii of curvature (m)
SP	solubilisation parameter (mol/mol)
$V_s$	volume om surfactant microemulsion phase (L)
$v_t$	volume taken by a surfactants hydrocarbon tail
$V_x$	volume of phase x (L)
$\gamma$	Surface tension (mN/m)
$\epsilon$	molar absorptivity ( $\text{mol}^{-1} \text{dm}^3 \text{cm}^{-1}$ )
$\mu$	viscosity (cP)
$\rho$	density ( $\text{g}/\text{cm}^3$ )
$\sigma$	interfacial tension (mN/m)
$\omega$	rotational frequency (rpm)



# Table of content

<b>Acknowledgement</b> .....	<b>iii</b>
<b>Abstract</b> .....	<b>v</b>
<b>Abbreviations and Symbols</b> .....	<b>vii</b>
<b>1 Introduction</b> .....	<b>1</b>
<b>1.1 Objective of the thesis</b> .....	<b>2</b>
<b>2 Theory/ Background</b> .....	<b>3</b>
<b>2.1 Crude Oil</b> .....	<b>3</b>
2.2.1 SARA classification.....	3
<b>2.2 Interfacial Forces</b> .....	<b>5</b>
2.2.1 Interfacial tension.....	5
2.2.2 Adsorption at the interface .....	6
<b>2.3 Effect of surface active agents on IFT</b> .....	<b>7</b>
2.3.1 Surfactant .....	7
2.3.2 Critical Micelle Concentration of surfactants .....	8
2.3.3 Surface active agents in crude oil .....	9
<b>2.4 Factors affecting the extent of interfacial absorption/activity</b> .....	<b>10</b>
2.4.1 Effect of surfactant concentration .....	10
2.4.2 Solubility/surfactant HLB value .....	10
2.4.3 Critical Packing Parameter.....	11
2.4.4 Electrostatic forces at the interface .....	12
2.4.5 Salinity .....	12
2.4.6 Temperature .....	16
2.4.7 pH.....	18
<b>2.5 Microemulsions</b> .....	<b>19</b>
2.5.1 Surfactant microemulsion for EOR.....	19
2.5.2 Phase studies and solubilisation parameter .....	21
<b>2.6 Surfactants on pore scale</b> .....	<b>23</b>
2.6.1 Capillary forces .....	23
2.6.2 Capillary number.....	24
<b>2.7 Characterisation by number of carbons</b> .....	<b>26</b>
2.7.1 Alkane carbon number .....	26
2.7.2 Equivalent alkane carbon number .....	26

<b>3</b>	<b>Method.....</b>	<b>27</b>
	<b>3.1 Chemical preparations .....</b>	<b>27</b>
	3.1.1 Preparations of Crude Oil .....	27
	3.1.2 Preparations of Brines.....	27
	3.1.3 Preparation of Surfactant Solutions .....	27
	3.1.4 Overview of chemicals used .....	28
	3.1.5 Different brine- and surfactant compositions.....	29
	3.1.6 Source of error in chemical preparation.....	29
	<b>3.2 Surface tension and Interfacial tension.....</b>	<b>30</b>
	3.2.1 Du-Nuöy ring method .....	30
	3.2.2 Spinning Drop method.....	32
	3.2.3 Pendant Drop method.....	34
	<b>3.3 Light absorption.....</b>	<b>37</b>
	3.3.1 Molecular bonding theory .....	37
	3.3.2 Molecular absorption of light.....	37
	3.3.3 UV-spectrophotometry.....	38
	<b>3.4 Volumetric calculations .....</b>	<b>40</b>
	3.4.1 Solubilisation parameters .....	40
<b>4</b>	<b>Results.....</b>	<b>41</b>
	<b>4.1 Determination of the surfactants' CMC .....</b>	<b>41</b>
	<b>4.2 The COB system.....</b>	<b>42</b>
	4.2.1 Effect of variation in brine salinity .....	42
	<b>4.3 The SCOB system .....</b>	<b>43</b>
	4.3.1 Effect of variation in surfactant concentration.....	43
	4.3.2 Effect of variation in salinity .....	46
	4.3.2.1 IFT / Solubilisation parameter- correlation .....	49
	4.3.2.2 IFT / Surfactant partitioning - correlation.....	51
	4.3.2.3 Effect of ion valence.....	52
	4.3.3 Effect of variation in pH .....	54
	4.3.4 Effect of variation in temperature .....	56
	<b>4.4 Effect of precipitation on surfactant concentration.....</b>	<b>57</b>
<b>5</b>	<b>Discussion .....</b>	<b>59</b>
	<b>5.1 The COB system.....</b>	<b>59</b>
	5.1.1 Effect of variation in brine salinity .....	59
	<b>5.2 The SCOB system .....</b>	<b>62</b>

5.2.1	Effect of surfactant on the oil-water IFT at LS conditions .....	62
5.2.2	Effect of variation in surfactant concentration.....	63
5.2.3	Differences in optimal salinities for different SCOB systems .....	64
5.2.4	Effect of Calcium on oil-water IFT at LSS conditions .....	67
5.2.5	Effect of variation in pH .....	69
5.2.6	Effect of variation in temperature .....	72
<b>6</b>	<b>Summary and conclusion.....</b>	<b>73</b>
<b>7</b>	<b>Further work.....</b>	<b>75</b>
<b>8</b>	<b>Bibliography.....</b>	<b>76</b>
<b>A.</b>	<b>Appendix A – Calculations.....</b>	<b>86</b>
A.1	Uncertainties .....	86
A.2	Ionic strength.....	86
<b>B.</b>	<b>Appendix B – Additional results.....</b>	<b>87</b>
B.1	Identification of CMC .....	87
B.2	Standard absorption curves for SDBS .....	90
<b>C.</b>	<b>Appendix C – Tables of data.....</b>	<b>91</b>
C.1	Additive- free variation in salinity .....	91
C.2	Variation in surfactant concentration .....	92
C.3	Variation in salinity .....	93
C.4	Variation in pH.....	96
C.5	Variation in temperature.....	98
C.6	Absorption of UV-light .....	98

# 1 Introduction

Hydrocarbons are the world's largest and most important source of energy, as well as supplying industry with many chemical feedstocks in the production of an enormous array of products. The global demand for hydrocarbons increases steadily in line with world economic growth, particularly within large developing economies in Asia. Current world production is approximately 96 million barrels per day, while consumption is increasing at over one million barrels per day annually [1]. Although current production is adequate to meet current demand, as demand increases, and as known oil and gas fields deplete, new sources of production will need to be exploited in the coming years. As well as exploring and discovering new oil and gas fields, the oil and gas industry is equally focused on producing the maximum economically possible from existing fields. This effort to optimise existing production goes under the general heading of Enhanced Oil Recovery (EOR) [2].

In general, there are three phases of recovering oil from a reservoir. *Primary recovery* occurs as a result of pre-existing pressure in the reservoir. Natural pressure within the formation push the fluids out the well bore. *Secondary recovery* includes methods used where gas or fluid is injected into the reservoir maintain reservoir pressure for an increased recovery. *Tertiary recovery* is where certain chemicals (e.g. surfactants or polymers) are added to the injected fluid to increase production even further [2, 3]. After a typical recovery process where only water has been injected for pressure support, there is still 50-65% of the OOIP (Oil Originally in Place) left in the reservoir. This oil can be mobilized by using tertiary recovery methods. The effectiveness of the process will however, depend on many factors like oil type, reservoir rock characteristics, rock formation and the injected brine [4]. The better the knowledge of the interactions between injected chemicals in a tertiary recovery process and the crude oil, the higher the potential oil recovery from the reservoir.

## 1.1 Objective of the thesis

The objective of this thesis is to investigate how three anionic, commercial surfactants with different structures affect the IFT between different oils and brines at different aqueous environments. The oils investigated are two alkanes and two crudes. An enhanced greater knowledge of the behaviour of surfactants of certain structures, will create an improved basis for choosing an appropriate surfactant for a given application.

To investigate the different structures, the physical- chemical properties of the three surfactants have been studied in systems containing both crude oils and n-alkanes. The surfactants have been tested with focus on changes interfacial tension, with regards to the different types of oils, and across a range of brine variables: pH, salinity, surfactant concentration, monovalent/divalent ion composition and temperature. This gives an insight into how the different surfactant structures affect the interfacial activity at the brine/oil interface. The three surfactants that are investigated in this thesis are Sodium dodecyl sulfate (SDS), Sodium dodecylbenzene sulfonate (SDBS) and sodium bis (2-ethylhexyl) sulfosuccinate (aerosol OT or AOT). The molecules of the three surfactants are illustrated in figure 1-1.

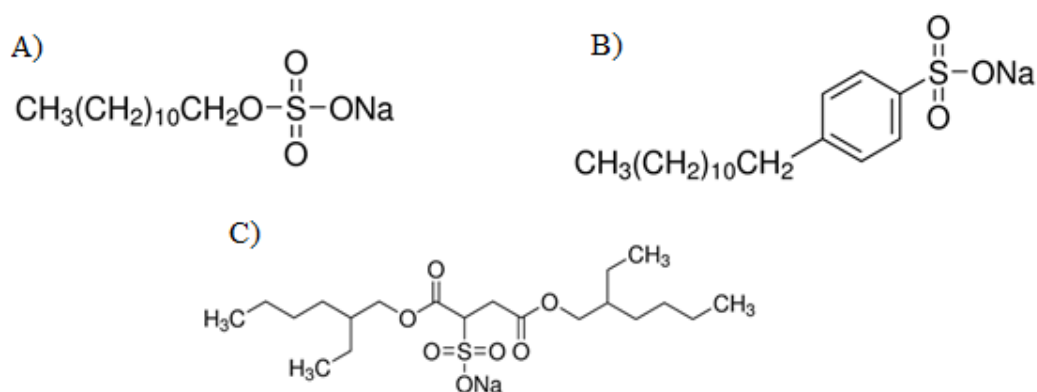


**Figure 1-1:** Surfactants used in this thesis. A) SDS B) SDBS C) AOT

## **2 Theory/ Background**

### **2.1 Crude Oil**

When organic matter is deposited and buried, the effect of continued deposition of sediments above will lead to an increase of temperature and pressure on the organic matter. Under certain conditions, and over a period of thousands to millions of years, this matter can form crude oil. The part of the organic matter that becomes crude oil, Kerogen, can have a wide range of origins, which results in crude oil from different sources often containing markedly different sets of components at the molecular level. Crude oil is one of a set of naturally occurring liquids and gasses resulting from the burial of organic material in the Earth's crust, known collectively as Hydrocarbons. So not surprisingly then, most common atoms found in crude oil are Hydrogen and Carbon, occurring in a wide range of complex molecular structures. Other atoms that are neither Hydrogen nor Carbon, called heteroatoms, also occur commonly. These heteroatoms are mostly Nitrogen, Sulphur and Oxygen (NSO), as well as traces of various metals. The set of components which finally make up a crude oil depends not just on type of Kerogen deposited, however, but also on the area of deposition, depositional environment, pressure and temperature. For this reason, we see in practice, that crude oils from different fields always differ in some way, though we do also see that oils from the same general province can in many cases share some of the same properties [5, 6].

#### **2.2.1 SARA classification**

Due to the almost infinite permutations of various atoms, molecules and compounds that can occur in a crude oil, classifying a crude oil based on its individual components is not realistic. To overcome this, a so-called SARA classification is useful, and is often the method of choice. SARA stands for Saturates, Aromatic, Resins and Asphaltenes. SARA is an analysis method that divides crude oil components according to their polarizability and polarity. Saturates are the most commercially desirable part of the crude, made up of carbon chains that incorporate the maximum numbers of hydrogen atoms possible, composed entirely of single bonds. Aromatics are hydrocarbons that contain one or more benzene rings. Resins and asphaltenes are bigger, polar, hetero-compounds which include NSO's and metals. Resins and asphaltenes are thus the heaviest fraction of the oil and might have molecular weights up to 500-1500 g/mol. See for example Fingas or Sjöblom [5, 7].

In the case of asphaltenes, they are not soluble in n-alkane, such as n-hexane for example, so this characteristic can be used to precipitate the asphaltene fraction. The remaining components can then be separated by polarity using the technique of High Performance Liquid Chromatography as described by Sjöblom [7]. Depending on the amount present of each class, the crude can then be assigned a definition of light (mostly saturates), intermediate (mix of all four classes) or heavy (mostly resins and asphaltenes) [6].

Naphthenic acids can act as interfacial active compounds, found in the resins- and asphaltene portion of the oil [6]. A parameter that defines the amount of naphthenic acids in a crude, is the total acid number (TAN) [8], and is given as the amount of potassium hydroxide in milligrams that is needed to neutralize the acids in one gram of oil. As the naphthenic acids have potential to be interfacial active compounds, the TAN will to some degree dictate the interfacial activity of the oil in a crude oil/brine (COB)- or a surfactant/crude oil/brine (SCOB) system.

## 2.2 Interfacial Forces

### 2.2.1 Interfacial tension

Interfacial tension (IFT) is a tension that arises when two immiscible fluids are in contact. The molecules of each fluid tend to stay in their bulk phase, rather than mixing with the other phase [9]. The resistance to mix occurs as the intermolecular forces in one of the immiscible fluids, pull on the molecules at the interface, towards the corresponding bulk phase. This pull on the interfacial molecules, results in a tension across the interface between the liquids. This is illustrated in figure 2-1.

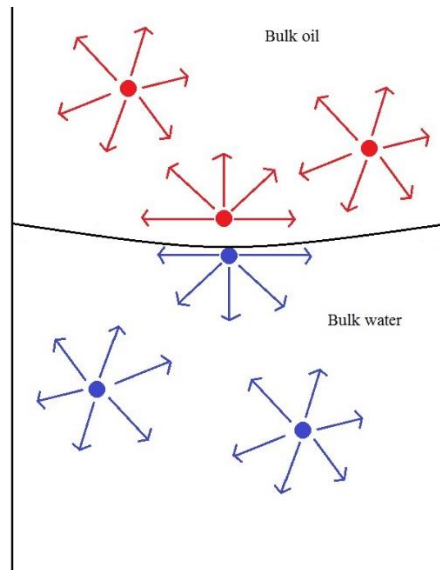


**Figure 2-1** Illustration of how the molecules at the interface get pulled by its corresponding bulk phase, creating interfacial tension.

The IFT can then be described as the difference in energy between molecules of two immiscible fluids, or work needed to keep the fluids apart at constant temperature (T), pressure (P) and number of moles (n). This energy is defined by Zolotukhin et.al. [10] as

$$\sigma = \left(\frac{\partial G}{\partial A}\right)_{T,P,n} \quad (\text{Equation 2.1})$$

Where G is Gibbs free energy, A the area of the interface between the immiscible fluids, and  $\sigma$  the interfacial tension. The molecules at the interface have a higher potential energy than the molecules in the bulk, which means that more work is required to move a molecule from the bulk to the interface, increasing surface area. This concept explains why a liquid always will minimize its surface area [10, 11].

The minimization of the surface area on a liquid drop, due to the intermolecular forces, makes the drop less easily deformed. Submerged in another immiscible liquid, the IFT between the liquids will dictate how easily the drop is deformed. In terms of oil recovery, an easily deformed drop is desired, as less energy is needed to deform the drop when flowing through the reservoir. A less easily



deformed drop (a higher IFT), will require larger amounts of energy to undergo enough deformation to travel through narrow pores, e.g. in an oil reservoir. This is due to the deformation being energetically unfavourable at high IFT's. On a microscopic scale, a high IFT will thus prevent oil droplets from moving across the reservoir, which in turn reduces total oil production [12].

### 2.2.2 Adsorption at the interface

Adsorption is adhesion of a large number of molecules or atoms of a particular specie, at a surface or an interface, where the concentration of the specie at the surface/interface is larger than the amount of the specie in the bulk. The molecular specie adsorbed to the surface or interface can be atoms, ions or molecules from a gas, liquid or a dissolved solid. The bulk compound in an adsorption process is known as the adsorbent, whilst the compound being adsorbed to the surface/interface are known as the adsorbate [13].

Much like interfacial tension, adsorption is a phenomenon that can be attributed to the intermolecular forces. Adsorption arises due to the intermolecular forces being unbalanced at the surface/interface, resulting in an attraction from the adsorbent on the adsorbate molecules. This attraction can result from electrostatic attraction, chemisorption (the adsorbate held on to surface/interface by van der Waals forces) or physisorption (the adsorbate held on to the surface/interface by chemical bonds) [13]. The concept of adsorption is illustrated in figure 2-2.

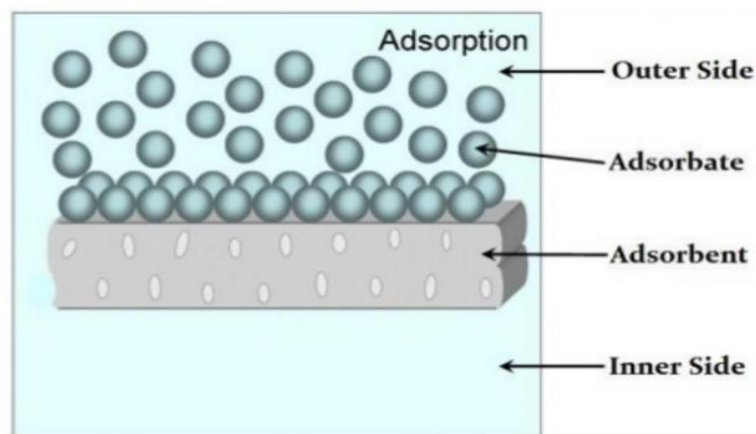


**Figure 2-2** Illustration of adsorption on a solid surface from a liquid or a gas. The same concept applies to a gas-liquid, liquid-liquid or a gas-solid interface. From [14].

## 2.3 Effect of surface active agents on IFT

### 2.3.1 Surfactant

Surfactants are amphiphilic molecules that consist of two parts. One part of the molecule is hydrophilic, which is soluble in the aqueous phase. This part of the molecule is commonly called the “head group”. The other part of the molecule is lipophilic, which is soluble in the oil phase. This part of the molecule is called the “tail group” [2, 10]. On a molecular level, the head group of the surfactant are a functional group that are either positively charged (cationic surfactant), negatively charged (anionic surfactant), positively and negatively charged (zwitterionic surfactant) or without a charge (non-ionic surfactant). The tail group is generally a hydrocarbon chain consisting of various lengths depending on the surfactant, but can also consist of several parallel chains connected to the same head group [2, 4, 11, 15]. The surfactants that will be studied in this thesis consist of a sulfonate group ( $R-O\text{SO}_3^-$ ) and an ion,  $\text{Na}^+$ , and are in other words anionic surfactants, as the head group has a negative charge. An example of the anionic surfactant SDS is seen in figure 2-3.

The amphiphilic nature of surfactants makes the molecules spontaneously adsorb in an interface between e.g. oil and water. The molecules will then reduce the energy difference created by the interfacial molecules getting pulled into their bulk phases by intermolecular forces [16]. This ability to spontaneously orient themselves at an interface, is what makes them interesting for both EOR and other processes, where it is desirable to mix, or reduce the IFT between two immiscible phases.

Anionic surfactants are the ones mostly used in EOR processes since they exhibit low retention in sandstone (a typical reservoir rock), which also are negatively charged [2]. One surfactant molecule is also often referred to as a *monomer*.

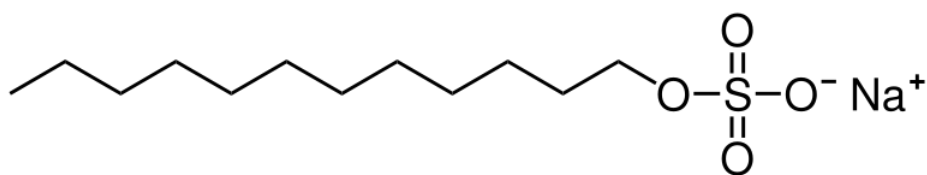


**Figure 2-3** Illustration of the anionic surfactant SDS, which is one of the three surfactants used in this thesis.

The fact that a surfactant/oil/brine (SOB) system will exhibit different IFT`s with regards to the microscopic environment, is well known. Factors like salinity, pH, temperature, surfactant concentration and presence of divalent ions have been reported to change the behaviour and/or efficiency of surfactants, and are why these factors are studied in this thesis [17-22].

### 2.3.2 Critical Micelle Concentration of surfactants

At a given surfactant concentration in a solution, micelles appear. Micelles are aggregates formed by the surfactant monomers. The cause of micelle formation is explained by thermodynamics, namely the balance between entropy and enthalpy [11]. As the concentration of surfactant is increased in a solution, an amount of surfactant molecules is reached, where the unfavourable entropy contribution from connecting the lipophilic tails of the monomers (i.e. creating a micelle), is overcome by an entropy increase due to the “distortion” of the surrounding water molecules when the micelle is formed. This is called the “hydrophobic effect”, and is the main force behind micelle creation [23]. The concentration in which this process takes place, is called the critical micelle concentration (CMC)

The CMC of a surfactant is an important parameter in the case of using surfactant for EOR. An increase in surfactant concentration above CMC will not lead to a further reduction in surface- or interfacial tension, but only lead to further creation of micelles, which have no surface- or interfacial effect [11]. As surfactants are expensive in terms of oil recovery [24, 25], a concentration at, but not above, CMC is most desirable.

An illustration of aggregation of surfactant monomers to micelles are illustrated in figure 2-4, as well as the surface- or interfacial tension as a function of surfactant concentration. The surface/interfacial tension remains close to constant when the concentration is increased above CMC, as the further addition of surfactant only lead to creation of micelles.

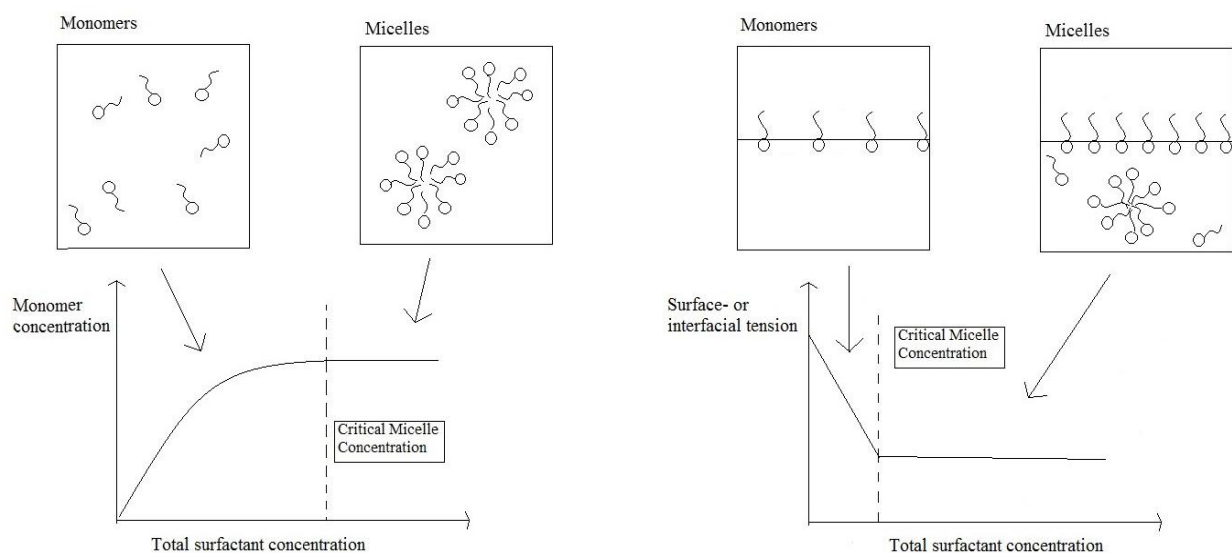


**Figure 2-4** Relationship between monomer and micelle concentration. Adapted partly from [10].

Changes in CMC for a surfactant system with regards to different parameters has been studied thoroughly [17, 26-30]. Wan & Poon [20] reported that all salts used in their experiments lowered the

CMC, as well as the surface tension (ST) of the liquid. They also found that no significant difference in a two-phase system as air was substituted for paraffin. However, this effect was only found when measuring on an ionic surfactant. No change in either CMC or surface/interfacial tension was found when a non-ionic surfactant was used. This phenomenon was explained by the possibility of the added electrolytes decreasing electrostatic repulsion between the charged head groups of the surfactant molecules. A decrease in electrostatic repulsion between the head groups makes the monomers more easily aggregate, and hence, the CMC is decreased for the surfactant with addition of salt. The same observations were found by Umlong & Ismail [31] on the anionic surfactant AOT. The concept of reduction of electrostatic repulsion is further explained in section 2.4.4.

### **2.3.3 Surface active agents in crude oil**

The polar components in a crude oil are as previously mentioned in the resin- and asphaltene fractions. One particularly significant component of the resin fraction, is the naphthenic acids. Naphthenic acids refers to an unspecific mixture of different types of carboxylic acids present in a crude oil, including both acyclic and aromatic acids, which can be interfacially active [32]. These acids are normally only present in the resin-group of the crude [7]. Asphaltenes in the crude are also polar and can be interfacially active. However, Varadaraj et.al. [33] reported that the naphthenic acids are more significant than the asphaltenes in terms of reducing IFT.

Varadaraj et.al. [33] further attempted to correlate crude oil composition with interfacial activity. They found that acids of lower molecular weight have more interfacial activity than acids of higher molecular weight. A probable explanation for this is that acids of a lower molecular weight are less soluble in the oil phase, than molecules of a higher molecular weight, and thus have the greatest affinity to the interface.

The effect of crude oil components on the IFT was further studied by Varadaraj et. al. [34], who observed a decrease in IFT with increasing concentration of asphaltenes in the crude. A suggestion was made that both asphaltenes and naphthenic acids contribute to interfacial activity for the crude. The polar compounds, the acids and the asphaltenes, are also able to react with divalent ions, such as calcium. Complexes made by compounds from the oil and calcium salt results in chemical compositions that are interfacially active [19]. A more precise explanation of how divalent ions can interact with the crude oil is presented in section 2.4.5.

## **2.4 Factors affecting the extent of interfacial absorption/activity**

### **2.4.1 Effect of surfactant concentration**

Change in surfactant concentration will affect the IFT in the SCOB system, as a higher concentration of surfactant in the solution will lead to a higher density of surfactant molecules at the interface, which in turn leads to a lower IFT. However, the concentration will reach a limit where the surfactant molecules begin forming micelles (CMC), where further addition of surfactant will not affect the IFT. Several studies have been conducted [35-38] where a correspondence between IFT and surfactant concentration has been investigated. The results obtained indicate that the measured IFT shows an abrupt decrease until a specific surfactant concentration (CMC), at which point the IFT remains approximately constant for all greater concentrations [39, 40]. This commonly accepted.

### **2.4.2 Solubility/surfactant HLB value**

The nature of the surfactant molecule enables it to be dissolved in both an aqueous and an oleic phase. The degree of preference to which phase the surfactant has a greater affinity to, is described by the surfactant's Hydrophile-Lipophile Balance (HLB). The HLB is a quantitative measure that indicates in which phase the surfactant is more soluble. The higher the HLB value is, the more water-soluble the surfactant. The lower the HLB, the more oil-soluble the surfactant. The HLB is in practice a function of the ratio between the molecular masses of hydrophilic and lipophilic part of the molecule [41-43]. Values for HLB normally range from 0 to 20 [44], where high values of HLB favours creation of o/w emulsions, while low values favour w/o emulsions. However, some ionic surfactants, due to their high solubility in water, may reach HLB's of up to 40 [11].

The IFT in a SOB system is reported by Granet et.al [45] to be at its minimum when the HLB is balanced ( $HLB \approx 10$ ) for a given surfactant. Generally, this is hard to achieve for single-chained surfactants. To the contrary, a two-chained surfactant holds a much more balanced HLB which in theory reduces the IFT to a greater extent than a single-chained surfactant [45]. Based on this, it can be assumed that the single-chained surfactants SDS and SDBS will exhibit a higher IFT than the double-chained AOT in general.

Further studies have shown that the HLB for SDS is 40 [46], 10.6 for SDBS [42] and 10 for AOT [47]. The HLB values are in agreement with theory, as SDBS has a longer tail than SDS (more lipophilic than SDS), and AOT being double chained (even more lipophilic and balanced).

Which type of emulsion that will appear from a given surfactant in a system follows Bancroft's Rule, which is based on HLB: "When an interfacial active agent is present along with two immiscible liquids, then after agitation the liquid that is the better solvent appears as the continuous phase" [48]. In other words, the HLB is a bridge between the surfactant structure and what type of emulsion, and

its properties, it will exhibit. In context with using surfactants in a EOR process, an o/w emulsion is desired, as w/o emulsions are related to loss of surfactant and changes in the systems viscosity [49].

### 2.4.3 Critical Packing Parameter

Another parameter based on the geometry of the surfactant, like the HLB is the Critical Packing Parameter (CPP). CPP is a function of the hydrocarbon chain length ( $l_t$ ), effective area of the head group ( $a_o$ ), and the volume of the tail group ( $v_t$ ), and the relation between the surfactants dimensions is explained by e.g. [50] with the following equation

$$CPP = \frac{v_t}{a_o l_t} \quad \text{(Equation 2.2)}$$

CPP determines the shape of the surfactant aggregate structure. A  $CPP < 1$  or  $CPP > 1$  describes a tendency to form spherical- or rod- formations respectively. Should, however, the CPP be close to 1, this will allow the tails of the surfactant to create a cylinder form, resulting in tight packing, which is the case for e.g. AOT (HLB = 10 [47]). With such tight packing, the IFT can reach minimum values [51].

The value of the CPP has been found by Wang [52] and Mittal [43], for some surfactants, to have a linear relationship with the HLB, as both parameters are a function of the surfactant molecule dimensions. A correlation between HLB, CPP and type of surfactant aggregate structure can be seen in figure 2-5. Figure 2-5 also shows whether the surfactant enhances a w/o or a o/w emulsion, depending on their HLB and CPP values.

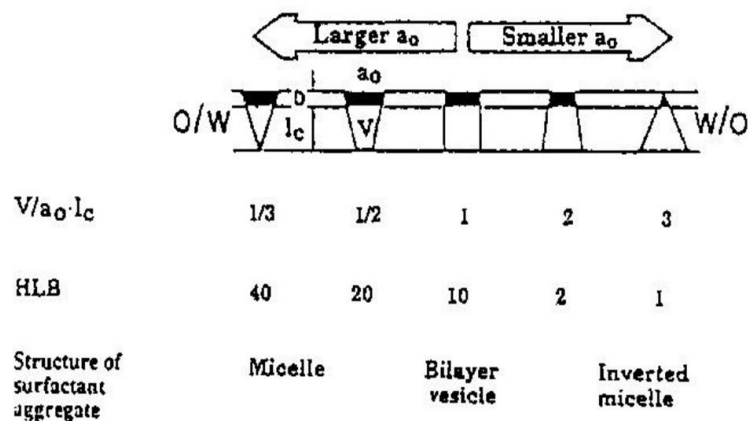


**Figure 2-5** Illustration of the scale of HLB and CPP. A larger headgroup area,  $a_o$ , makes the surfactant more hydrophilic, thus a high HLB, o/w emulsions and creation of micelles. A smaller  $a_o$  promotes a lower HLB, w/o emulsion and creation of inverted micelles. From Mittal & Kumar [43].

#### 2.4.4 Electrostatic forces at the interface

When a charged particle is present in a solution containing excess ions, those ions will orient themselves around the charged particle to electrostatically neutralize the particle. Closest to the particle, a layer consisting of only ions with opposite charge of the particle will accumulate. Further out from the charged particle, both ions of the same charge and the opposite charge will accumulate in a layer, larger than the inner one. These two layers, are what is called the electrical double layer (EDL) [11, 53, 54]. Illustration of the EDL can be seen in figure 2-6.

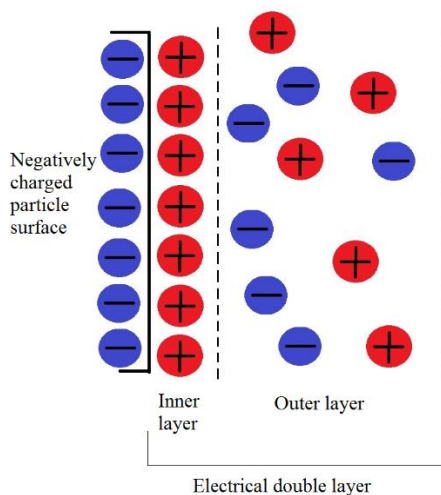


**Figure 2-6** Illustration of the electrical double layer present at a charged surface.

When two surfactant monomers with the same charge of the head group is present at an interface, their EDL will interact and repel each other, as the two monomers have the same charge. However, when salt is introduced to the system, positive and negative ions will interact with the double layer, decreasing the size of the EDL, and hence the repulsion between the two monomers [55]. This is the reason why CMC, as well as IFT, decrease in a surfactant-containing system when salt is introduced to the system.

#### 2.4.5 Salinity

All three surfactants investigated in this thesis are ionic surfactants. This means, that in an emulsion or at an interface, there will be some repulsion between the surfactant head groups as they carry the same charge. This, in turn, makes the effective head-group-area large due to its EDL. Addition of electrolyte, however, will weaken the repulsive forces between the head groups. The weakening of the repulsion allows a higher concentration of surfactants at the interface/surface [56]. An increase in surfactant/area ratio will decrease IFT [51]. The addition of electrolyte, and thus a tighter packing of monomers at the interface, is illustrated in figure 2-7.

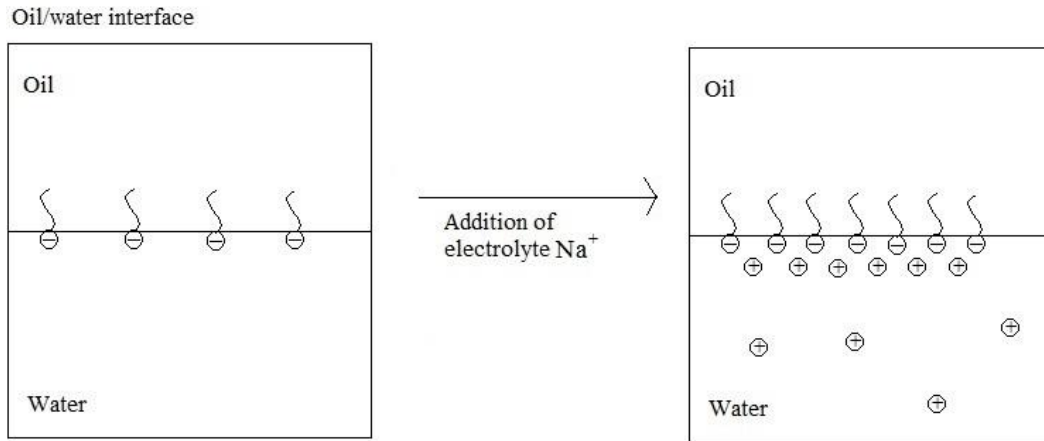


**Figure 2-7** Illustration of the effect of adding electrolyte to an aqueous surfactant solution on IFT/surfactant density

The effect of increasing salinity does not only have an effect with regards to the charge of the head group of the surfactant, it also alters the aqueous phase' solubility. As concentration of salt increases, the solubility of surfactant in the aqueous phase decreases. As the solubility decreases, the surfactant starts accumulating at the interface instead of in the bulk. The salt concentration where the solubility of the surfactant is equal in both the oil- and the water phase, is where the surfactant has its highest affinity to the interface. This salinity is defined as the optimal salinity (OS) for that given system, as this is the salinity where the solubility of the surfactant is equal in both phases, resulting in the tightest possible packing at the interface [57, 58]. Increasing the salinity above the OS, the solubility at the interface starts to decrease, and the surfactant move in to the oil phase.

The change in IFT as a function of salinity is illustrated in figure 2-8. An increasing salinity will increase the surfactants affinity to the interface, resulting in a higher concentration of monomers at the interface, and thus a lower IFT. After a minimum IFT are reached at the OS, IFT increases again as the surfactant move in to the oil phase. Which kind of Winsor microemulsion that is created are also indicated on the figure, and the differences between them is discussed further in section 2.5.1.



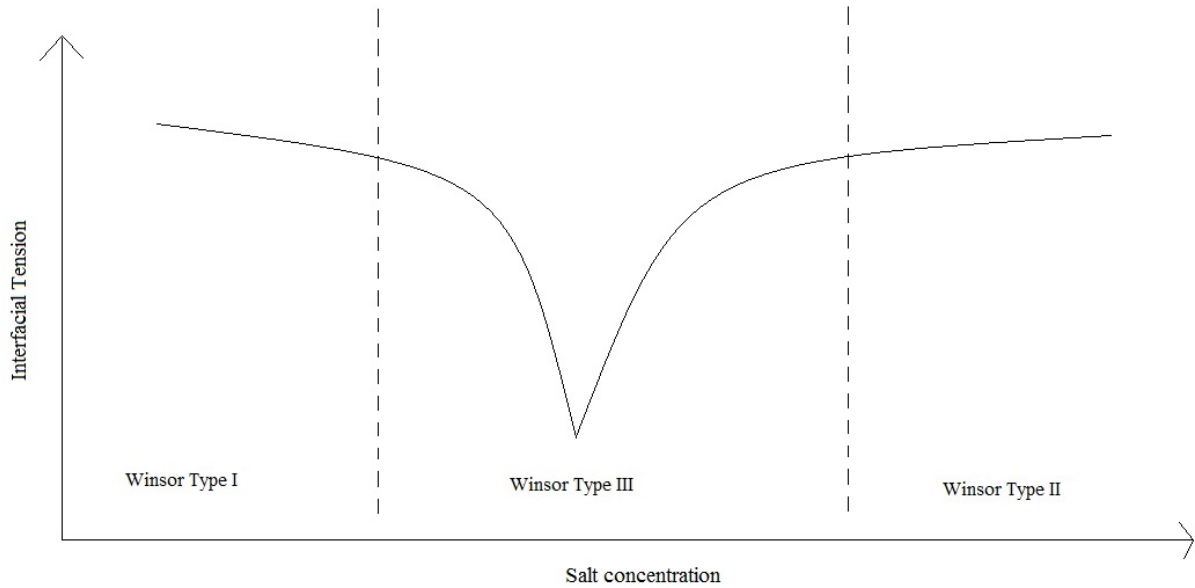


**Figure 2-8** Interfacial tension as a function of salinity. The IFT is lowest at a salinity where the surfactant has equal solubility in the water and oil phase, and thus a largest affinity to the interface. Illustration redrawn from [59].

Kumar & Mandal [30] studied the IFT between three different surfactants (SDS, CTAB and Tween-80) against a crude oil with variation in brine salinity. They observed that the IFT will decrease towards a minimum, to further increase with an increasing salinity. The measured IFT for the SCOB system against different wt% of NaCl, showed a IFT minimum for all three surfactants [30].

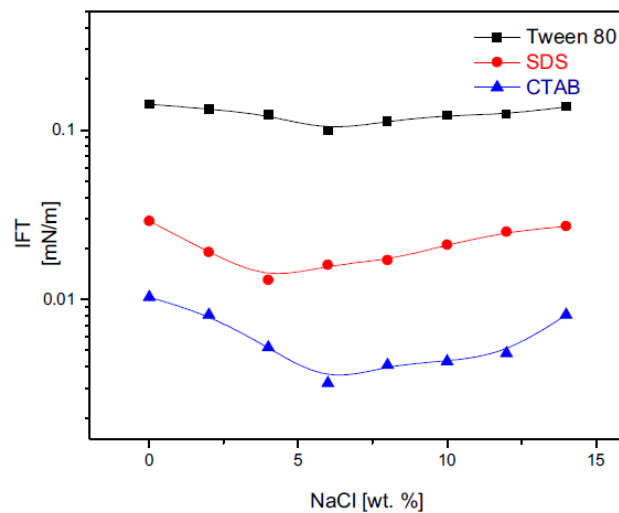


**Figure 2-9** Identification of optimal salinity for three different surfactants. From Kumar and Mandal [30].

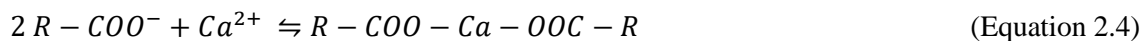
The results were explained by the fact that the presence of salts increases the tendency of surfactants to accumulate at the interface, due to reduction in surfactant solubility in the water phase. At some optimal electrolyte concentration, a minimum in IFT was reached. At salinities, higher than the optimal salinity, IFT then increases. They explained the increase in IFT being due to the salinity being

at a level where the surfactants migrate into the oil phase, rather than orienting themselves at the interface. The same concept is investigated by several other studies [40, 59-62], where the same observations have been made.

This optimal salinity will, according to Aarra et.al [63], vary with temperature, pressure and microemulsion composition of a given SCOB system. That being said, Puerto & Gale [64] reported the optimal salinity to decrease with an increasing surfactant molar weight, probably due to the fact that a higher molar weight would arise from a longer hydrocarbon chain. The length of the hydrocarbon chain will dictate how lipophilic the surfactant molecule is. More lipophilic molecules will be less soluble in water, and hence, less salt is needed to induce an affinity to the interface for the surfactant.

#### *Addition of divalent ions*

Addition of divalent metal ions (e.g. calcium, magnesium) has been observed to lower the optimal salinity for given SOB system by Reed & Healy [57]. Tichelkamp et.al [19] explained that this effect, should it be on a crude, arises from the fact that calcium ions can form 1:2 ion pairs with naphthenic acids in the crude oil. The 1:2 calcium-naphthenic-acid-complexes will be adsorbed to the interface due to its solubility in both oil and water [19]. The reaction of naphthenic acids with divalent  $Ca^{2+}$  can be written as the following equations proposed from Buckley & Liu and Farooq et.al [65, 66] respectively



An illustration of calcium ions reacting with naphthenic acids in the crude can be seen in figure 2-10.

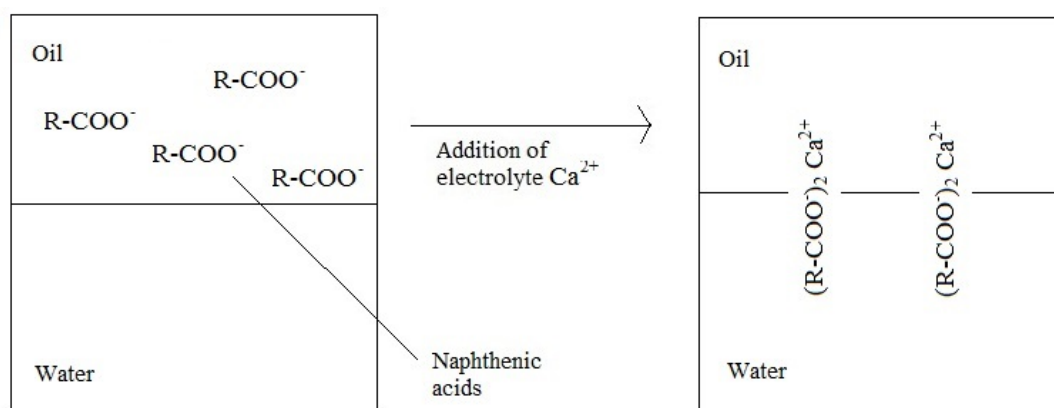


**Figure 2-10** Illustration of the effect of divalent metal ions on naphthenic acids in crude oil, creating interfacial active compounds which adsorb to the interface and reduce IFT.

#### 2.4.6 Temperature

HLB temperature, or phase inversion temperature (PIT), for a surfactant is another way of classifying surfactant emulsifiers. PIT is defined as the temperature for a given SOB system with equal amounts of an oil phase and an aqueous phase, where the emulsion changes from an o/w to a w/o emulsion. For standardisation, it is required that the surfactant concentration is in the range of 3-5 wt% [11]. It is important to realize that the PIT value is not associated with the specific surfactant per se, as it relates to the total oil–water–surfactant system [15]. At a temperature equal to the PIT for a given system, the system will exhibit the lowest interfacial tension [67]. The more balanced the HLB of the surfactant molecule is, the more it will be sensitive to change in temperature [67, 68].

The inversion of emulsions and change in effective HLB occurs as the temperature for the system increases. The temperature increase results in a decrease in the intermolecular forces between the surfactant head group and the water phase. During a temperature increase, the effective HLB of the surfactant will therefore decrease. The decrease in HLB will continue until the properties of the surfactant molecules promote a w/o emulsion rather than o/w [68]. The temperature where this transition takes place, is the SOB systems PIT, and is also where the system will reach its lowest IFT [40]. Factors that change the PIT for a system are salinity of the aqueous phase, type of salt dissolved, relative volumes of water and oil, oil composition and surfactant concentration [67].

Ye et.al. [69] studied the effect of temperature on IFT between a crude oil and a gemini surfactant. They found that the system's IFT decreased with increasing temperature, until a minimum was reached. At temperatures higher than the temperature where the minimum was observed, IFT increased with temperature. The same trend is also found earlier by Healy et.al [70] with the use of an anionic surfactant, and also by Aveyard et.al [40] by the use of surfactant AOT. Aveyard et.al. [40] explained the change in IFT with temperature, being due to the entropy change of transferring a mole of surfactant from the bulk to the interface, being approximately equal to the entropy of formation of micelles containing a mole of surfactant. Temperature induced minimums in IFT for AOT at different salinities are found by Aveyard et.al and can be seen in figure 2-11.

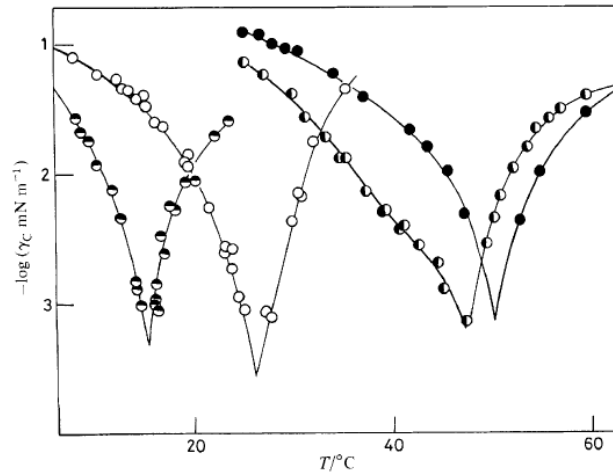


**Figure 2-11** IFT minimums found by Aveyard et.al [40] at different temperatures. Each curve has a different salinity, while surfactant concentration is kept constant.

Karnanda et.al [27] however, found some contradicting results on the SCOB IFT's response to change in temperature. They found that the relation between the IFT and temperature in a SCOB system varies with type of surfactant. They tested surfactants Triton X-100 (non-ionic), Triton X-405 (non-ionic) and Zonyl FSE (anionic).

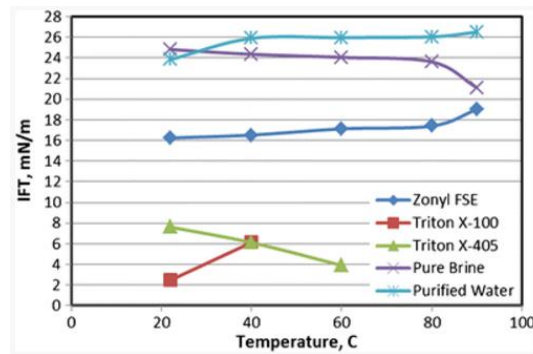


**Figure 2-12** Change in IFT as function of temperature, contradicting the observations done by Aveyard. From [27]

A probable explanation is the degree of solubility of the surfactant in the water phase, as explained by Miquilena et.al [71]; If the solubility of a surfactant in water increases with temperature, then the IFT will decrease, as the surfactant molecules rather exist in the bulk, than at the interface. In the opposite case, if the solubility decreases with temperature, the surfactant molecules orient themselves rather at the interface, hence, IFT decreases. The surfactants response to change in temperature will therefore be dictated by its response in solubility to temperature change.

### 2.4.7 pH

The direct effect on a surfactant by change in pH is strongest at low pH values [51]. At low pH, anionic surfactants can react with  $H^+$  and convert from an anionic to a non-ionic surfactant by the following mechanism (here illustrated with anionic surfactant SDS) [72]:

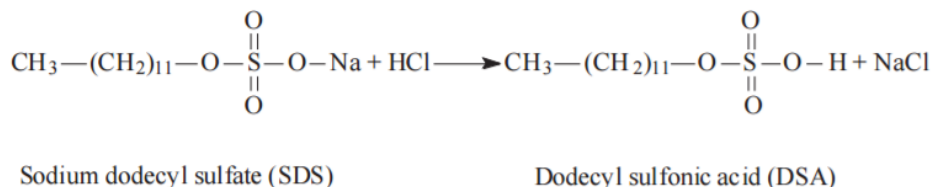


**Figure 2-13** Reaction of anionic to non-ionic surfactant at low pH. Represented here by anionic surfactant SDS.

Further, for anionic surfactants in distilled water or at very low salinities, the addition of  $H^+$  will to some degree reduce electrostatic repulsion between the surfactant molecules, thus enhanced tighter packing in the interface, which in turn, lowers the IFT [51]. The same effect in reverse also takes place, as the IFT of a non-ionic surfactant increases with increasing pH, due to the high pH ionising the carboxylic head group, and thereby making the surfactant more hydrophilic, and thus inducing a lower affinity to the interface [73].

Considering the effect of pH on the SCOB system, the composition of the crude is of importance. Addition of inorganic acids or bases to the brine (i.e. change of pH) in contact with the crude, will strongly influence the surface activity of the acidic and/or basic components of the crude. This has been documented by several studies [51, 74-76]. Like the creation of in-situ surfactants when  $Ca^{2+}$  ions are present, changes in pH will, given appropriate components in the crude, further induce amphiphility to the molecules. Dissociated acidic and basic components in the oil will be protonated or deprotonated depending on the pH [77]. A molecule that has reacted with a  $H^+$  or  $OH^-$  ion, will have a be amphiphilic, and orient itself at the interface, thus the IFT is decreased [78].

These naphthenic acid components in the resin- and asphaltene fraction of the oil are of significance in relation to injection of alkalis in an oil reservoir. The acidic compounds in the crude will become interfacially enhanced should they react with alkalis. Depending on the properties of the crude, this can to different degrees enhance the oil recovery. Alkali can therefore be favourably employed as a flooding agent [2, 30, 32]. A synergy effect between this creation of in-situ surfactants and injected surfactant has been observed by Liu et.al. [79]. Herein lies a commercial benefit as alkalis are in general cheaper than pure surfactants, so co- injection of alkali has the potential to significantly reduce the cost of an EOR-process [30].

## 2.5 Microemulsions

### 2.5.1 Surfactant microemulsion for EOR

A desired scenario in petroleum production is to create a microemulsions zone displacing the oil. The reason that this is desirable in an oil reservoir, is that a characteristic of microemulsions are that they exhibit low IFT`s. Low IFT`s are favourable for mobilizing residual oil [80, 81]. Microemulsions are in practice transparent homogeneous mixes of oil/hydrocarbons and water, with the presence of large amounts of surfactant, that are thermodynamically stable, have high surface area of the emulsified liquid and are able to create a bi-continuous phase [82].

The commonly used microemulsion system was first introduced by Winsor [83], and later by others [84, 85] , who explained that microemulsion phases can co-exist in equilibrium with other excess phases. Definitions of different systems containing microemulsions were defined by Winsor [83] as:

*Winsor I* - Excess oil phase and a water-continuous microemulsion phase.

*Winsor III* – Excess water phase, a bi-continuous microemulsion phase and an excess oil phase

*Winsor II* – Excess water phase and an oil-continuous microemulsion phase.

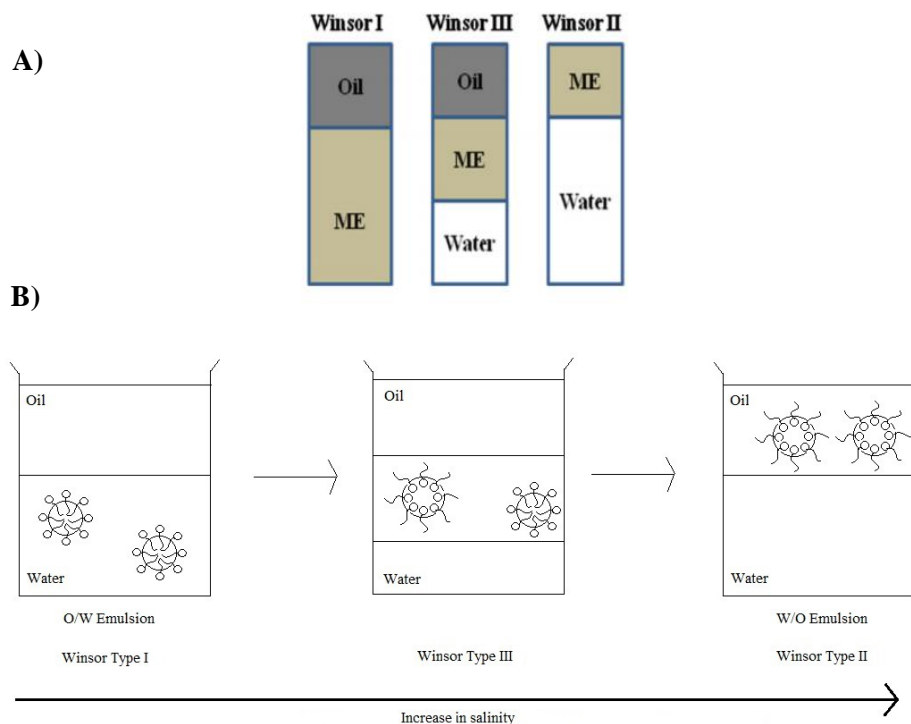


**Figure 2-14** A) Illustration of the Winsor-systems from [85] and B) Illustration of surfactant behaviour at increasing salinity defined by Winsor systems and type of microemulsion. The microemulsions exhibits its lowest IFT where both o/w and w/o emulsions appear.

In a Winsor I system, a lower phase microemulsion exists with excess oil. In the opposite case, Winsor II, an upper phase microemulsions exists with excess brine [70]. The surfactant- rich middle

phase, is as noted, called a Winsor III system. In a Winsor III system there exists a bi-continuous structure consisting of equal amounts of both w/o and o/w emulsions, with a very low IFT between the liquids [86].

The behaviour of the microemulsions is key to optimizing the SCOB system for EOR. Identification of properties of different microemulsion systems is often done by laboratory screenings [85]. This screening is done by varying the factors affecting the system, e.g. salinity, temperature and surfactant concentration. Studies by Reed & Healy [57] have shown that the formulation of the system is crucial to the performance of the oil production, as IFT of the system depends on the type of formulation. Given an optimal formulation, i.e. the optimal conditions with regards to salinity, temperature, surfactant type, co-surfactant etc., a Winsor III microemulsions exists, and the system will exhibit its lowest IFT [87].

In a Winsor III system there is a balance between the solubility of surfactant in the oil-phase and the water-phase, resulting in highest surfactant solubility in the interface [2]. It is also in this phase that the system will exhibit  $IFT < 10^{-3}$  mN/m, also known as “ultralow” IFT [51]. Other studies [40, 57, 59] have shown that the IFT in of a SOB system will reach its minimum when the contributing factors promote a Winsor III microemulsion.

Another mechanism that increases oil recovery by creation of microemulsions, is swelling. As the Winsor III microemulsion is created, water and oil solubilizes in each other. In this middle phase, in the reservoir, the oil saturation increases, hence the relative permeability of the oil. A higher relative permeability means the oil flows more easily though the reservoir, which leads to a higher oil recovery [24]. A Winsor III is thus the favourable case for creating a mobile oil bank in the reservoir, as droplets are more easily deformed and mobilised due to the low IFT. An illustration of this concept on a reservoir scale can be seen in figure 2-15. WIII indicates the Winsor III region where oil is mobilised by a microemulsion.

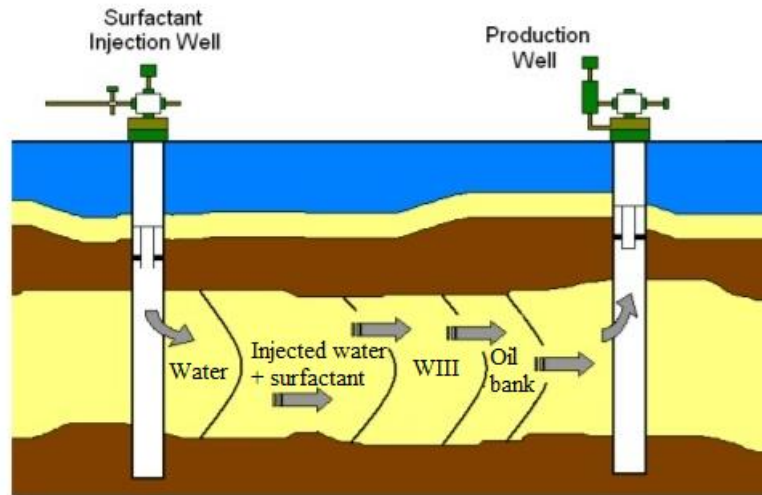


**Figure 2-15** Illustration of surfactant injection with a mobile zone with preferably Winsor III conditions, mobilizing an oil bank which is pushed to the production well. Redrawn from [88].

### 2.5.2 Phase studies and solubilisation parameter

Huh [89] found that the IFT of the SOB system can be correlated to the systems geometry, and using the same method, identify optimal salinity. By studying the volume of water emulsified in oil, and volume oil emulsified in water over a series of samples with different salinities, he found that the volumes of liquid solved in each respective phase could be correlated to the optimal salinity. In addition, the method proved useful for identifying the salinity range in which a Winsor III microemulsion appears. Puerto & Gale [64] showed in addition that the interfacial tension is inversely proportional to the magnitude of the solubilisation parameter at optimal salinity.

A simplified version of Huh's calculations is made by Salager et.al. [90] where the IFT of a system at optimal salinity can be written as

$$\sigma SP^{*2} = constant \quad \text{(Equation 2.5)}$$

Where  $\sigma$  is the IFT, and  $SP^*$  is the solubility parameter at optimal salt concentration. Solubility parameters are a function of the volumes solved in each respective liquid for the different phases. The constant in equation 2.5 is empirically validated from several studies, by e.g. Fotland and Skauge [91, 92], and is found usually to be at a value of  $0.30 \pm 0.05$  mN/m when the IFT is expressed as mN/m and  $SP$  in vol/vol [90]. The equation, however, is not valid at other salt concentrations than the optimal.

Solubilisation parameters are a measure of the amount of oil emulsified in water and water emulsified in oil in terms of volumes. A definition of this is given by e.g. Broze [93] as



$$SP_w = \frac{V_w}{V_s} \quad (\text{Equation 2.6})$$

$$SP_o = \frac{V_o}{V_s} \quad (\text{Equation 2.7})$$

Where  $SP_x$  is the solubilisation parameter for each respective phase,  $V_x$  the volume of oil or water per  $V_s$ , volume of surfactant. The two equations are simply the difference between the initial oil volume and excess oil (at the top) at equilibrium condition after proper shaking [94].

At optimal salinity, equal amounts of water and oil per volume surfactant are assumed, thus at optimal salinity the solubility parameter can be written [61]

$$SP^* = \frac{V_w}{V_s} = \frac{V_o}{V_s} \quad (\text{Equation 2.8})$$

In order to calculate the solubilisation parameter, however, it must be assumed that there are no volume changes upon mixing, and that all the surfactant is retained in the microemulsion phase [61].

The parameters can be used to identify the optimal salinity of a SOB system. As equation 2.8 states, the optimal salinity is where the solubilisation parameters are equal. Thus, a plot of solubilisation parameters as a function of, e.g. salinity, will reveal the optimal salinity for the system. An illustration of this is shown in figure 2.16.

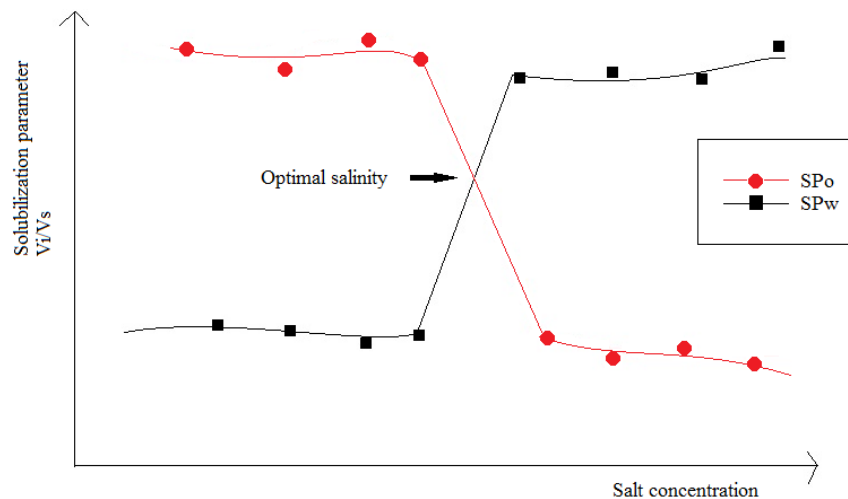


**Figure 2-16** Illustration of determination of optimal salinity from solubilisation parameters.

## 2.6 Surfactants on pore scale

### 2.6.1 Capillary forces

As discussed in section 2.3, surfactants decrease the IFT in a liquid-liquid non-miscible system. The decrease in IFT happens as the surfactant molecules replace the water molecules at the interface. As the surfactant molecules are soluble in both phases, the energy difference across the interface decreases, and hence the IFT [95]. The decreasing effect on IFT is why surfactants are interesting in terms of EOR. This is due to two effects:

1) The reduction in IFT makes the drop more deformable, making it mobile enough to travel through narrow pores in the reservoir. An example of deformation due to lower IFT is illustrated in figure 2-17.

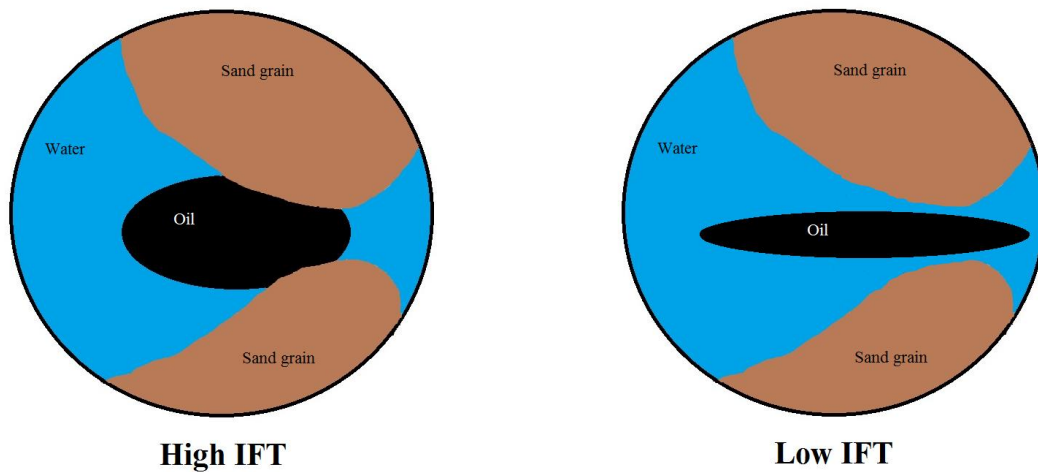


**Figure 2-17** Illustration of mobilization and deformation of an oil drop with regards to the IFT between the liquids.

2) Residual oil in a reservoir that is trapped and immobilized due to the restraint of capillary forces, will be released with a lower IFT [96]. The capillary forces in a pore is a function of the IFT, and is defined by Berg [11] as

$$P_c = P_o - P_w = \Delta P = \sigma_{ow} \left( \frac{1}{R_1} - \frac{1}{R_2} \right) \quad (\text{Equation 2.9})$$

Where  $R_1$  and  $R_2$  are the principal radii of the curvature of an oil drop,  $\sigma$  the IFT, and  $\Delta P$  is the pressure difference across the interface for the two liquids (in this case between oil and water). Equation 2.9 states that the capillary pressure is a function of the IFT. As seen from the equation, a decrease in IFT will lead to a decrease in capillary pressure, which will mobilize residual oil, and increase the total oil recovery.

## 2.6.2 Capillary number

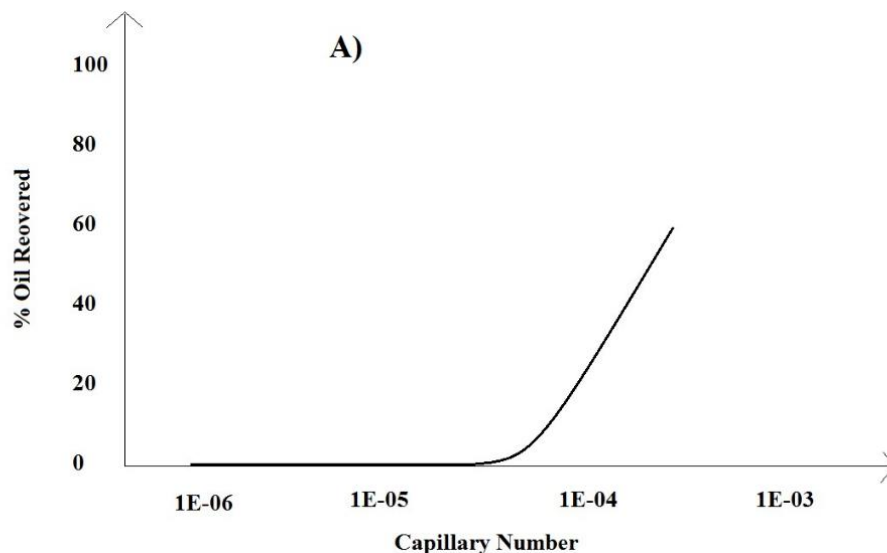
It is generally accepted, and empirically verified, that residual oil saturation in a given reservoir correlates with the capillary number  $N_c$ , defined by several authors [10, 62, 97] as

$$N_c = \frac{\text{Viscous forces}}{\text{capillary forces}} = \frac{V\mu}{\sigma \cos\theta} \quad (\text{Equation 2.10})$$

In terms, the capillary number is a dimensionless ratio between the capillary forces and the viscous forces in an oil displacement. The viscous forces are a function of the viscosity  $\mu$  of the injected liquid and the displacing Darcy velocity  $V$ . The capillary forces are a function of IFT  $\sigma$ , and the contact angle  $\theta$ .

Equation 2.10 states that an increase in capillary number can be achieved by either a) increasing injection fluid velocity, b) increasing injected fluids viscosity or c) decreasing IFT between oil and water [24]. However, method a) and b) can in practice not increase the capillary number by a large enough amount that there is a significant increase in oil recovery (cf. figure 2-19 A). There are e.g. technical limitations to which degree the velocity of an injection fluid can be increased. Studies from Reed and Healy [57] have, however, shown that IFT between oil and water can be reduced from 25-30 mN/m, to magnitudes of  $10^{-3}$  mN/m, by the use of surfactant. A reduction in IFT by this magnitude will decrease the capillary number in the range of  $10^{-1}$ -  $10^3$ . A decrease in capillary number of a size like this is shown by Butt [98] to decrease the residual oil saturation by tens of percent.

A decrease in residual saturation and increase in oil recovery by increasing capillary number in the range of  $10^2$ -  $10^3$  is shown on figure 2.18.



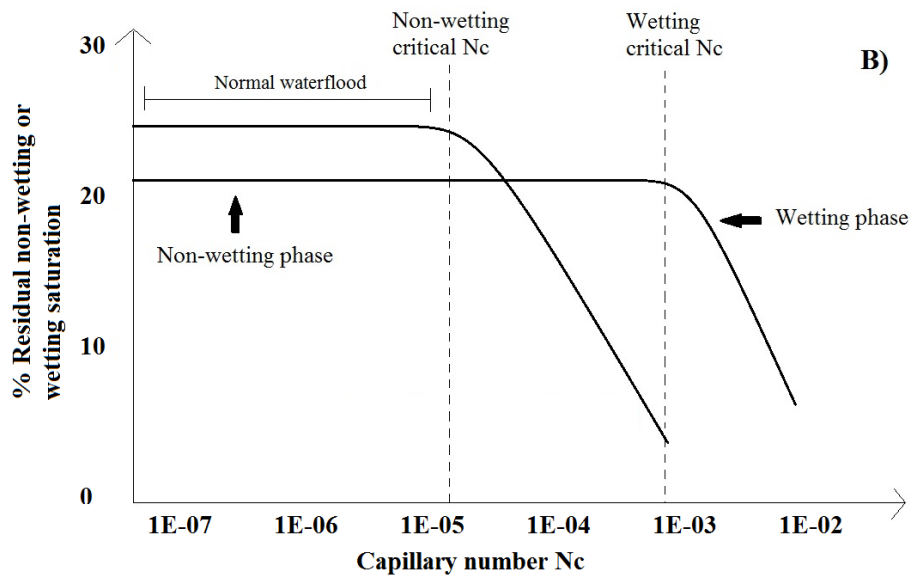


**Figure 2-18** Schematic of A) Oil recovery as a function of capillary number. Redrawn from [99].  
 B) residual saturation for wetting- and non-wetting fluid respectively, as a function of capillary number. Redrawn from [100].

## 2.7 Characterisation by number of carbons

### 2.7.1 Alkane carbon number

Alkane carbon number (ACN) is the number of carbon atoms in the chain of an n-alkane. E.g. Heptane has an ACN of 7, decane an ACN of 10 and dodecane an ACN of 12. This follows for all straight alkane chains. The ACN concept satisfactorily characterizes the hydrophobicity of hydrocarbons of an alkane type, where a higher ACN indicates a more hydrophobic compound [101].

### 2.7.2 Equivalent alkane carbon number

Crude oils on the contrary to alkanes, do not consist of straight chain alkanes, but are rather a mix of several different organic species. To more easily classify/ predict the behaviour of crude, Wade et.al. [102] introduced the concept of equivalent alkane carbon number (EACN). This is a dimensionless value that represent to what degree the oil is lipophilic, much like ACN for alkanes. EACN is a measurement of both the oil bulk, and its possible polarity, should it possess one [103]. The parameter is applicable for determining the stability of emulsions, much like the HLB parameter for a surfactant. That being said, the EACN is independent of which surfactant used in terms of microemulsions [87].

Observations e.g. by Cayias et.al. [104], showed that if a crude is replaced with an alkane, or alkanes, of similar ACN in the presence of a sulfonate type surfactant, the interfacial tension can be modelled using that/those same alkanes. To create a model oil with the same properties as a crude, an averaging rule can be applied to calculate the EACN of the mix [104]

$$(EACN)_M = \sum_i (EACN)_i * x_i \quad (\text{Equation 2.11})$$

Where  $EACN_i$  is the EACN of component i, and x the mole fraction of compound i. The equation is useful for determining physiochemical properties of a mix of compounds in applications where it will act as a model oil. The correlation can also aid in identifying the EACN of a crude, by variation in which alkanes that can be mixed to mimic the behaviour of the crude. Knowledge of the EACN of a crude could possibly save time in screening for an optimal surfactant [87].

## **3 Method**

### **3.1 Chemical preparations**

#### **3.1.1 Preparations of Crude Oil**

In this thesis, two different crude oils from the North Sea are used. These oils are throughout the thesis denoted A and C. The crude oils were heated in a water bath at 60°C for 30-40 minutes, with the lid slightly opened to avoid pressure build-up, before each set of measurements. During the 30-40 minute warm up, the samples were softly shaken 10-15 times to ensure the oil was homogenous. Both Crude Oils were supplied by Centre of integrated Petroleum Research (CiPR) at the University of Bergen.

#### **3.1.2 Preparations of Brines**

Monovalent brines were prepared with NaCl, which was used as received from supplier. For solutions containing divalent ions, CaCl<sub>2</sub> is the chemical used, also used as received from supplier. The salt was weighed in to correct amount and left to stir on a magnetic stirrer for 4-5 hours to ensure total dissolution. In the brines involving different pH values, 0.1M HCL and 0.1M NaOH were used to adjust the pH. The added volumes of HCL and NaOH were so small that changes in both salinity and surfactant concentration, due to the additional volume, were neglected. The pH values were measured by using a Metrohm pH-meter equipped with a Cl-Ag electrode.

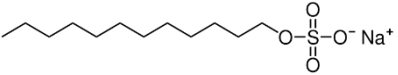
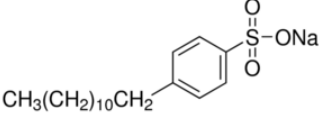
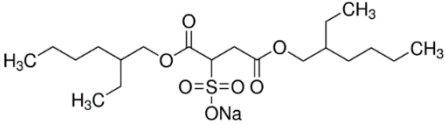
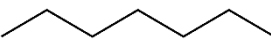
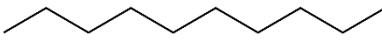
#### **3.1.3 Preparation of Surfactant Solutions**

All three surfactants SDS, SDBS and AOT were used as received from supplier. Solid surfactant was weighed and mixed with either brine or distilled water depending on the desired fluid composition. Surfactants were then left on a magnetic stirrer for 6-12 hours to ensure total surfactant dissolution. All surfactant solutions used in this thesis are, unless otherwise specified, at a surfactant concentration of 10xCMC. This concentration is chosen specifically, as small or no changes would be made in terms of physical-chemical properties, should the surfactant concentration somehow be altered during a measurement (precipitation, evaporation of liquid etc.). A concentration at a such degree above CMC makes the system more robust, and is why this concentration was chosen.

### 3.1.4 Overview of chemicals used

Table 3-1 gives an overview of all the chemicals used.

**Table 3-1** Overview of the IUPAC names and abbreviations, molecular weights, structures, suppliers and purity of the chemicals used. Purity of SDBS could not be obtained.

IUPAC name (Abbreviation)	M <sub>w</sub> [g/mol]	Structure	Supplier	Purity [wt%]
Sodium dodecyl sulfate (SDS)	288.38		Sigma-Aldrich	≥ 99
Sodium dodecylbenzenesulfonate (SDBS)	348.48		Sigma-Aldrich	- *
Sodium dioctyl sulphosuccinate (AOT)	444.56		Sigma-Aldrich	> 98
Sodium Chloride	58.44	NaCl	Sigma-Aldrich	> 98
Calcium dichloride dehydrate	147.01	CaCl <sub>2</sub> * 2H <sub>2</sub> O	Sigma-Aldrich	> 99.5
n-Heptane (C7)	100.21		Sigma-Aldrich	> 99.5
n-Decane (C10)	142.29		Sigma-Aldrich	≥ 95
Hydrogen chloride (HCL)	36.46	HCL	Sigma-Aldrich	> 99
Sodium hydroxide (NaOH)	40.00	NaOH	Sigma-Aldrich	> 98

\* Purity for SDBS could not be obtained.

### 3.1.5 Different brine- and surfactant compositions

Different heavy phase compositions are used throughout this thesis. An overview of the different heavy phase abbreviations, compounds present in the solutions, concentrations of each compound,  $\text{Ca}^{2+}/\text{Na}^+$  ratios and ionic strengths given in table 3-2.

**Table 3-2** Abbreviations and compositions of different heavy phase systems used. The table shows the different brine/surfactant compositions, their abbreviation,  $\text{Ca}^{2+}/\text{Na}^+$  ratio as well as ionic strengths.

Abbreviation	Solution	$\text{Ca}^{2+}/\text{Na}^+$ ratio	Ionic strength
LS	0.02M NaCl	0	0.02
LSS	0.02M NaCl + surfactant concentration of 10xCMC	0	0.02
LS-Ca	7.14mM NaCl + 4.29mM $\text{CaCl}_2$	0.6	0.02
LSS-Ca	7.14mM NaCl + 4.29mM $\text{CaCl}_2$ + surfactant concentration of 10xCMC	0.6	0.02

### 3.1.6 Source of error in chemical preparation

In all measurements, unless otherwise specified, the surfactant concentration is kept at approximately 10 times the concentration of CMC. For surfactant SDS however, a mistake in calculating the amount of solid surfactant needed, led to the concentration being 16 times CMC, rather than 10. This was not realized until several measurements had been conducted. The concentration is therefore kept the same, at 16xCMC, throughout all measurements, unless otherwise noted. However, since the concentration is well above CMC, the mistake should not to any significant degree have affected the physical-chemical properties, and thus the results obtained. The high concentration of surfactant could, however, explain the large degree of precipitation observed during the scan for optimal salinity for SDS.



## 3.2 Surface tension and Interfacial tension

### 3.2.1 Du-Nuöy ring method

CMC for the surfactants was identified by use of the Sigma 700 Tensiometer (KSV Instruments Ltd., Finland) and the Du Nöuy ring method. The method is based on measuring the forces pulling on a ring as it is lifted through, and out of a liquid. Due to the intermolecular forces, the surface molecules of the liquid will be drawn to the bulk rather than air, resulting in a surface film, and hence, a surface tension. This film will to some extent prevent the ring from leaving the liquid, exhibiting a force  $F$ . This force can be correlated to the ST ( $\gamma$ ) of the liquid by the following equation explained by Butt.et.al [105] and originally from Du Nöuy [106]:

$$F = 2\pi * (r_i + r_o) * \gamma \quad (\text{Equation 3.1})$$

Where  $r_i$  and  $r_o$  are the inner and outer radii of the ring respectively, and  $\gamma$  is the surface tension. Illustration of the method are shown in figure 3-1.

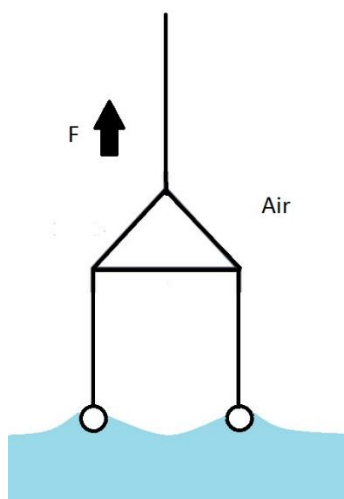


**Figure 3-1** Illustration of the Du-Nuöy ring being drawn through a liquid-air interface.

The platinum ring used in the method was thoroughly cleaned with ethanol, and heated on a bunsen burner before each measurement. The burning process was done to remove any organic residue that might be present on the ring, as presence of organic residue would affect the forces working on the ring. Data from the measurements were provided by associated software to the Sigma 700 Tensiometer. Measurements were done at room temperature ( $\approx 23\pm 2^\circ\text{C}$ ).

To successfully identify CMC, surface tension is measured at several surfactant concentrations. The surfactant concentration was automatically altered during the measurements by the apparatus, based on original surfactant concentration, and pre-set steps for addition of solvent. This results in a plot where surface tension is plotted against surfactant concentration. On a plot like this, abrupt change in

surface tension, and hence identification of CMC, can be found either from the plot itself (figure 3-2 A), or approximated by the use of trendlines (figure 3-2 B). Both methods was used in thesis to identify the surfactants CMC.

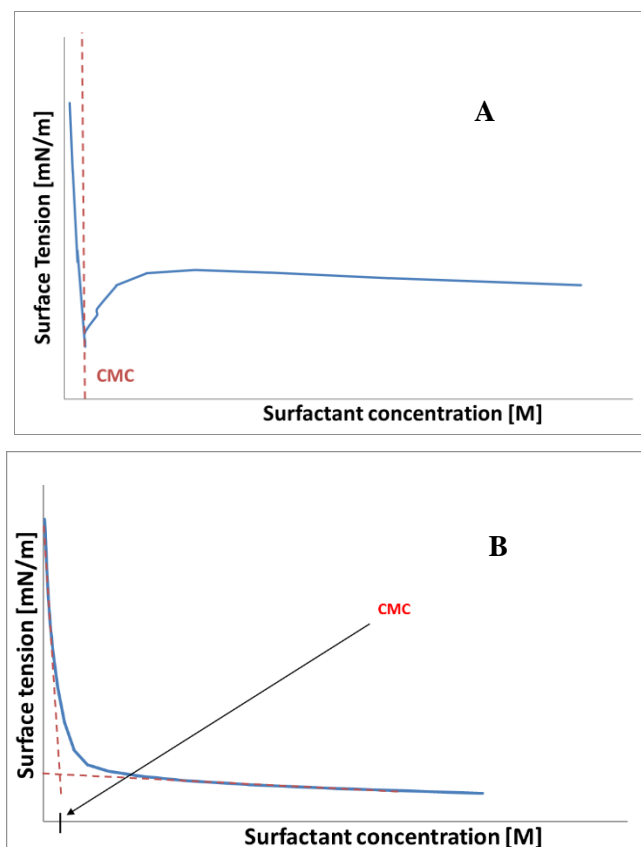


**Figure 3-2** Example of a curve of surface tension vs. surfactant concentration, where A) CMC is read directly of the plot, or B) CMC is identified by the use of trendlines.

#### *Source of error – Du Nüoy ring*

If the ring is covered by organic residue before the measurement is started, the residue will affect how the liquid clings to the ring. This will result in an incorrect surface tension measurement for the liquid, and thus an incorrect CMC. As the ring was cleaned and burned before each measurement this source of error is not believed to have affected the results in any way. However, when measuring CMC on SDS and AOT, up to three parallels were measured, with one off-set parallel for each surfactant. As one parallel showed an off-set, and the others were close to identical, the off-set parallel was discarded for both surfactants. The origin of the off-sets is unknown, but as it happened two times with two different surfactants, it can be assumed that it was a human-made error in the process of setting up the measurements that created the off-set.

During one of the measurements, a valve in the system responsible for emptying the sample container when changing surfactant concentration loosened from the system. This resulted in no liquid output,

and only input. The error caused the apparatus to overflow with water. As the ring is calibrated at a certain height, no useful data was found, and all the data in the given measurement were discarded. The valve was secured and put back in place after the measurement, and is not believed to have affected any of the other measurements.

### 3.2.2 Spinning Drop method

All interfacial tension measurements where the IFT is in the range of 0-10 mN/m, are done by the use of the Spinning Drop method. This is a method where a drop of the light phase is placed in a cylinder containing the heavy phase fluid, and spun at high rpm's. Apparatus used in this thesis is the Krüss Site 100 Tensiometer with Drop Analysis Software v.2.6.

Before each measurement the apparatus was cleaned with distilled water and acetone and then filled with the heavy phase by the use of a BD Plastipak 10mL syringe. The cylinder was then spun at 5000rpm to remove air bubbles from the system. A drop of the light phase was then injected into the cylinder with a Hamilton 1.0mL syringe. The system was then tilted to horizontal position so the light drop phase was placed approximately in the center of the spinning cylinder. Further, the rotational frequency was adjusted so the length of the drop was approximately 5 times the width.

During measurements, the rotating cylinder is surrounded by a circulating oil with an adjustable temperature, which made it possible to adjust the temperature of the system.

The spinning drop apparatus is shown in figure 3-3.

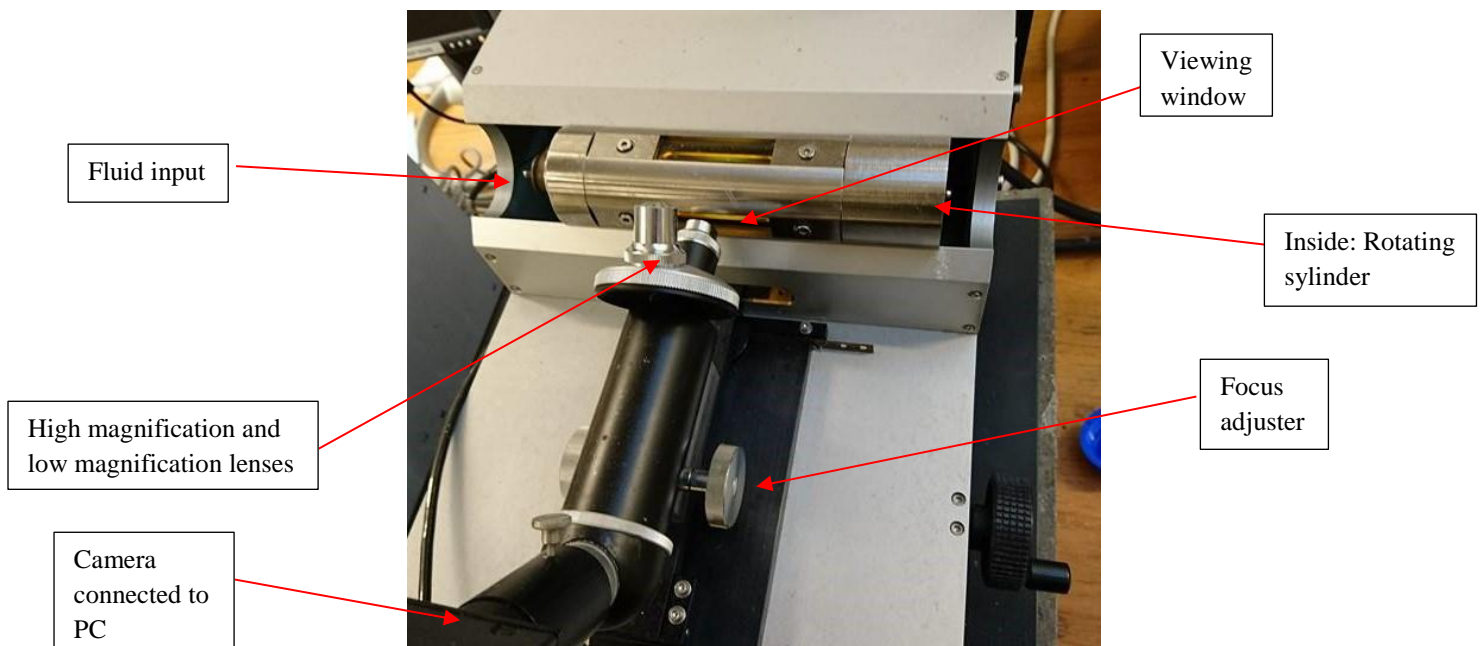
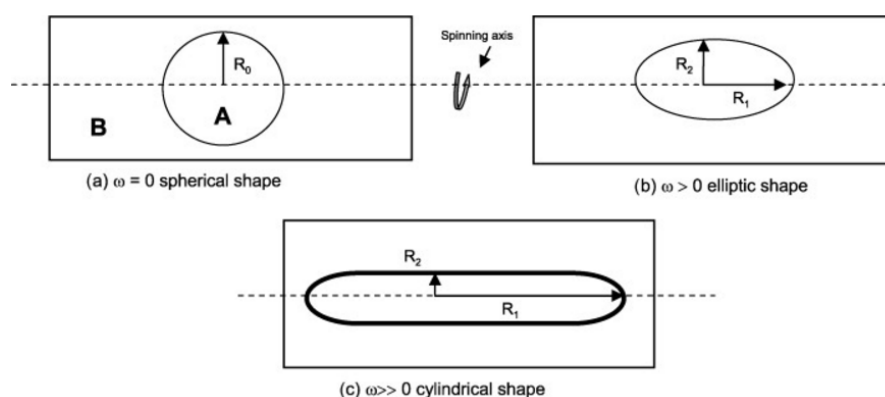


Figure 3-3 Setup for measurements of IFT with the Spinning Drop method.

With known densities ( $\Delta\rho$ ), drop shape and rotational frequency ( $\omega$ ), equation 3.2 are used to determine the IFT between the light and heavy phase depending on the spinning drops radii ( $r$ ). The equation is written by e.g. Viades-Trejo & Gracia-Fadrique [107]:

$$\gamma = \frac{r^3 \omega^2 \Delta\rho}{4} \quad (\text{Equation 3.2})$$

The calculations are done automatically by the supplied software, and the IFT is presented on associated computer, in units of mN/m. Figure 3-4 illustrates the drop behaviour inside the rotating cylinder as rotational frequency is increased.



**Figure 3-4** Illustration of deformation of a light drop when spun in presence of a heavy bulk phase by the spinning drop method.  $R_2$  is equivalent to variable  $r$  in equation 3.2. Illustration from [107].

The results from the spinning drop apparatus will vary according to which kind of measuring protocol that is used [108, 109]. In this thesis, the IFT has been recorded when equilibrium between the light- and heavy phase is reached. After the drop was injected, IFT was manually measured continuously as a function of time, as surfactants make IFT a time-dependant value [78]. When the IFT stabilized at a certain level, the drop was kept spinning for 1-2 additional minutes to ensure equilibrium. The IFT value was then recorded. Depending on the light phase/ heavy phase – system, the time until equilibrium varied from 2-3 minutes to 10-15 minutes.

After each measurement the spinning cylinder containing both the light and heavy phase was cleaned with distilled water, acetone and more distilled water. This was to ensure that there would not be any remaining fluids from either the aqueous or the oleic phase from the previous measurements inside the cylinder. The cylinder was then dried using compressed air before the next measurements were initiated.

### *Source of error – Spinning Drop*

The Krüss Site 100 Tensiometer with Drop Analysis software v.2.6 is supplied with a thermostat making it possible to adjust the temperature of an oil circulating around the system, and hence, the temperature of the system. The temperature-adjusting oil is at no point in direct contact with the fluids being measured. However, without any form of cooling applied, the temperature will rise to approximately 28°C, independently of which temperature set on the thermostat. For temperatures lower than 28°C, the apparatus can cool down using water. The water-cooling-application for the system was not known about until several measurements with the apparatus had been carried out. Therefore, most measurements carried out with the spinning drop are done at 28°C, instead of the ideal 23±2°C (room temperature). However, this is not believed to have affected the results to any significant degree.

### **3.2.3 Pendant Drop method**

For higher IFT's ( $\approx 10$  mN/m and higher), the spinning drop method is inaccurate and insufficient, and other methods are required. For measurements of IFT's higher than 10 mN/m the Pendant drop method is used. When measuring IFT between two liquids by use of the Pendant Drop, a drop of one phase is dispensed in the other phase by the use of a syringe. Apparatus used for the measurements is the Dataphysics OCA20 with the corresponding SCA20U software. A criteria for this method to work, is that the ambient phase is transparent, so a clear image of the drop shape can be analyzed by the software corresponding to the apparatus. An example of a crude dispensed in a brine as shown through the computer software are shown in figure 3-5. The apparatus has a piston that controls drop volume attached to a syringe and a homogeneous light source to create a clear drop shape for the software to measure. The exact setup can be seen in figure 3-6.

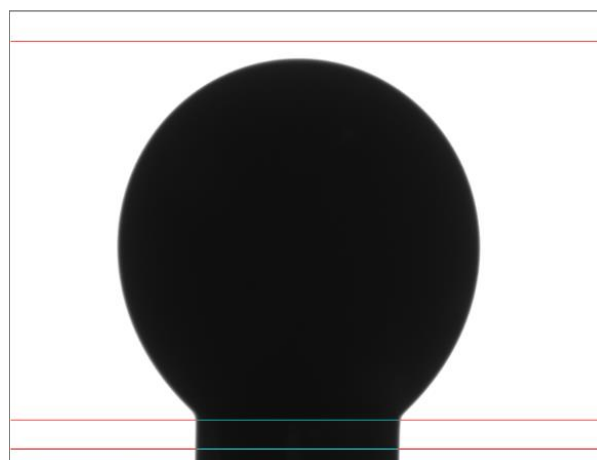


**Figure 3-5** Example of measurement done with pendant drop as represented by the apparatus software. The example shows a drop of Crude C submerged in a brine. The software uses the density differences as well as the curvature of the drop to calculate IFT.

Calculations of IFT are then based on the curvature of the drop, density difference between light- and heavy phase, as well as the effect of gravity [110]. Calculations are done by use of equation 3.3, where the effect of gravity is accounted for by measuring the drop shape. The equation is written by e.g. Berry et.al. [9].

$$\Delta P = (P_i - P_o) = \sigma \left( \frac{1}{R_1} + \frac{1}{R_2} \right) = \Delta P_0 - \Delta \rho g z \quad (\text{Equation 3.3})$$

Where  $\sigma$  is the interfacial tension,  $\Delta P$  the Laplace pressure across the interface,  $\Delta \rho$  the density difference, and  $R_1$  and  $R_2$  the principal radii of the drop.  $\Delta P_0$  is the reference pressure [9].

The oil phase (a crude or an alkane) was used as the drop phase in the measurements, as the crudes are not transparent. As the oil phases have a lower density than the heavy phases (water, brine or surfactant + brine), an inverted needle was used to submerge a drop of the light phase in the heavy phase to create a measurable drop. The needle was attached to a 1.30mL Braun syringe. The heavy phase (water, brine or surfactant + brine) was kept in a special cuvette with optical glass so the image read by the software would not be altered by how the light hit the glass.

When using an inverted needle, it is crucial that the needle is completely free of all organic substances. Presence of organic compounds on the needle will lead to the oil-drop having an affinity to the needle-tip. This in turn makes the drop cling to the needle, rather than expand in the heavy phase and create a measurable drop. To avoid this, the needle was thoroughly washed between each measurement with a 50/50 mix of toluene and ethanol.

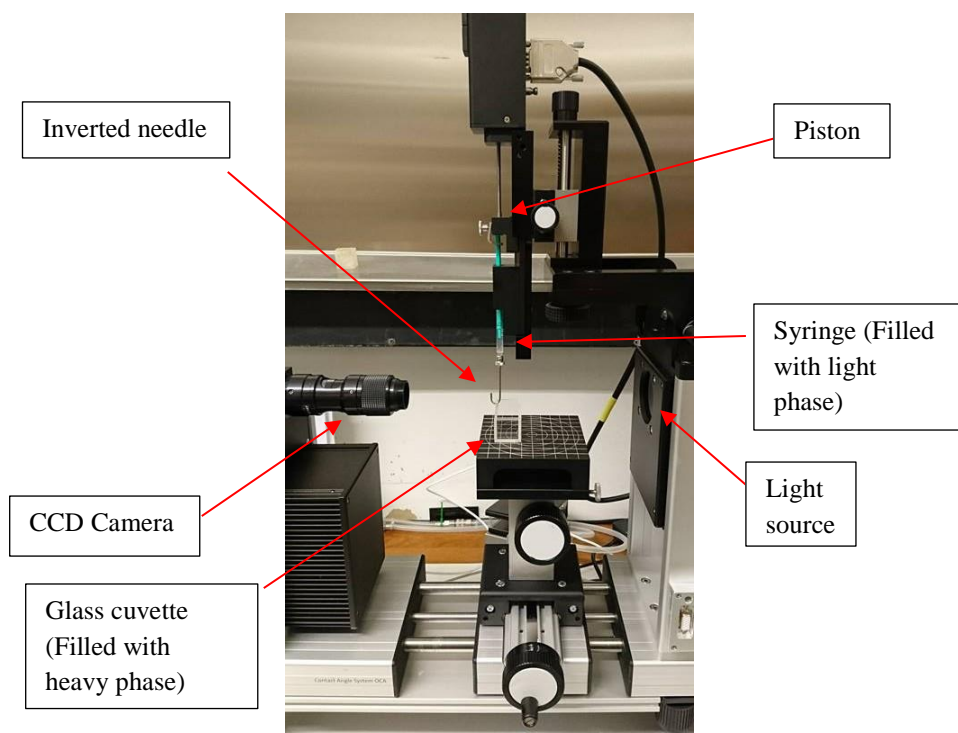


**Figure 3-6** Setup for IFT measurements with Pendant Drop method.

For each pendant drop measurement, there was a 5-10-minute wait for the drop phase to equilibrate with the bulk phase. When equilibrium was reached, the IFT value was recorded.

*Source of error – Pendant drop*

At some low IFT's, the light phase would flow out of the pipette without being able to create a full drop shape. In these cases, the IFT was measured with the spinning drop method instead.

The glass-cuvette used to contain the heavy phase liquid was about 2cm in height. This would in some cases limit the size of the drop, which in terms could have affect the drop shape parameter, used by the software to calculate IFT. This may to a small degree have affected the precision of the measurements, but not the significance of them.

The drop is also sensitive to vibrations and noises near the apparatus. Noise and vibrations caused the drop to vibrate. A vibration will alter how the apparatus reads the drop shape. However, after the noise and/or vibration stopped, the drop quickly reached equilibrium with the heavy phase again. As the IFT was taken after the noise and/or movements were gone, this is not believed to have had any influence on the results.

### 3.3 Light absorption

#### 3.3.1 Molecular bonding theory

If the atoms in a molecule are bonded with covalent bonds, there is an overlap between their electron orbitals. An electron orbital is considered to be a “cloud” surrounding the nucleus of the atom, where the electron(s) is most likely to be found. The type of overlap is called either a  $\sigma$ -bond or a  $\pi$ -bond. The  $\sigma$ -bonds are a covalent bond where there is an end-to-end overlap of the electron orbitals. A  $\pi$ -bond on the other hand, is a side-to-side overlap between the orbitals, where the distance to the nucleus is longer than for a sigma-bond. The longer distance means that a lower amount of energy is needed to move, or excite the  $\pi$ -electrons. All single covalent bonds are sigma-bonds, while double bonds have one  $\sigma$ - (end-to-end) and one  $\pi$ - (side-to-side) bond. A triple bond consists of one  $\sigma$ - and two  $\pi$ -bonds [111]. An example of the types of bonds in an ethene molecule are shown in figure 3-7.

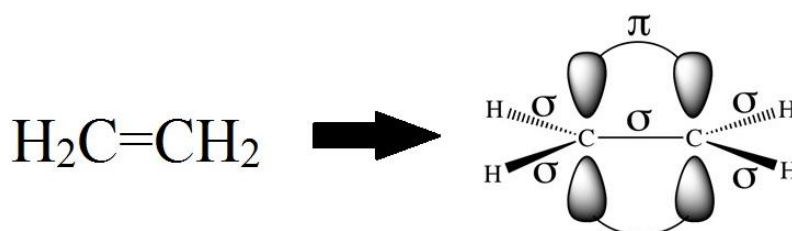


**Figure 3-7** Illustration of the types of bonds present in ethene. The double bond consists of one sigma- and one pi bond. The electrons in the pi-bond are further away from the nuclei and are more easily excited. Redrawn from [112].

The type of bonds in a molecule are important in terms of how the molecule absorbs light, and at which wavelength, as the energy needed to excite an electron in a  $\pi$ -bond is lower than for a  $\sigma$ -bond [113].

#### 3.3.2 Molecular absorption of light

A molecule absorbs UV-light as the light excites electrons in the molecule to a higher state of energy. The energy needed to excite an electron is reversely proportional to the wavelength of the incoming light. This follows from the energy ( $E$ ) of a photon being equal to Planck's constant ( $h$ ) times the photon's wave frequency ( $\nu$ ). The frequency is a ratio between the speed of light ( $c$ ) and the wavelength ( $\lambda$ ). The equation for this is shown in equation 3.4. This concept is generally accepted, and further explained by Becchi & D'Elia [114] among others.

$$E = h\nu = \frac{hc}{\lambda} \quad (\text{Equation 3.4})$$



In other words, light at a given wavelength will have a given energy [115]. Should this energy match up to the required energy to excite the one or more of the electrons in the molecule, the light will be absorbed. These energy “jumps” of the electrons a molecule, depend on the type of bonds between the atoms in the molecule.

The part of a molecule that is eligible for absorbing UV-light due to the atomic structure, is called the chromophore of the molecule [116]. The benzene-ring is the chromophore in SDBS, and due to its conjugated  $\pi$ -bonds, the electrons need a relatively low amount of energy to be excited. An absorbance peak can be measured at  $\approx 225\text{nm}$  in a compound containing a benzene ring by spectrophotometry [117]. The other two surfactants, SDS and AOT, do not have chromophores which absorb light in the same fashion as SDBS. That being said, the ester group in AOT do absorb UV light at  $\approx 205\text{nm}$  [118] due to its  $\pi$ -electrons. However, the relative intensity of the absorption is of a such small degree [119], that when measured, even at high surfactant concentrations, no absorption is detectable.

The straight hydrocarbon chains in the surfactant molecules, which are common for all three surfactants, do absorb light, but only at low wavelengths. This is because the C-atoms in the chain are bonded only with  $\sigma$ -bonds. The electrons in the  $\sigma$ -bonds demand, as mentioned, a higher energy to get excited [120], and thus absorb light at a lower wavelength than the regular Spectrophotometer can measure (190-800nm) [121]. This is the reason why standard curves and UV-measurements were only done for SDBS in this thesis.

### 3.3.3 UV-spectrophotometry

UV-spectrophotometry uses absorption of UV-light to determine the concentration of a certain compound in a solution. When the light passes through the solution, a given amount of light will be absorbed by the dispersed molecules, should the molecules possess a chromophore that can absorb light in the range of wavelengths in the incoming light. The intensity of light exiting the solution will be lower than the light entering, due to absorption. The difference between the intensities is measurable. Given the measured difference, the concentration of the molecules which possess the chromophore can be calculated from Beers Law, as explained by e.g. Ball [122]:

$$A = \log_{10} \frac{I_0}{I} = \epsilon * b * c \quad (\text{Equation 3.5})$$

Where  $I_0$  and  $I$  is the intensity of the light entering the sample and the light exiting the sample respectively,  $b$  the length of the sample,  $c$  the concentration of the compound that can absorb light and  $\epsilon$  the molar absorptivity of the compound.

In theory, given this relationship between absorption and concentration, a linear plot can be created correlating concentration and absorbance for a specific compound. Given such a plot, an unknown concentration of the compound in a solution can be determined by measuring the amount of UV-light absorbed in the solution. Illustration of Beers Law and example of a standard curve correlating concentration an absorption can be seen in figure 3-8.

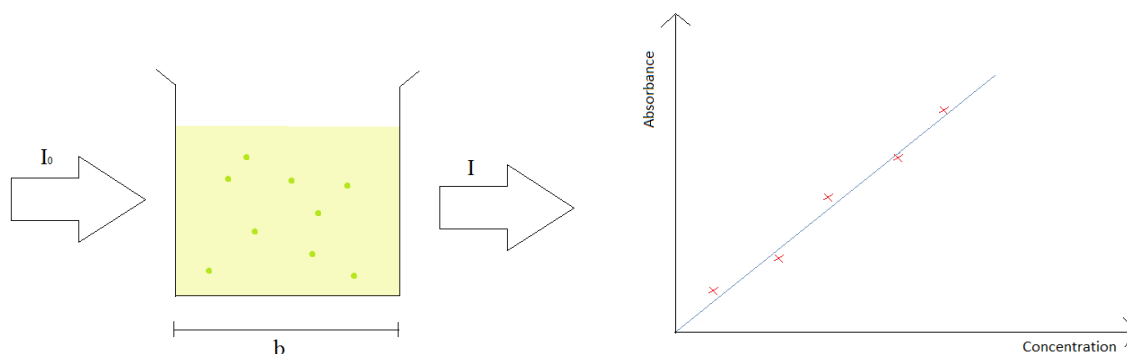


**Figure 3-8** To the left: Illustration of Beers law in practice. To the right: illustration standard curve correlating concentration with absorbance.

Beers Law as illustrated is only valid for low concentrations. If the concentration of the compound exceeds a certain amount, total absorption will be too high for the apparatus to measure a valid result. This happens as higher concentrations of molecules will lead to the molecules interacting with each other, thus changing the molar absorptivity of the compound [122]. If a high, unknown concentration is to be determined in a solution, the sample needs to be diluted down to a lower measurable concentration to create a valid result. As the relationship between absorbance and concentration is linear, the result can then be scaled up to find the original concentration before the dilution was made.

Appratus used for the measurements of absorbance in this thesis are the VWR UV-3100PC Spectrophotometer. A quartz cuvette, neutral even at high energy (low wavelengths) light was used. Before all measurements a benchmark absorbance was set, measuring the light intensity through a sample of pure solvent. All measurements were performed at room temperature ( $\approx 23\pm 2^\circ\text{C}$ ).

#### *Source of Error – UV spectrophotometry*

Type of cuvette/cell used for UV measurements is critical. Before the standard curves were made, several attempts were conducted without satisfactory results. The reason was the disposable plastic cuvettes used in the failed attempts. These types of cuvettes will not interfere with the incoming light, given that the light is in the visible spectrum (380-780nm). As the desired spike in absorbance was at 223nm, the apparatus gave noisy and inconsistent readings as this was outside the range of functional wavelengths for the disposable plastic cuvettes (380-780nm) first used. However, fused quartz

cuvettes will not interfere with the incoming light for wavelengths down to 190nm. After the plastic cuvettes were exchanged for quartz cuvettes, the standard curves were created as expected.

After each measurement, the quartz cuvette was cleaned with acetone and distilled water to avoid any residue that could affect the results, as residue could absorb incoming light. The cuvettes were washed carefully, as any scratches or marks on the glass could interfere with the light going through the sample.

### **3.4 Volumetric calculations**

#### **3.4.1 Solubilisation parameters**

Surfactant solutions with constant surfactant concentration respective to each surfactant, were mixed with NaCl. 10mL of the brine/surfactant solution and 10mL heptane was mixed in a 20mL glass tube (Water/oil ratio (WOR) = 1:1). The samples were then shaken carefully and left for 2-3 weeks at room temperature ( $\approx 23\pm 2^\circ\text{C}$ ) to reach equilibrium. After equilibrium was reached, volumes of oil solubilized in water and water solubilized in oil were measured. The height, and thus the volumes, of the different phases solved in the samples were measured with a standard ruler. The volume of each phase was calculated using the measured height, and converted to solubilisation parameters using equations showed in section 2.5.2.

#### *Source of error – Solubilisation parameter*

Some of the glass tubes were not properly sealed, leading to vaporization of the oil phase during the time to reach equilibrium. This did not change the surfactant concentration in the oil phase, as only pure alkane had vaporized and no surfactant. As soon as it was realized that the sealing was not sufficient, the samples were filled with oil to reach original oil volume. The samples in question were once again softly shaken, and left to reach equilibrium. The seals of the samples were changed, to prevent further vaporization. This source of error should in theory not have affected the measured surfactant concentration in either the oil- or water phase.

It should also be noted that in the context of comparing results from the solubilisation parameters, UV- measurements and the IFT measurement, the solubilisation parameter-measurements are done at room temperature of ( $23\pm 2^\circ\text{C}$ ), as opposed to the IFT measurement where the temperature was kept at  $28^\circ\text{C}$ . A direct comparison will therefore in theory have an off-set due to the difference in temperature.

## 4 Results

### 4.1 Determination of the surfactants' CMC

CMC for each of the three surfactants was successfully identified. All obtained CMC's were without significant deviation from literature values. An overview of the CMC's measured and corresponding literature values can be found in table 4-1. Plots of ST against surfactant concentration used to obtain CMC's are shown in appendix B.1.

**Table 4-1** Overview of measured CMC's for the three different surfactants.

	Literature CMC in 0.02M NaCl [M]	Measured CMC in 0.02M NaCl [M]
<b>SDS</b>	3.4E-03 <sup>[123]</sup>	2.0E-03
<b>SDBS</b>	1.9E-03 <sup>[124]</sup> , 1.7E-03 <sup>[51]</sup>	2.0E-03
<b>AOT</b>	1.1E-03 <sup>[31]</sup>	2.6E-03

## 4.2 The COB system

### 4.2.1 Effect of variation in brine salinity

The effect of change in salinity in the brine was investigated by measuring the IFT between the two crude oils, and brines with different salinities without the presence of a surfactant. Only NaCl was used to change salinity of the brine, hence salinity is represented as NaCl concentration. No further measurements could be done above 5.0M NaCl as the water became saturated with salt and a further increase in salinity was not possible. Results are shown in figure 4-1.

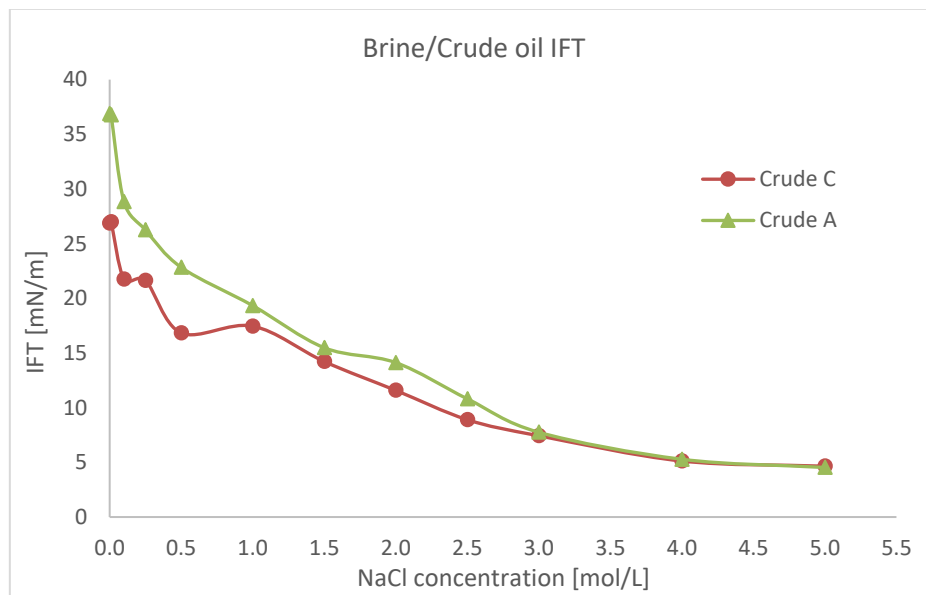


**Figure 4-1** Interfacial tension between Crude oils and brines at different salinities without the presence of a surfactant.

The main trend in figure 4-1 for both crude oils is a decrease in IFT with increasing salinity. Despite that their IFT's against distilled water differs, the IFT's seem to converge to approximately the same value.

### 4.3 The SCOB system

#### 4.3.1 Effect of variation in surfactant concentration

IFT for each SOB system was measured at three different surfactant concentrations. Surfactant concentrations were chosen to be  $1/10 \times \text{CMC}$ ,  $\text{CMC}$  and  $10 \times \text{CMC}$ . All surfactant solutions were made in a 0.02M NaCl brine. For SOB systems with  $\text{IFT} > 10\text{-}12 \text{ mN/m}$ , the pendant drop method was used to determine IFT. For  $\text{IFT} < 10 \text{ mN/m}$  the spinning drop was used. Comparison of IFT for the systems at the same relative concentration of surfactant is shown in figure 4-2. The relationship between IFT and surfactant concentration for each surfactant is shown in figure 4-3 to 4-5. Measurements are made at  $28^\circ\text{C}$ .

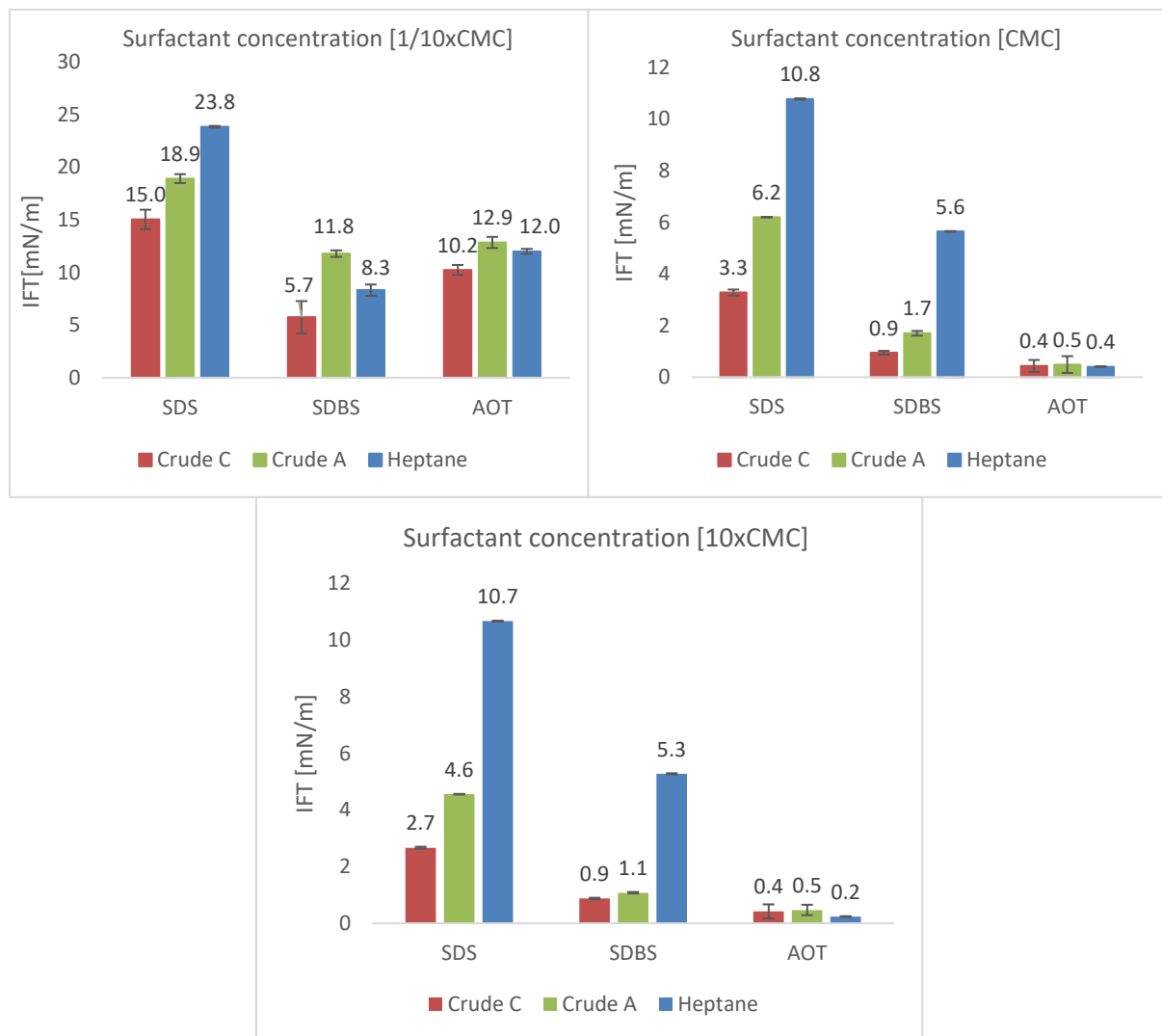


**Figure 4-2** Difference in interfacial tension for the three surfactants with regards to oil phase at surfactant concentrations of  $1/10 \times \text{CMC}$ ,  $\text{CMC}$  and  $10 \times \text{CMC}$

With regards to surfactant efficiency, it is clear that AOT is the most efficient surfactant, i.e. the surfactant that provides the lowest IFT at concentrations  $\text{CMC}$  and  $10 \times \text{CMC}$ , whilst SDBS is most efficient at  $1/10 \times \text{CMC}$ .

Further, figures 4-3 to 4-5 indicates that all the SOB systems to some extent exhibit the same behaviour. The difference in IFT for surfactant concentrations at CMC and 10xCMC is small compared to the concentration at 1/10xCMC. This is as expected according to the effect of surfactant concentration explained in section 2.3.

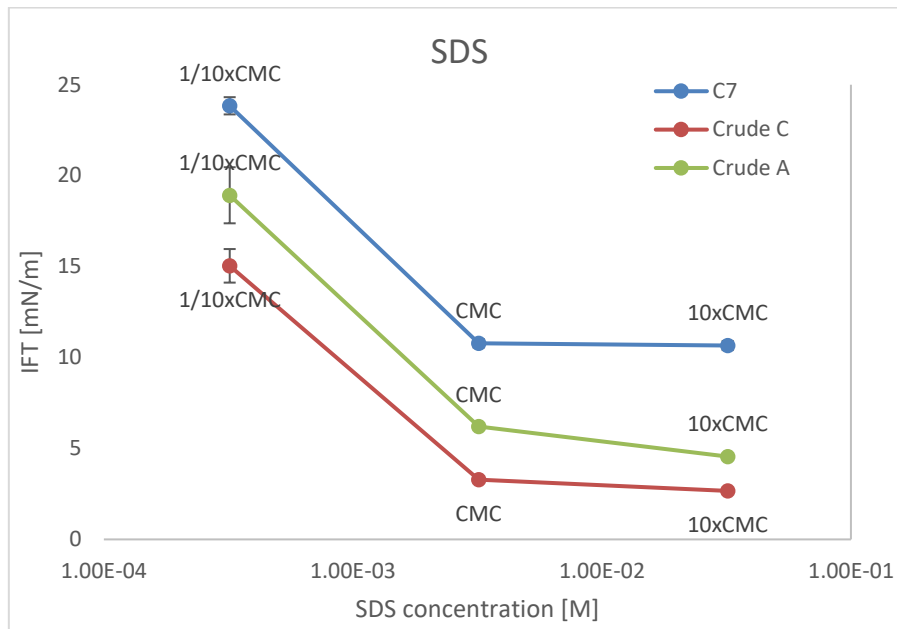


**Figure 4-3** Change in IFT for three different SOB systems with regards to concentration of SDS. Each data point represents 1/10xCMC, CMC and 10xCMC respectively.

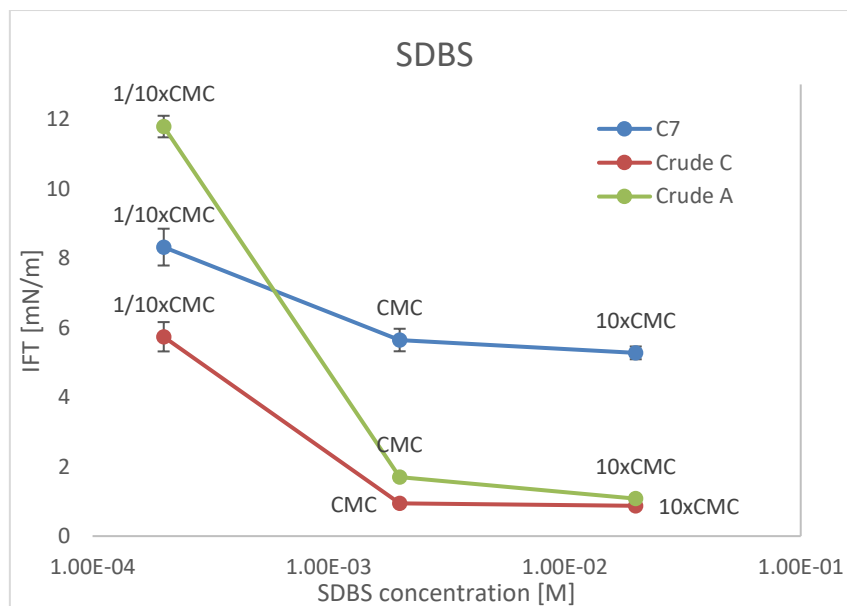


**Figure 4-4** Change in IFT for three different SOB systems with regards to concentration of SDBS. Each data point represents 1/10xCMC, CMC and 10xCMC respectively.

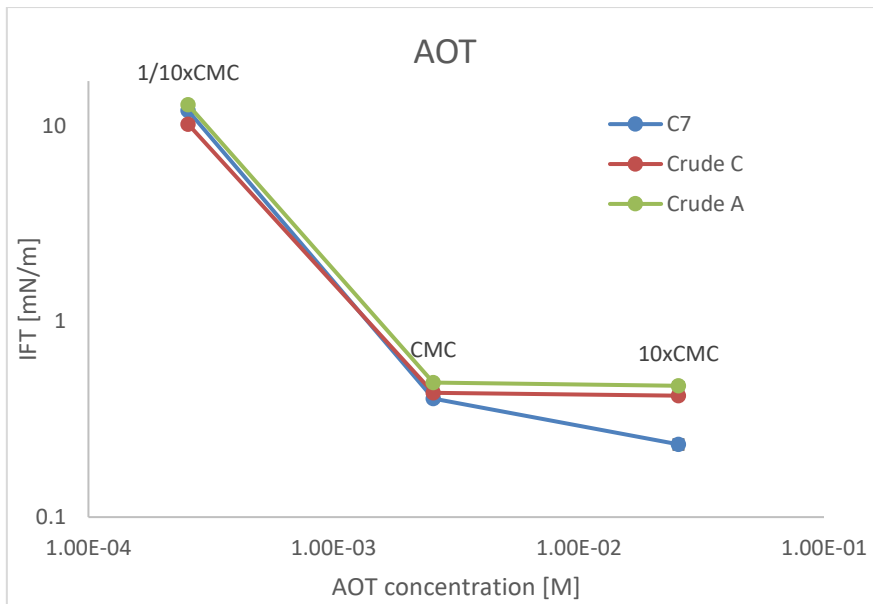


**Figure 4-5** Change in IFT for three different SOB systems with regards to concentration of SDBS. Each data point represents 1/10xCMC, CMC and 10xCMC respectively.

Common for all three surfactants is that the IFT for each system has an abrupt decrease from surfactant concentration of 1/10 CMC to CMC. The IFT furthermore remains quite constant when the surfactant concentration is increased from CMC to 10xCMC.



### 4.3.2 Effect of variation in salinity

Each surfactant was tested against 4 different oils, 2 crude oils and 2 n-alkanes, to identify the system's optimal salinity. Optimal salinity would be indicated by a minimum in IFT. IFT's for the systems are plotted against salinity, given in mol per litre of NaCl. Surfactant concentrations are kept constant at 10xCMC. Figure 4-6 to 4-8 shows the obtained results.

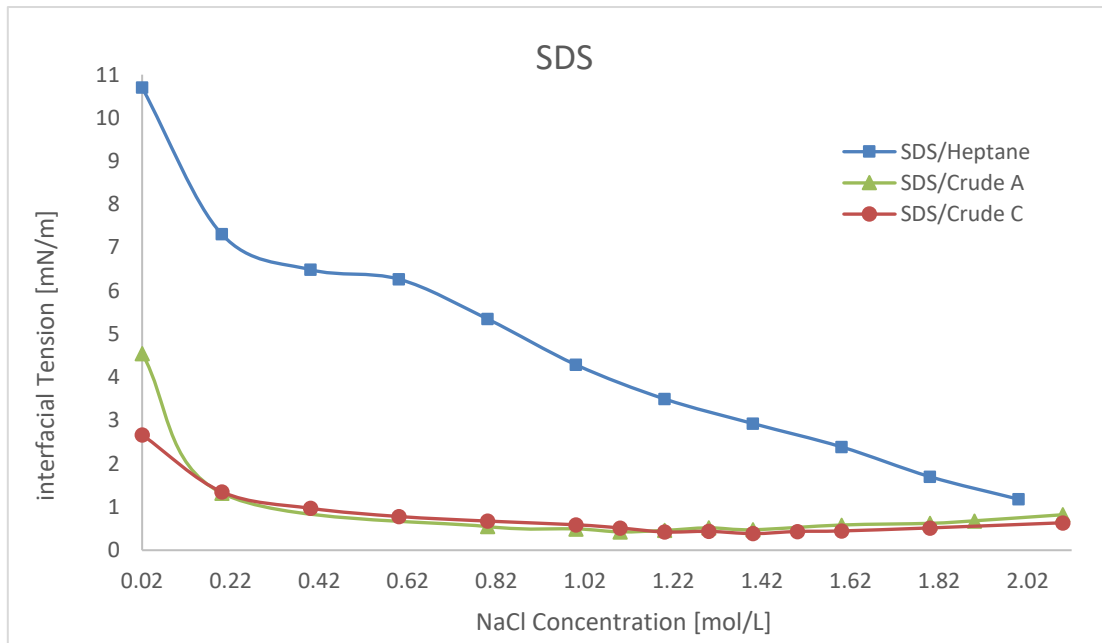


Figure 4-6 Variation in IFT at different salinities to identify optimal salinity for systems containing different oils and SDS.

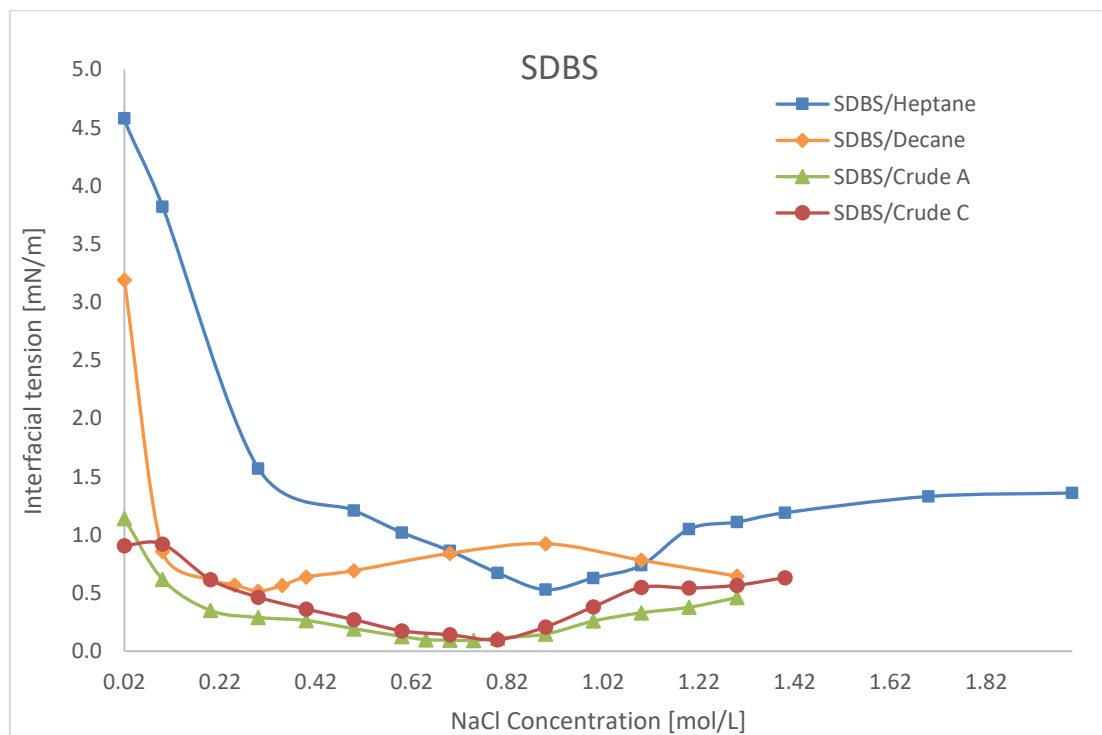
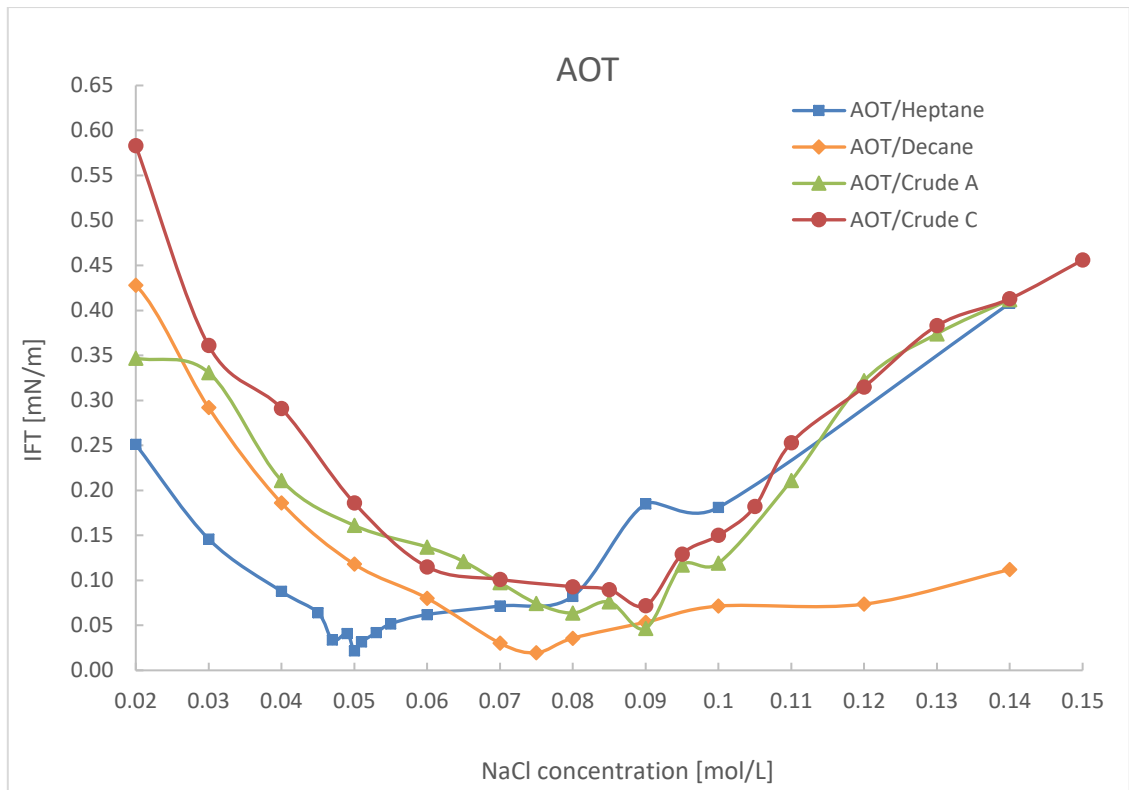


Figure 4-7 Variation in IFT at different salinities to identify optimal salinity for systems containing different oils and SDBS.



**Figure 4-8** Variation in IFT at different salinities to identify optimal salinity for systems containing different oils and AOT.

### *SDS*

For systems containing SDS, measurements were only conducted on 3 oils. SDS exhibited the highest IFT's in the measured systems. Evaluation of the optimal salinities was not possible as the optimal salinities were not found. Before optimal salinity could be reached, the high amounts of solids in the solutions caused solid surfactant to precipitate out of the solution, changing surfactant concentration. In addition, as a result of the precipitation the solution too unclear for the apparatus to identify a measurable drop.

### *SDBS*

For systems containing SDBS, an optimal salinity was found for all four systems. The optimal salinities identified are 0.3M for SDBS/decane, 0.9M for SDBS/heptane, 0.75M for SDBS/Crude A and 0.80M for SDBS/Crude C. All curves show that the IFT decreases with increasing concentration of NaCl, until optimal salinity is reached, where the IFT convergely increase. These results are according to theory.

### *AOT*

Optimal salinities were found for all four AOT systems. Similar to the curves for SDBS, all four systems decrease with increasing IFT up to optimal salinity. After optimal salinity was reached, the

IFT's increased with increasing NaCl concentration. The optimal salinities are 0.075M for AOT/decane, 0.05M for AOT/heptane, and 0.08M for both AOT/Crude C and AOT/Crude A.

To summarize, the optimal salinity (OS) was found for all systems containing SDBS and AOT, but only for the crudes when surfactant SDS was used. The optimal salinities and corresponding IFT's for the surfactant systems are summarised in table 4-2.

**Table 4-2** Overview of the optimal salinities and IFT's found for each surfactant/brine/oil system. Neither the optimal salinities nor the corresponding IFT shows an uncertainty as only one parallel was measured during the salinity screenings.

Oil	SDS		SDBS		AOT	
	OS [M]	$\sigma$ [mN/m]	OS [M]	$\sigma$ [mN/m]	OS [M]	$\sigma$ [mN/m]
<b>C7</b>	-†*	-*	0.90	0.529	0.050	0.0216
<b>C10</b>	-*	-*	0.30	0.517	0.075	0.0196
<b>Crude A</b>	1.2**	0.422**	0.75	0.0928	0.080	0.0637
<b>Crude C</b>	1.1**	0.424**	0.80	0.0991	0.090	0.0720

---

\* Optimal salinity could not be found as the surfactant precipitated to a such degree that the surfactant concentration most likely changed, as well as the solution being too unclear to identify a drop shape in the apparatus.

\*\* IFT minimums were identified for the crudes, however due to the large degree of precipitation the OS's are not believed to be valid.

#### 4.3.2.1 IFT / Solubilisation parameter- correlation

Phase study samples for the AOT/heptane and SDBS/heptane systems were prepared over a range of salinities, including optimal salinity obtained from the spinning drop method. As no optimal salinity was found for the SDS/Heptane system by IFT measurements, phase studies, and hence, solubilisation parameters, are only calculated for AOT and SDBS. Ideally, the lowest measured IFT and the crossing point of the solubilisation parameters would be at the same salinity, as the surfactant solubility of each phase would be equal at optimal salinity. This is shown in figure 4-9 and 4-10 for SDBS, and in figure 4-11 and 4-12 for AOT.

#### SDBS

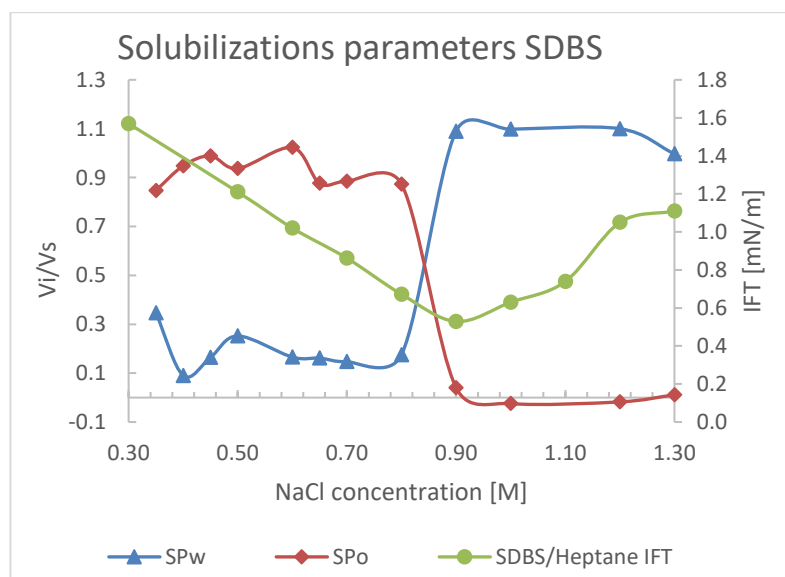


**Figure 4-9** (Left) Solubility parameters for water and oil for SDBS/Heptane system calculated by volume of each phase solved in the other. The IFT measured with spinning drop is also included in the plot.

**Figure 4-10** (Right) Phase studies for SDBS. The amount of water solubilised in oil, and oil solubilised in water vary with salinity. The solubilisation of each phase in the other is seen by the visible interface between the liquids changing with increasing salinity. NaCl concentration is indicated on the figure.

## AOT

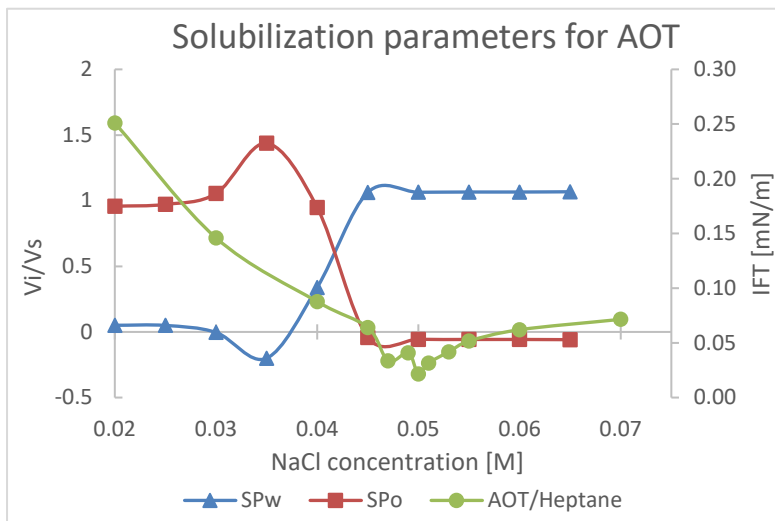


**Figure 4-11** (Left) Solubilization parameters for water and oil for AOT/Heptane system calculated by volume of each phase solubilised in the other. The IFT measured with spinning drop is also included in the plot.

**Figure 4-12** (Right) Phase studies for AOT. The amount of water solubilised in oil, and oil solubilised in water varies with salinity. The solubilisation of each phase in the other is seen by the visible interface between the liquids changing with increasing salinity. NaCl concentration is indicated on the figure.

The optimal salinities found by IFT matches the optimal salinities found by solubilisation parameters. For SDBS the optimal salinity is found to be at 0.90M NaCl with the spinning drop, and 0.84M NaCl with solubilisation parameters. For AOT the optimal salinity is in close proximity by both methods, as the optimal salinities are found to be 0.050M NaCl with the spinning drop and 0.043M with solubilisation parameters.

#### 4.3.2.2 IFT / Surfactant partitioning - correlation

Standard curves for the relation between surfactant concentration and absorbance were made for SDBS in water- and oil phase. This was only done for the SDBS/heptane, as there are no chromophores in SDS or AOT that absorb light in the UV-vis spectrum, and the phase studies only were made with heptane. The standard curves created can be seen in appendix B.2. Based on absorbance measurements and use of the standard curves, surfactant concentration in the oil- and water phase at different salinities was calculated by measuring absorbation. Figure 4-13 shows the surfactant concentration in both oil- and water phase as function of salinity of the brine. The salinity where the concentration in the oil- and water phase is equal, is where the surfactant solubility is the same in both phases, ergo the optimal salinity. The secondary y-axis shows the IFT measurements for SDBS/heptane at different salinities done by the spinning drop method. In theory, the lowest point on the curve should correspond to the crossing of the concentration curves.

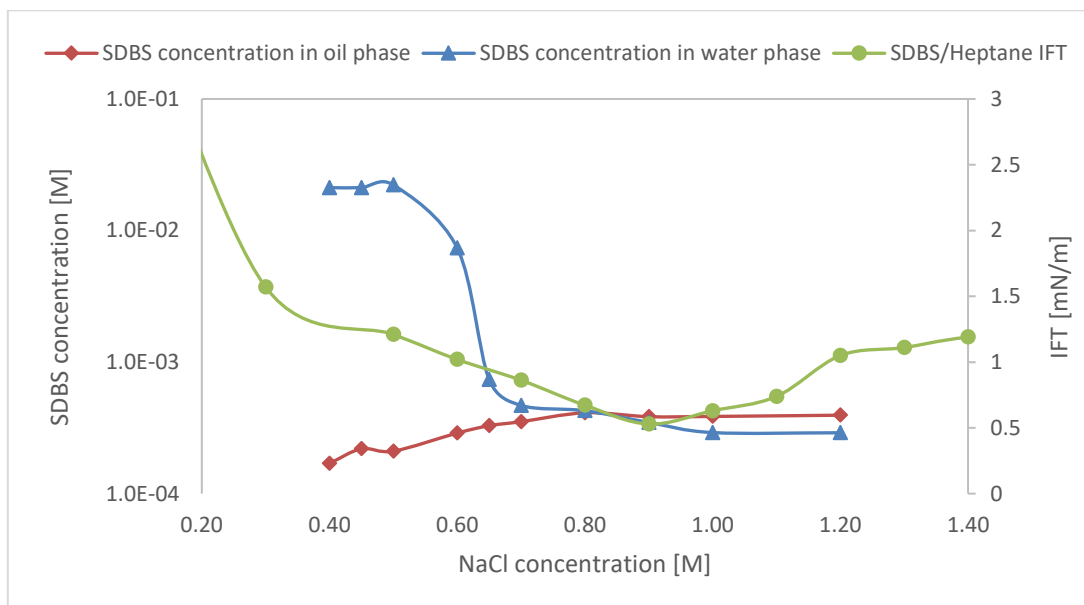


**Figure 4-13** Concentration of SDBS in water- and oil phase. The concentrations are equal approximately at the minimum measured IFT.

The optimal salinity found by IFT measurements match the crossing point of the concentration curves, with only a slight deviation. Optimal salinity found by IFT measurements is at 0.90M NaCl, whilst the optimal salinity found from concentration in the phase studies gives an optimal salinity at approximately 0.83M NaCl – the same optimal salinity as found by the method of solubilsation parameters.

### 4.3.2.3 Effect of ion valence

Variations in IFT by addition of ions with difference valence was studied. Ionic strength was kept constant at 0.02 with variation in  $\text{Ca}^{2+}/\text{Na}^+$  ratio. Note that the x-axis is the ratio between  $\text{Ca}^{2+}$  and  $\text{Na}^+$ , not mole fraction. Ionic strength was chosen to be 0.02, as this is the same ionic strength used in the measurements where surfactant concentration was varied (section 4.3.1), and later during the temperature measurements (section 4.3.4). Surfactant concentration is kept at 10xCMC and temperature at 28°C. Results are shown in figure 4-14 to 4-16.

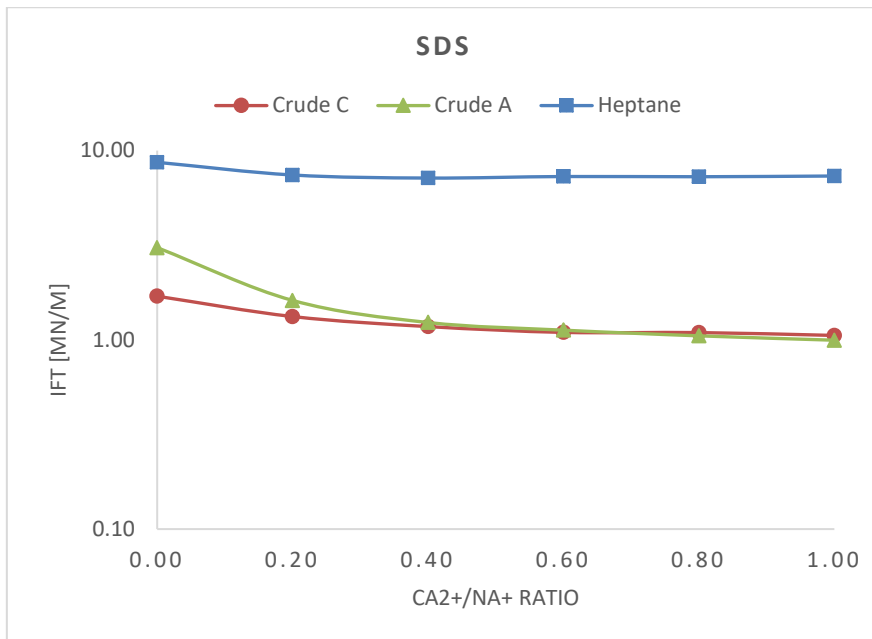


Figure 4-14 Variation in IFT with increasing  $\text{Ca}^{2+}/\text{Na}^+$  ratio for SDS.

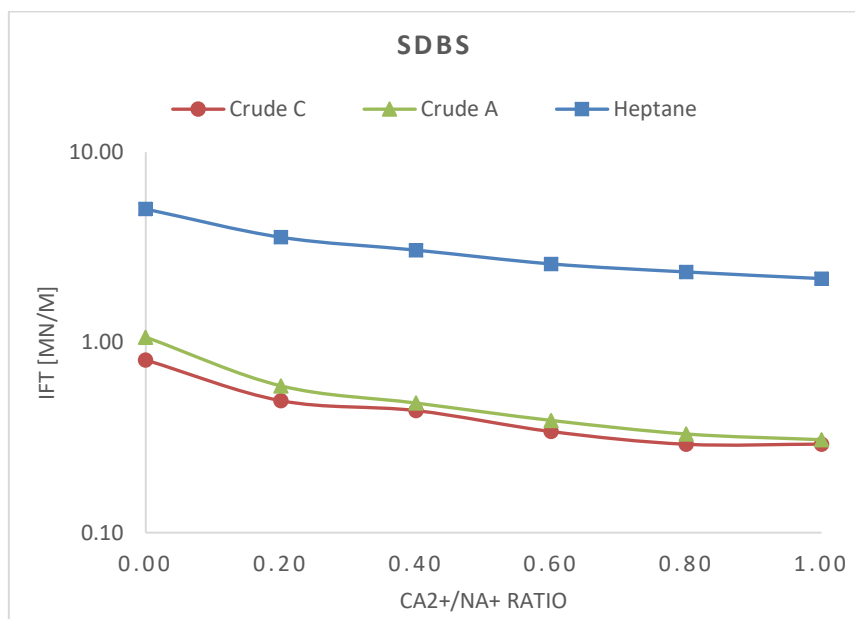
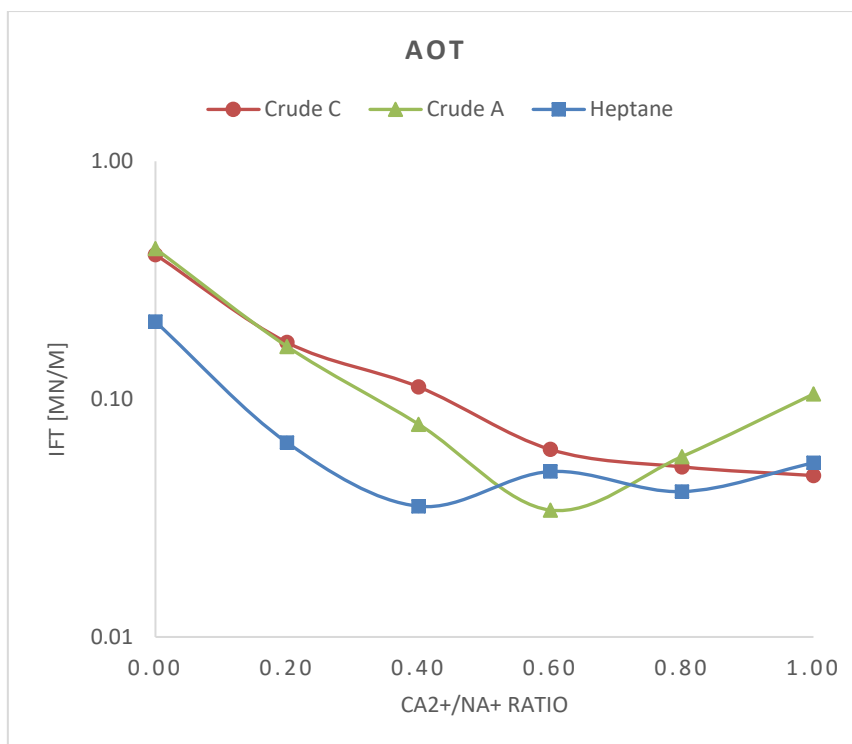


Figure 4-15 Variation in IFT with increasing  $\text{Ca}^{2+}/\text{Na}^+$  ratio for SDBS.



**Figure 4-16** Variation in IFT with increasing Ca<sup>2+</sup>/Na<sup>+</sup> ratio for AOT.

Figure 4-14 to 4-16 shows that the IFT decreases for all SOB systems with increasing Ca<sup>2+</sup>/Na<sup>+</sup> ratio. A minimum ratio is found for AOT against heptane and Crude A. The IFT increases after this minimum with increasing salinity, due to the decrease in surfactant solubility as amount of calcium rises. At a higher ratio of Ca<sup>2+</sup>/Na<sup>+</sup>, the SDS and SDBS systems might decrease to a minimum as there is a decreasing trend in IFT with Ca<sup>2+</sup>/Na<sup>+</sup> ratio. See further work.



### 4.3.3 Effect of variation in pH

Change in pH was investigated at three different salinities for AOT and SDBS. No measurements was done on SDS, as no optimal salinity was identified. Three benchmark salinities was chosen for the pH measurements per surfactant – a lower salinity (LS), the optimal salinity (OS, varies with type of oil phase) and an upper salinity (US). Table 4-3 lists the brine salinities for each SOB system at LS, OS an US. Each salinity is given as concentration of NaCl. At each salinity, IFT between the surfactant/brine solution and oil was measured at a pH of 3, 6 and 9. The surfactant concentrations was kept at 10xCMC, and measurements are done at 28°C. Results are shown in figures 4-17 and 4-18.

**Table 4-3** Overview of salinities used for each surfactant on each oil at LS, OS and US.

	AOT				SDBS			
	<i>Heptane</i>	<i>Decane</i>	<i>Crude A</i>	<i>Crude C</i>	<i>Heptane</i>	<i>Decane</i>	<i>Crude A</i>	<i>Crude C</i>
<b>LS [M]</b>	0.02	0.02	0.02	0.02	0.02	0.02	0.02	0.02
<b>OS [M]</b>	0.050	0.075	0.080	0.090	0.90	0.30	0.75	0.85
<b>US [M]</b>	0.14	0.14	0.14	0.14	1.30	1.30	1.30	1.30

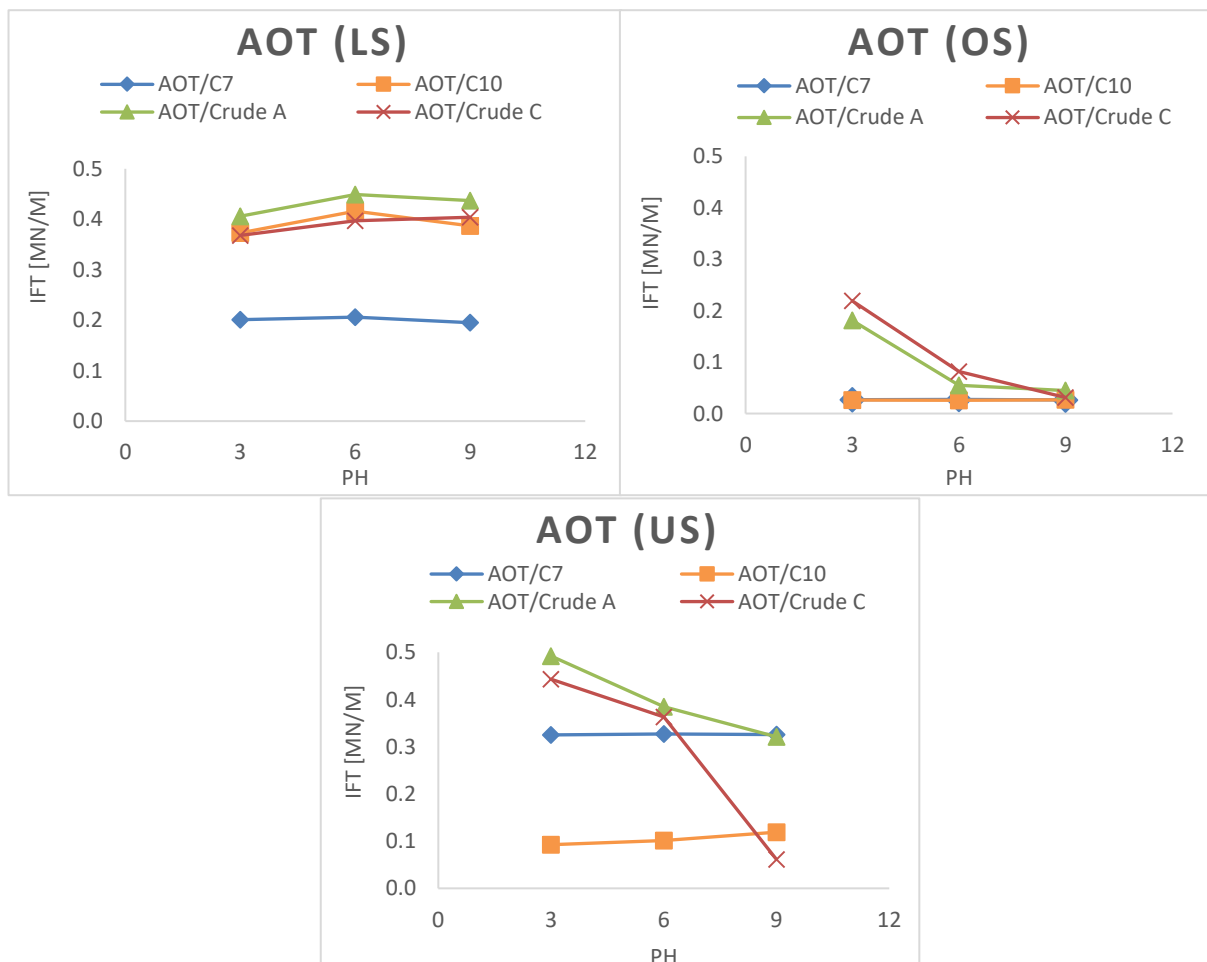


**Figure 4-17** Change in IFT as a function of pH at LS, OS and US for AOT. C7 and C10 curves are close to identical at optimal salinity.

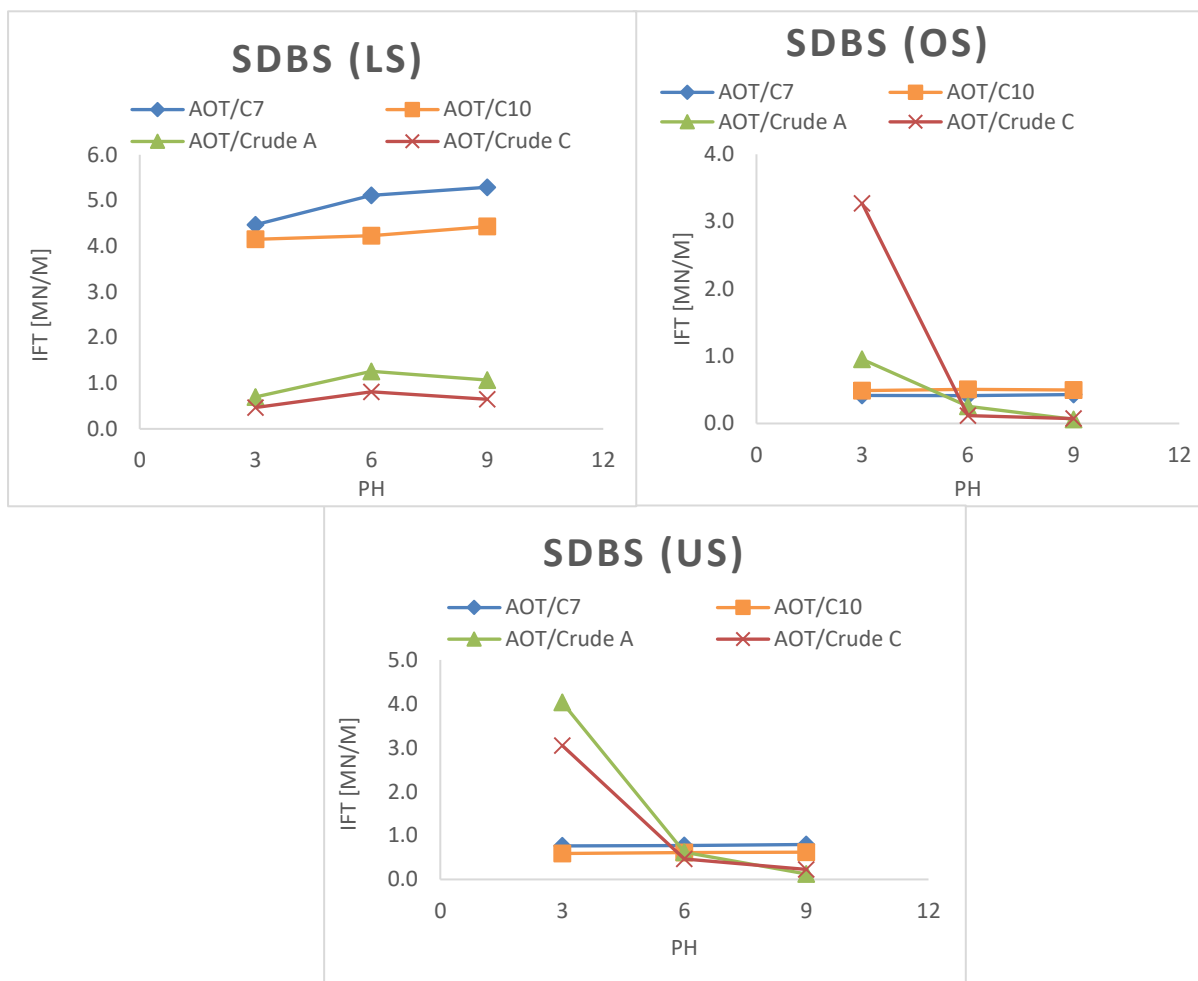


**Figure 4-18** Change in IFT as a function of pH at lower-, upper- and optimal salinity for SDBS.

The trends for both surfactants is that the change in IFT with pH are smaller at LS than at OS and US. It is interesting to notice, that in general, the IFT's are lower for AOT. However, SDBS at the most optimal conditions exhibits the lowest IFT in total (at OS and pH = 9). In addition, the change in IFT with regards to pH is observed to be greater for the crude oils than for the alkanes.

#### 4.3.4 Effect of variation in temperature

The temperature dependency of the IFT in the SOB systems was measured using the spinning drop method. Surfactant concentrations were kept at 10xCMC, and made in a 0.02M NaCl brine.

Measurements were done at temperatures of 28°C\* and 50°C for SDS and SDBS, and at 28°C\*, 40°C and 50°C for AOT.

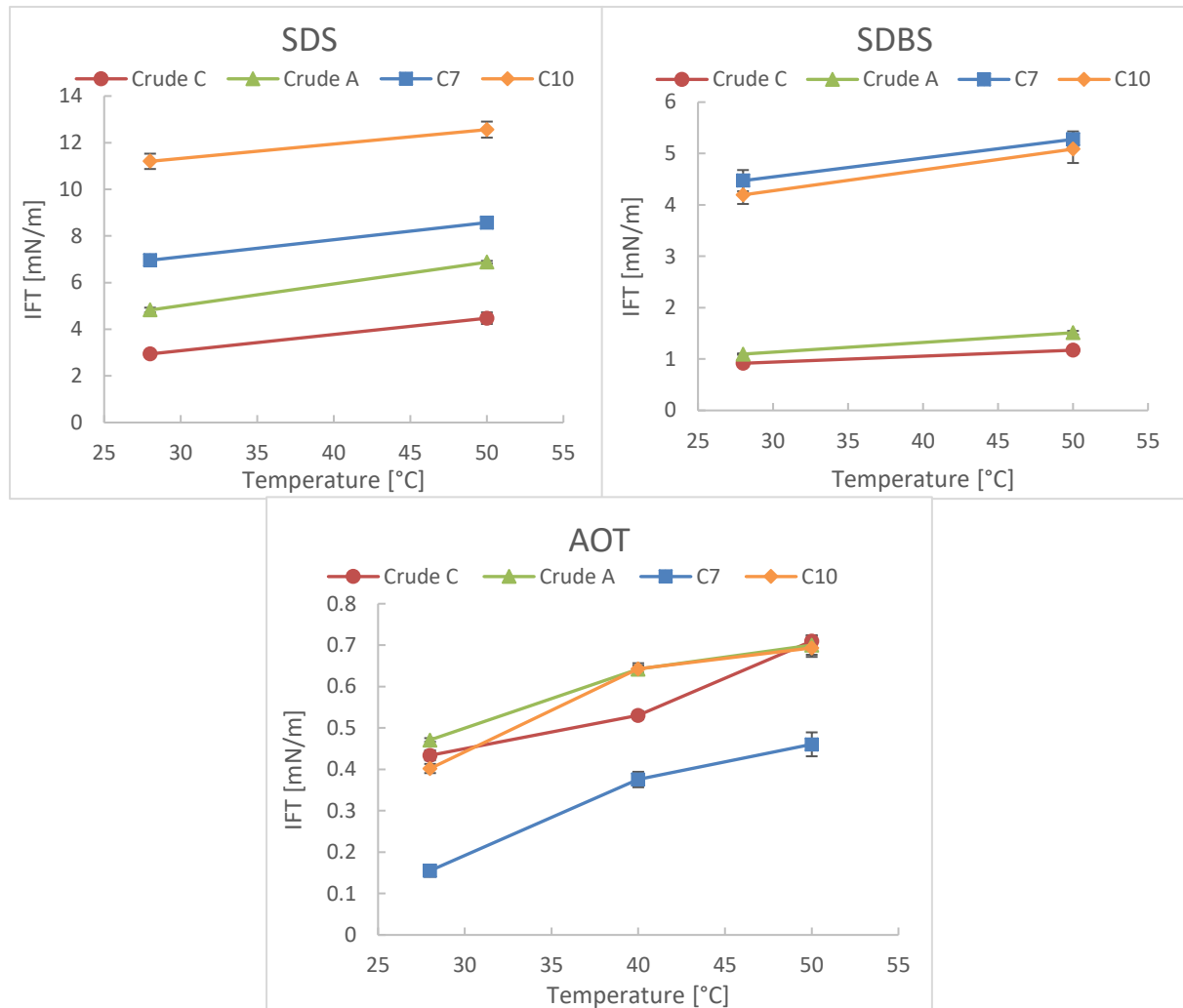


**Figure 4-19** Temperature dependency of IFT for the different brine/surfactant/oil systems.

As seen from figure 4-20, the general trend is that the IFT increases with increasing temperature for all the SOB systems. For AOT it is evident that the change in IFT is larger from 28-40°C than for 40-50°C. Surfactant AOT was measured at three temperatures as opposed to two, in an attempt to further investigate the similarity in behaviour between decane and the crude when AOT is the present

\* See section 3.2.2.

surfactant. The efficiencies of the surfactants are the same throughout all temperatures. IFT Ranked from lowest to highest for the SOB systems is AOT < SDBS < SDS.

#### 4.4 Effect of precipitation on surfactant concentration

For solutions containing brine and SDBS, at salinities higher than 0.3M NaCl, some solid surfactant precipitated out of the solution. An example of the precipitation can be seen in figure 4-21. To validate that the precipitation was not to such a degree that the surfactant concentration in each sample dropped below CMC, and would affect the interfacial properties, UV- vis spectrophotometry was used to measure the absorbance in each SDBS/brine solution. The absorbance was further used to calculate surfactant concentration by use of standard curves. The standard curves are shown in appendix B.2.

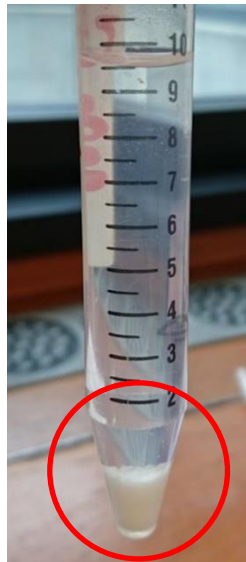


**Figure 4-20** Example of solid surfactant precipitation out of the solution. Picture is taken at a SDBS concentration at 10xCMC and a NaCl concentration of 0.7M.

The ratio between surfactant concentration in a sample at a given salinity ( $C_i$ ), and base surfactant concentration ( $C$ ), is plotted against NaCl concentration. As the start concentration of surfactant was  $\approx 10xCMC$ , the interfacial properties are not to a significant degree changed if  $C_i/C$  is kept above 0.10, as this would indicate a concentration below CMC. If the concentration decreased below CMC, surfactant concentration, i.e. amount of surfactant precipitated out of the solution, would affect IFT, and thus the optimal salinity measured.

As seen from figure 4.21, the ratio does not decrease below 0.10. As a result, the precipitation of surfactant should not have affected the measured IFT's, and thus, the optimal salinities identified.

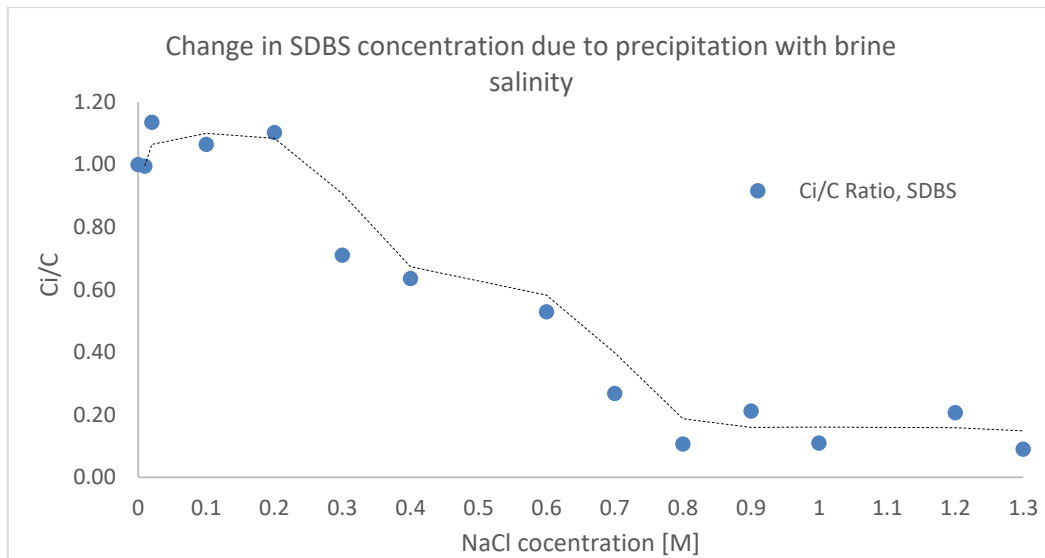


**Figure 4-21** Ratio between surfactant concentration at a given salinity ( $C_i$ ) and base surfactant concentration ( $C$ ), plotted against NaCl concentration. The ratio does not decrease below 0.10.

## 5 Discussion

### 5.1 The COB system

#### 5.1.1 Effect of variation in brine salinity

The IFT in a COB system is a result of complex interactions between solubility, intermolecular forces (both electrostatic and van der Waals), specific interaction (e.g. when  $\text{Ca}^{2+}$  forms complexes with compounds in the crude) and what kind of surface active components present in the natural occurring system. Which part of the system or the crude that has the largest effect on the IFT are debated [2, 125].

Addition of salts and salinity will affect the IFT in a COB system. To which degree the salt affects the IFT, depends on the type, and amount of surface active material present in the crude. Changes in the COB system with monovalent ions are in general due to the salinity altering the distribution of the surface-active species in both the oil- and water phase, as well as at the interface. Divalent ions alter the system by altering the distribution as well, in addition to create surface active complexes from the compounds in the crude [19].

Figure 4-1 shows that the IFT for both Crude A and Crude C decrease with increasing salinity. The same trend was observed by Isaacs and Smolik [126] when measuring the IFT between a Athabasca bitumen and an aqueous phase. However, this is in contradiction to the findings of Bai et.al [127], who concluded that NaCl concentration had no significant effect on the IFT in a COB system. They argued that all the surface-active substances in the oil they studied were oil-soluble, and not to any degree water soluble, and thus a change in IFT by increasing the salinity in the aqueous phase would be minimal. Price [128] on the other hand reported that the trend should be the opposite of that shown in figure 4-1, as he reported that the aqueous solubility of the interfacial active species in the crude decreases with increasing salinity. According to that theory, IFT should have been observed to increase with increasing salinity.

Crude C has a lower IFT against distilled water (zero salinity) than Crude A. This indicates that there are either a larger amount of interfacially active compounds, or that the compounds are more interfacially active in Crude C than Crude A. As a significant amount of interfacial components in a crude are found in the asphaltene fraction [6], the IFT distribution at zero salinity agrees with the asphaltene content in the oils reported by Sørbrø [109], who found that Crude C has a higher asphaltene content than Crude A. It should also be noted, however, that acids and bases from the crude can also be found in the de-asphalted portion of the crude. Isolating of the factor of asphaltene content alone, will therefore not be representative for the total systems IFT.

It could also be expected that the crude with the highest TAN would be the crude that exhibits the lowest IFT. The reason being that a higher TAN indicates more acids in the crude that can migrate to

the interface. However, this is not the case. Table 5-1 shows that Crude A has the highest IFT, as well as the highest TAN. As there do not seem to be a direct correlation between the measured IFT's and the crudes TAN, an assumption can be made that the acidic species in Crude C are more interfacially active than the species in Crude A. According to Varadaraj [33, 129], the degree of interfacial activity from the acidic compounds will depend on the type and structure of the acidic molecules. As Varadaraj et al. [33] and Acevedo et al. [130] suggests that acids of a lower molecular weight will have a higher affinity to the interface than acids of higher molecular weight, it can be assumed that the acids in Crude C are of a lower molecular weight than those in Crude A.

Results from Kolltveit [131] gives further insight in the interfacial behaviour of the crudes, as she found that the viscosity is higher for Crude A than Crude C. Authors [33, 130] have, as mentioned in the previous paragraph, reported that acidic compounds in a crude of lower molecular weight, are more interfacially active than those of a higher weight. As larger molecules will promote a higher viscosity, the measured viscosities agree with the assumption made, that the acidic molecules in Crude C are smaller, and thus more interfacially active, than the acids in Crude A. The measured IFT's, viscosities and TAN's, given that acids of a lower molecular weight are indeed more interfacially active than those of a higher weight, do to some degree match. It should however be noted, that both crudes consist of complex mixtures of compounds, hence, it is plausible that the matching of the viscosities with the other values are more a coincidence than a direct correlation.

Table 5-1 shows the numeric values for the IFT, asphaltene content and viscosity for the two crudes, which are all in agreement.

**Table 5-1** The table shows the IFT against distilled water, asphaltene content, TAN and viscosity for Crude A and C. No uncertainty is given for the asphaltene content of Crude A.

	IFT [mN/m] [NaCl] = 0	Asphaltene [wt%] <sup>[109]</sup>	Viscosity [mP*s] <sup>[131]</sup>	TAN [mgKOH/g] <sup>[109]</sup>
<b>Crude A</b>	36.9	0.25	36 ± 2	3.01 ± 0.04
<b>Crude C</b>	26.9	0.39 ± 0.01	22 ± 1	0.98 ± 0.05

However, as the IFT's for the crudes converge to approximately the same value with increasing salinity, it can be assumed that the effect of the difference in asphaltene content, TAN, viscosity and IFT decreases with increasing salinity.

An explanation for the decrease in IFT as salinity increases is that some of the naphthenic acids are water-soluble. When monovalent ions are added to the aqueous phase, it will alter the distribution of the naturally occurring surfactants in the oil due to changes in the electrostatic forces involved, which is the case for the IFT for both Crude A and C. The monovalent ions will also contribute to decreasing the IFT by decreasing the EDL between charged headgroups of the naturally occurring surfactants in

the crude. This happens as a decrease in EDL results in a tighter packing of the interfacially active compounds at the interface. A tighter packing, in turn, lowers IFT.



## 5.2 The SCOB system

The reason for the LSS environment being emphasized in this thesis, and being the most used environment for the measurements carried out, is that previous studies has shown a positive effect on an oil recovery when combining injection of low salinity water and surfactant [2, 66, 125, 132, 133]. Even though the positive effect is observed, the mechanisms behind the combined injection is not fully understood, and is why investigations of a combined system of surfactant and low salinity brine is of interest.

### 5.2.1 Effect of surfactant on the oil-water IFT at LS conditions

Figure 5-1 shows the percentage decrease in IFT from a LS system to a LSS system. Equation used to calculate the percentage decrease in IFT are

$$\Delta IFT_{LS \rightarrow LS+surf} [\%] = \left( \frac{IFT_{LS} - IFT_{LSS}}{IFT_{LS}} \right) * 100 \quad (\text{Equation 5.1})$$

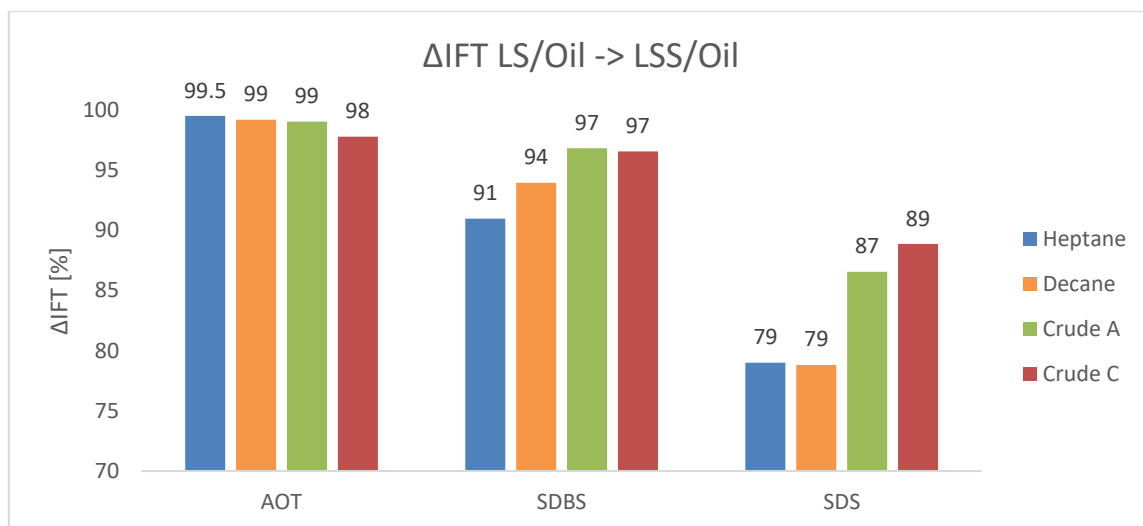


**Figure 5-1** Effect of surfactant on oil-water IFT at LS conditions

From figure 5-1 it is evident that AOT is the most efficient surfactant in general, decreasing IFT for all tested oils by > 97%. AOT also exhibit the lowest variations in percentage change in IFT across the different oils. The two-tailed nature of AOT and its balanced HLB [42] is probably why the AOT is the surfactant that decreases IFT the most. The balanced HLB makes the surfactant equally less soluble in each phase, thus increasing its affinity to be positioned at the interface. Higher affinity to the interface results in more surfactant molecules at the interface, which in turn decreases IFT.

The two crude oils seem to exhibit approximately the same decrease in IFT, for each of the three surfactants respectively. This indicates that the effect of adding surfactant overrides the effect of interfacial active compounds in the crude, as the decrease in IFT for the crudes is similar for a specific surfactant, but changes as the surfactant is changed. Probably due to the fact that the crudes have different TANs, densities and viscosities [109], a difference in IFT when no surfactant is present is

observed (see figure 4-1 at 0.02M NaCl) . After IFT is decreased by addition of surfactant, the relative difference between the IFT`s are smaller than before surfactant was added.

The decrease in IFT is significantly larger for the crudes than for the alkanes when SDS and SDBS are the present surfactant. The reason for the decrease being larger for the crudes, is that there is a synergy effect between the natural occurring interfacially active compounds in the oil, and the added surfactants. This effect was reported to be significant by Trabelsi et.al. [134] for surfactant SDBS and Touhami et.al. [135] for surfactant SDS, and is assumed to exist also for AOT.

Additionally, in a SCOB system, the interfacially active compounds in the crudes will compete with the commercial surfactant molecules for a position at the interface [78]. As alkanes do not contain surface active compounds themselves, there will not be any competition for a position at the interface for the alkane SOB systems. As the decrease in IFT is greater for the crudes than the alkanes by several percent, it appears that the decreasing effect of synergy (as shown by Chu et.al [136]) between active compounds in the crude and the commercial surfactants, gives a larger decrease than if commercial surfactant alone is present at the interface. This seems to be the case despite there being an increased molecular competition for a position at the interface when both commercial- and natural occurring surfactants are present.

### 5.2.2 Effect of variation in surfactant concentration

All the SOB systems show to some extent the same behaviour. The difference in IFT in the systems with surfactant concentrations of CMC and 10xCMC are minor, compared to the difference to the IFT with a concentration of 1/10xCMC. This is as predicted by the theory, which states that the IFT will decrease with increasing surfactant concentration until CMC is reached [24], and further addition of surfactant over CMC, will only lead to the creation of more micelles, which have no interfacial effect [15].

The efficiency (i.e. which surfactant that lowers IFT the most) of the surfactants with regards to each other, varies for each concentration. At a concentration of CMC and 10xCMC, the most efficient surfactant is AOT. However, at a concentration of 1/10xCMC, SDBS lowers IFT the most. This is illustrated in table 5-2, based on data from figure 4-2.

**Table 5-2** Overview of the efficiencies of the three surfactants at different concentrations.

10xCMC		CMC		1/10xCMC	
<i>Efficiency rank</i>	<i>Surfactant</i>	<i>Efficiency rank</i>	<i>Surfactant</i>	<i>Efficiency rank</i>	<i>Surfactant</i>
1	AOT	1	AOT	1	SDBS
2	SDBS	2	SDBS	2	AOT
3	SDS	3	SDS	3	SDS

Smit et.al [137] found, by use of both simulations and experimental data, that increasing the tail length of a surfactant makes the surfactant more effective at low concentrations. As SDBS has a longer tail-group than AOT and SDS, this might explain why SDBS gives the lowest IFT at concentration of  $1/10 \times \text{CMC}$ . Another possible explanation for this, is the decline rate of ST or IFT with surfactant concentration. This rate is not equal for all surfactants. A steeper decline rate will give a greater difference in IFT when concentration is reduced from CMC to  $1/10 \times \text{CMC}$ .

### 5.2.3 Differences in optimal salinities for different SCOB systems

Aveyard et.al. [40] found the OS for the AOT/Heptane system by measuring IFT, to be at 0.05M NaCl. This agrees with the optimal salinity for the AOT/Heptane system found and presented in table 4.8.

Kellay et.al. [138] reported that the OS for the AOT/Decane system to be at approximately 0.077M NaCl. Bastidas et.al [139] also investigated the AOT/Decane system at different salinities by use of phase behaviour, and reported the OS for the system to be between 0.070M NaCl and 0.077M NaCl.. Both reported OS`s agree with the value of 0.075M NaCl obtained here with the spinning drop method.

No values for the OS of the SDBS/Decane system could be obtained, as most studies use an alcohol as co-surfactant, or a mixture of surfactants, when identifying optimal salinity for the system. These studies are e.g. [140-142]. However, Skauge & Fotland [92] reported the optimal salinity for the SDBS/Decane system to be at 0.58M NaCl with the presence of 4 wt% n-butanol, in comparison to the OS of 0.30M NaCl found for the pure SDBS/Decane system in figure 4-7. A higher optimal salinity for the system from Skauge & Fotland with presence of an short chain alcohol is as expected, as theory from e.g. Miller et.al. [143] states that the optimal salinity will increase when short chain alcohols are added to the system. This is due to the fact that as the alcohol increases the solubility of the surfactant in the water phase, and thus more salt is needed for the solubility of the surfactant to be equal in both phases.

Aarra et.al. [63] investigated the OS of SDS/Heptane with the use of solubilisation parameters, and found the OS to be at 8.3 wt%. No OS was found for the SDS/Heptane system due to the precipitation when using the spinning drop method, a problem that would not arise when conducting the measurements by use of solubilisation parameters as performed by Aarra et.al [63]. Thus, there is no basis to compare with Aarra`s [63] value.

From table 4-2 it is observed that the OS for a system is decreasing with increasing hydrocarbon length- or number of tails on the surfactant. A longer hydrocarbon chain (or double tailed chain) gives a more lipophilic surfactant, with a more balanced HLB. The decreasing OS arises from the fact that the more lipophilic a surfactant is (e.g. the longer the tail group or more number of tails), the less salt is needed in the water-phase for the surfactant molecules to be salted out of the bulk, and rather have an affinity to the interface, or the oil phase [45]. Given one specific oil tested, the OS ranked from high OS, to low OS are SDS > SDBS > AOT. This rank corresponds to the surfactants HLB`s, which are SDS (HLB = 40) > SDBS (HLB = 10.6) > AOT (HLB = 10).

Both crudes do have their OS at approximately the same NaCl concentration, as well as being quite similar in the corresponding IFT to the OS`s. As this trend extends across all three surfactants, the assumption can be made both crudes exhibit approximately the same EACN. Further, the OS for each surfactant decreases the greater the similarity between ACN of the alkane and the EACN of the surfactant hydrocarbon chain. AOT, with an EACN of 8 [144], has a lower OS against heptane with its ACN of 7 [103], than against decane with its ACN of 10. The same trend is observed for SDBS. SDBS has a EACN of 12 [144], and exhibit a lower OS against decane (ACN = 10) than against heptane (ACN = 7). A hypothesis can therefore be proposed that the OS of a system has a minimum the more the ratio between the ACN (or EACN) of the oil, and the EACN of the lipophilic part of the surfactant, is equal to 1. The same trend is not applicable to the crudes, as EACN for neither of the crudes is known. However, based on the theory above, it can be assumed that they have approximately the same EACN, as OS for both crudes are in close proximity across all three surfactants used. Illustration of suggested correlation between OS and ACN or EACN can be seen in figure 5-2.

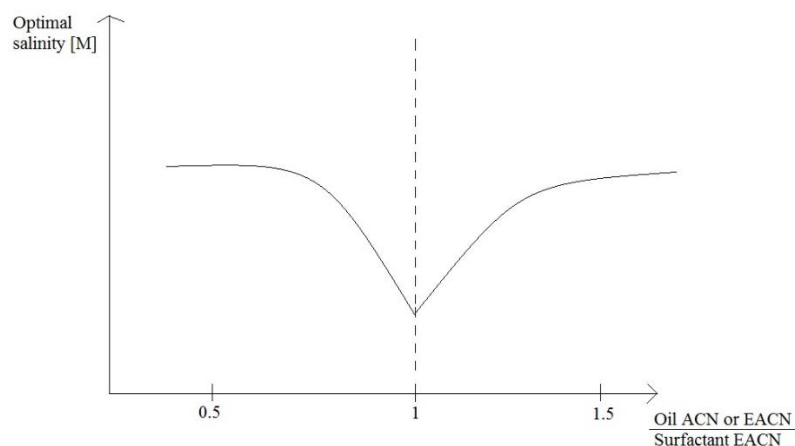


**Figure 5-2** Illustration of the suggested hypothesis of the correlation between optimal salinity for the given system and the ratio between the oil ACN or EACN, and the surfactants EACN.

Other researchers have, however, reported that the relationship in figure 5-2 is not the case. Salager et.al. [87], and later Skauge & Fotland [92] , reported that for a given surfactant, the natural logarithm

of the optimal salinity increases linearly with increasing ACN of the oil. The relationship can be expressed as [87]

$$\ln S^* = K (ACN) + \dots \quad (\text{Equation 5.2})$$

Where  $S^*$  is the optimal salinity, and  $K$  is an empirically determined constant, shown to be  $0.16 \pm 0.01$  when  $S^*$  is expressed in grams of NaCl per  $100\text{cm}^3$ . The value of  $K$  is, according to Salager et.al. [87] constant for all alkyl aryl sulfonates that they tested, an isomeric mixture of sodium dodecylbenzene sulfonate species. The dots in the equation represent that other variables are included to determine the optimal salinities. Such variables are e.g. the addition of alcohols or other co-surfactants [87], which is not investigated in this thesis, and therefore not written out in the equation. It is worth mentioning that the studies referred to [87, 92] used different alcohols as co-surfactants as they identified their linear relationships.

In other words, the trend of decreasing OS to a minimum where EACN of the lipophilic chain of the surfactant match the EACN does not seem to be a general trend, but rather a coincidence in the measurements done in this thesis. Identifying OS for alkanes of other ACN's will give a more complete picture.

### 5.2.4 Effect of Calcium on oil-water IFT at LSS conditions

Figure 5-3 shows the percentage decrease in IFT from a LSS to a LSS-Ca system. Equations used to calculate the percentage decrease in IFT are

$$\Delta IFT_{LSS \rightarrow LSS-Ca} [\%] = \left( \frac{IFT_{LSS} - IFT_{LSS-Ca}}{IFT_{LSS}} \right) * 100 \quad (\text{Equation 5.3})$$

for solutions containing surfactant and

$$\Delta IFT_{LS \rightarrow LS-Ca} [\%] = \left( \frac{IFT_{LS} - IFT_{LS-Ca}}{IFT_{LS}} \right) * 100 \quad (\text{Equation 5.4})$$

for the additive-free solutions.

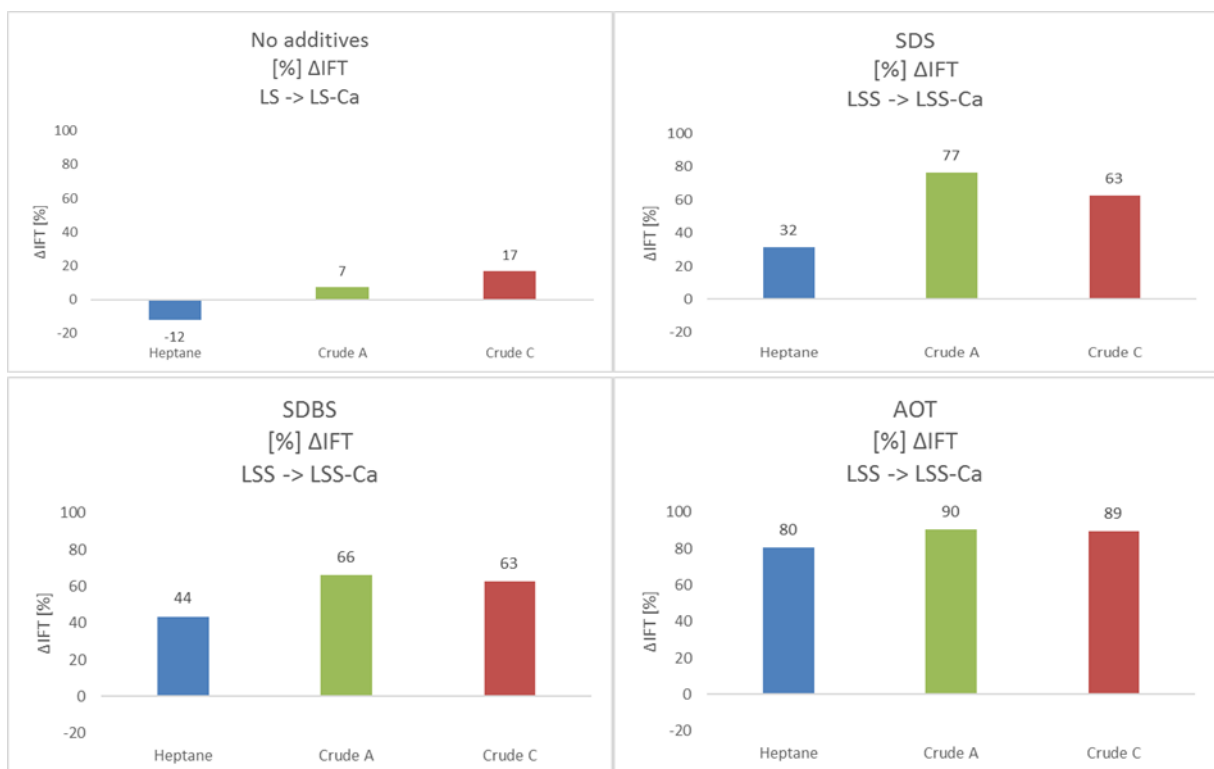


**Figure 5-3** Percentage decrease in IFT from LSS to LSS-Ca systems for each surfactant and with no additives. Upper left: No additives. Upper right: SDS. Lower left: SDBS. Lower right: AOT. Which oils the IFT's are measured against are shown on the figure.

As figure 5-3 illustrates, the presence of calcium changes the IFT for each system. It is evident that when the brine is changed from LSS to LSS-Ca, there is a decrease in IFT for all systems containing commercial surfactants.

The decrease in IFT when  $Ca^{2+}$  ions are added to the system can mainly be contributed to three mechanisms. The first one being a tighter packing of anionic surfactants at the interface, as the EDL are reduced due to the addition of divalent ions [18]. Secondly, the added calcium is able to create ion pairs with acids from the crudes. These ion pairs can precipitate, or partition into the oil phase and

then act as a surfactant, and thus reduce the IFT [19]. Third, the addition of divalent ions reduces the water solubility, which gives surface active compounds a lower affinity to the bulk phase. As a result, they orient themselves at the interface, resulting in a lower IFT. This is called a salting out effect [145].

When taking the differences in decrease in IFT between the oils when  $\text{Ca}^{2+}$  are added in to consideration, the decrease in IFT is slightly larger for crude A than crude C when SDS is the surfactant present. This can be attributed to the TAN in the crude. Crude A has a TAN of 3.01 mgKOH/g and Crude C 0.96 mgKOH/g [109]. The higher the amount of acids in the crude, the more compounds are present that are interfacially active, and can react and make complexes with  $\text{Ca}^{2+}$  [19, 21]. A higher amount of said complexes will in turn lower the IFT. The difference in decrease in IFT between Crude A and Crude C, can therefore possibly be due to the difference in TAN.

However, when AOT or SDBS is present, the difference in TAN does not make an impact on the decrease in IFT, as the crudes exhibit approximately the same percentage decrease. Even though Crude A has a higher TAN than Crude C, when no surfactant is present, Crude C shows a larger decrease in IFT than Crude A. This is contradictory to what is expected in terms of the TAN's mentioned in the previous paragraph. Correspondingly to how the classes acidic species in the COB systems discussed in section 5.1.1 dictate the IFT of the systems, the same classes of acidic species in the crudes are believed to dictate how the crudes react to addition of calcium. This is due to some acids being more reactive with calcium than others. As which types of acidic species present in each of the crudes are not known, an investigation of the different types of acidic compounds would help to better the understanding of calcium addition. See further work.

Heptane, which has the lowest relative decrease in IFT across all three surfactants, does not contain any naphthenic acids ( $\text{TAN} = 0$ ), or other compounds that would influence on the interface. This explains why the decrease in IFT when calcium is added is lowest for heptane when surfactants are present. The decrease taking place despite the absence of naphthenic acids or other compounds in the crude, can be contributed to calcium having a higher valence than sodium. As a result, calcium increases the effect of minimizing the EDL between the charged head groups of the surfactants. A lesser EDL makes the surfactant able to pack tighter, which in turn decreases the IFT.

It is also interesting to note that when no surfactant is present, addition of calcium ions leads to an increase in IFT for heptane. The reason for this is the increase in intermolecular forces in the brine when ions are added. The interaction between the anions from the salt and the partial positive hydrogen in the water molecules, along with the cations from the salt and the partial negative oxygen in the water molecule, leads to increased intermolecular forces between the molecules in the brine. This will in turn increase the interfacial tension, as the intermolecular energy-difference between the liquids will increase [146, 147]. Even though total ionic strength is kept constant, an increasing amount of divalent  $\text{Ca}^{2+}$  increases the strength of the intermolecular forces, as calcium is of a higher

valence than Na<sup>+</sup> [148]. Thus, an increase in IFT is observed for the brine/heptane system when calcium is added.

### 5.2.5 Effect of variation in pH

Common for both surfactants that pH measurements are carried out with, is that the change in IFT at different pH values is more significant at OS and US than at LS. The effect of change in pH decrease with decreasing salinity. It can therefore be assumed that for these SCOB systems, the changes in salinity are more dominant than changes in pH. This follows from that if change in pH was the dominating factor on IFT, the same relative change from pH 3 to 6, and 6 to 9 would have been observed over all three salinities. Hence, the effect of salinity is more dominant. These observations are the opposite of that reported by Tichelkamp et.al. [51], who investigated the effect of change in pH for SDBS solutions of no salt, low salinity and a solution low salinity + calcium. In their observations, the effect of change in pH decreased with the increase of salinity and/or presence of calcium in the water phase.

As expected, the change in pH did indeed have a larger impact on the crude oil than the alkanes. This is evident from figure 5-4, where the percentage change in IFT can be observed at OS and US for SDBS and AOT. Difference in IFT for pH changes at LS is not presented in this figure, as the relative change in IFT is modest compared to the changes at OS and US.

The reason for the crude oils exhibiting a significantly greater change in IFT as the pH changes, is that crude oils have polar compounds - asphaltenes and naphthenic acids. These compounds interact with OH<sup>-</sup> and H<sup>+</sup> ions in the brine, depending on the pH, making these compounds into in-situ surfactants with a polar-, hydrophilic, end and a lipophilic, hydrocarbon end [78]. The results obtained in figure 5-4 indicates that these compounds contribute to decreasing IFT, as the IFT reduction is significantly larger for the crude oils.

Percentage decrease in IFT as pH is changed is calculated by

$$\Delta IFT_{pH=3 \rightarrow pH=6} [\%] = \left( \frac{IFT_{pH=3} - IFT_{pH=6}}{IFT_{pH=3}} \right) * 100 \quad (\text{Equation 5.5})$$

and correspondingly for change in pH from 6 to 9.



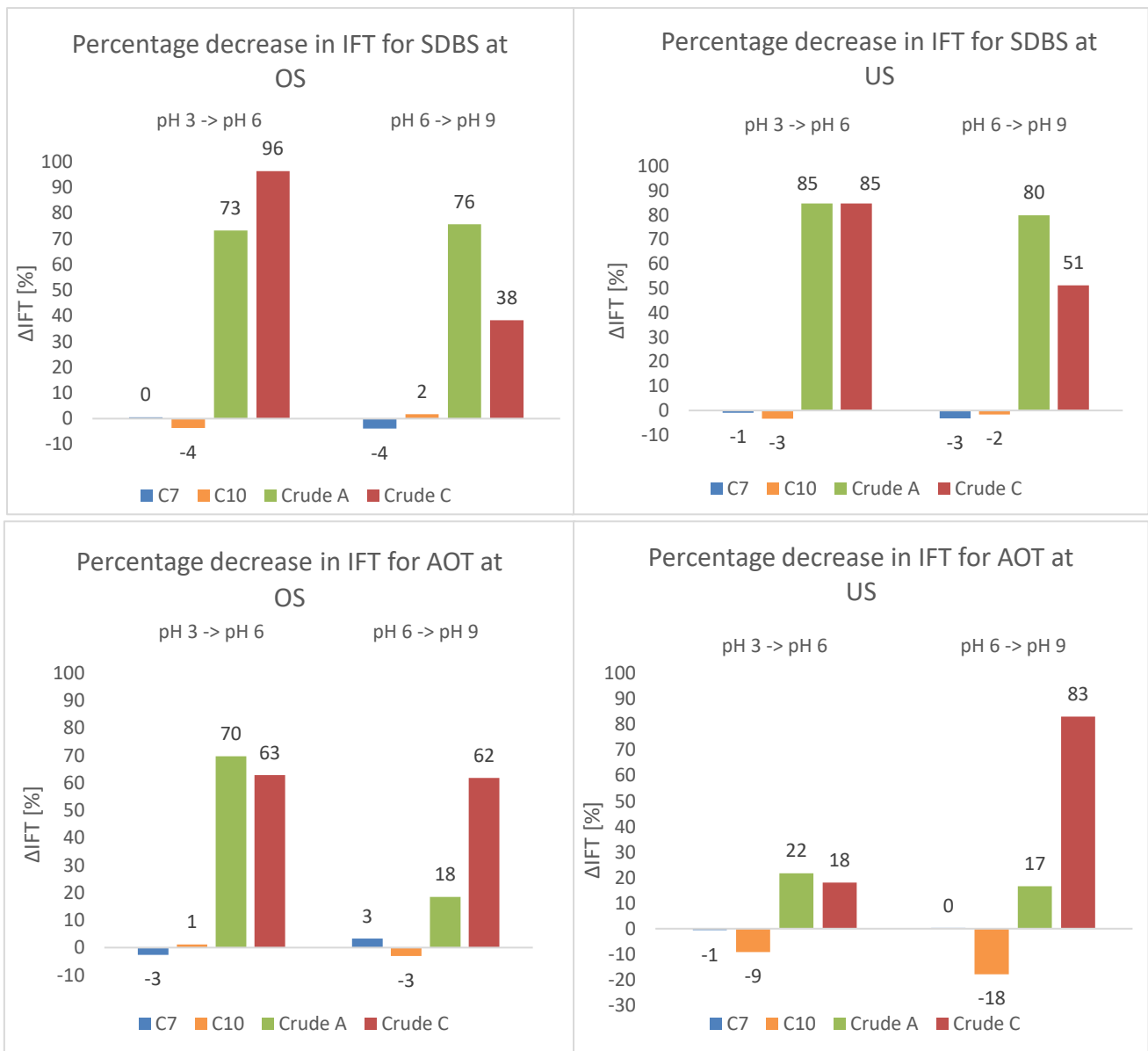


**Figure 5-4** Percentage decrease in IFT as pH is changed from 3 to 6 and 6 to 9 for SDBS and AOT, at OS and US respectively. Changes in IFT with respect to pH at L.S are not presented as the change in pH are less significant compared to the changes at OS and US

Given that the surfactants used are anionic surfactants, a low pH, i.e. addition of  $H^+$  ions, will to some degree contribute to lowering the EDL between the headgroups of the surfactant. The same concept applies here, as to why CMC of an anionic surfactant decreases at lower pH values, as explained by Bhuyan et.al. [149]. However, the decrease in the EDL between the headgroups is not observed to affect the results compared to the creation of in-situ surfactants from the oil, as the IFT consistently decreases with a higher pH. In addition, Tichelkamp et.al [51] reported that the decrease in the EDL only occurs at very low pH values.

As the IFT's measured are consistently lowest for a *higher* pH value for the crude oils, it appears that the crudes have more acidic than basic components –  $OH^-$  ions interact with easily “detachable”

hydrogens from the acidic components, creating polar compounds that are both water- and oil soluble. These compounds then orient themselves in the interface, decreasing IFT. If the oils contained a larger number of basic components than acidic, the IFT would have rather decreased at *low* pH values.

In theory, a higher TAN for the crude will lead to a lower IFT, as TAN is an indication of the amount of acids present in the crude, i.e. acids that at a high pH can create in-situ surfactants. Sørbø [109] reported as previously mentioned that Crude A has a TAN of 3.01mgKOH/g and that Crude C has a TAN of 0.98 mgKOH/g. This indicates that Crude A has more acid-components than Crude C, and thus, in general has a greater possibility to create interfacially active compounds. Based on this, it would be expected that Crude A would exhibit the lowest IFT of the two crudes at high pH. However, from both the percentage decrease in IFT (figure 5-4) and the variation of IFT with pH (figure 4-17 and 4-18), it is evident that the difference in TAN is not great enough to consistently make a significantly difference in IFT when a surfactant is present.

Another interesting observation is that even though AOT exhibits the lowest IFT in both the concentration- (figure 4-2) and the temperature measurements (figure 4-20), it is not the most efficient surfactant when the pH is varied. This could be explained by Trabelsi et.al. [134], who compared the efficiency of SDBS with SDS, as well as a non-ionic surfactant Triton X405 against a crude oil with variations in pH. They concluded that at high pH values, SDBS was by far the most efficient surfactant, due to the synergistic effect with acids in the crude. They explained this effect existing due to the highly reactive  $\pi$ -electrons in the benzene-ring in SDBS being able to link to compounds in the crude.

Another reason why SDBS is more efficient than AOT when the pH is varied, could be attributed to the fact that when a certain number of in-situ surfactants is created from the components in the oil at medium- and high pH values, the in-situ compounds compete with the commercial surfactant molecules for a position at the interface. As the double chained AOT molecule will take up more volume than the single chained SDBS at the interface (follows from their molecular structure), the net amount of surfactant + in-situ surfactant possible at the interface is lower for AOT than SDBS. This could be the reason why the percentage change in IFT is generally larger for SDBS than AOT across the crudes, at both OS and US.

### 5.2.6 Effect of variation in temperature

As seen from figure 4-20, the IFT for all SOB systems increases with increasing temperature. This behaviour is due to the surfactant solubility, in both the oil- and water phase, increasing proportionally with the temperature. A higher solubility in the bulk phases, leads to the surfactants having a lower affinity to the interface, thus increasing the IFT [92]. The measurements also indicate that the efficiencies of the surfactants relative to each other remains the same at higher temperatures (from most to least efficient); AOT > SDBS > SDS.

An interesting observation is that the behaviour of each oil phase relative to each other, vary with the type of surfactant used. When SDS is the present surfactant, the increase in IFT by increase in temperature is observed to be approximately equal for each of the SCOB systems, but at different IFT`s. Heptane and Crude A are the alkane and the crude exhibiting the closest behaviour, as they are the closest with regards to IFT, and showing approximately the same slope. However, they cannot be said to exhibit the same behaviour.

When SDBS is the present surfactant, the difference between the crudes and the alkanes are greatest for all SCOB systems investigated. The behaviour of heptane and decane are similar. The same can be said for the behaviour of Crude A and C. However, a large difference between the crudes and the alkanes is present. Comparing the crude to the alkanes, it is evident that the crudes in general exhibits the lowest IFT, and the alkanes exhibiting a greater slope when the temperature is increased.

AOT is the surfactant where behaviour of the alkanes matches the behaviour of the crudes the most. Crude A and decane exhibits to a large degree similar behaviour, with curves being in close proximity from 28°C – 40°C, and identical from 40°C – 50°C. This, however, is contradicting to when SDS is the present surfactant, where it was observed that heptane and Crude A had the most similar behaviour.

No alkane did consistently behave like one of the crudes across all three surfactants, as which alkane that matched the most which one crude varied across the three surfactants. Due to the difference across the three surfactants, an assumption can be made that which type of surfactant, and its structure, dictates the systems response to changes in temperature. This assumption is supported by finding by Karnanda et.al [27]. No certain similarity between a specific alkane and a specific crude could be found.

## 6 Summary and conclusion

The objective of this thesis has been to investigate how different surfactants with different structures affect the IFT between a brine and different oils at different aqueous environments. The aim was to identify how different surfactants of different structures behave when taking crude oil compositional parameters into consideration. In the measurements, two crude oils have been used, as well as two n-alkanes. The investigation has been done by studying the effect of variation in surfactant concentration, brine salinity, ion-valence composition, pH and temperature on the SCOB and SOB systems IFT. The differences between the crude oils were small, as they exhibited the same behaviour for each individual surfactant.

Regardless of the oil, AOT was in general the surfactant that gave the lowest IFT for the systems investigated, probably due to its balanced HLB and molecular structure, which makes it have equal solubility in both the oil- and water phase. SDBS was in general the second most effective surfactant, with SDS being the least effective surfactant in terms of IFT. This agrees with the surfactants HLB.

For surfactant addition to a LS system to create a LSS system, AOT was the most effective surfactant. In terms of comparison of the oils, the percentage change in IFT when adding surfactant was similar for both crudes. In addition, the crudes had a larger decrease in IFT compared to the alkanes. This arises from the fact that the crudes, unlike the alkanes, have interfacial active components present in the oil. A synergy effect between the added surfactants and the natural occurring surfactants are believed to be the reason why the percentage decrease was highest for the crudes.

The optimal salinities for the systems was identified for AOT and SDBS. AOT had the lowest OS across all oils measured. Due to its surfactant structure, only small amounts of salt are needed to change to which part of the system (oil, aqueous or interface) the surfactant has a greater affinity to. SDBS had a lower OS's across all the oils. OS for SDS was only identified for the crudes, however, even at low salinities, solid surfactant precipitated out of the solution. The surfactant concentration is thus believed to have changed during the process of identifying OS for the SDS, and changed the system to a such degree that the OS's found are not valid. In addition, for all systems regardless of precipitation and type of surfactant, both crudes behaved similarly during the salinity scans. The corresponding IFT's to the OS were also similar for the crudes, for each respective surfactant. The similarities in OS and IFT indicate that differences in crude oil properties that can affect IFT, are overridden by the effect of surfactant addition, as neither of the crudes had a significantly different OS or IFT than the other for a given surfactant. A hypothesis was suggested that the closer the ratio between the ACN of the oil and the EACN of the surfactants lipophilic group was to one, the lower the optimal salinity. This theory held for heptane and decane, but the literature proved otherwise.

With regards to ion valence, the IFT was decreased for all the systems containing crude oils when  $\text{Ca}^{2+}$  was added to the system ( $\text{LSS} \rightarrow \text{LSS-Ca}$ ) and ionic strength was kept the same before and after

calcium addition. A decrease in IFT was observed for all the systems, except for heptane when no additive was present. The decrease was highest for the crudes, likely due to the calcium ions creating 2:1 complexes with the compounds in the crude, creating in-situ surfactants. These complexes would in addition have a positive charge, interacting with the negative head group from the anionic surfactants, further reducing IFT due to tighter packing. There was also a decrease in the IFT for the alkane systems, due to a decrease in the EDL between surfactant headgroups, and hence, tighter surfactant packing when calcium ions replaced sodium. The IFT for the heptane/brine system without surfactant present, behaved opposite of the other systems, as IFT increased with addition of calcium. The increase happened as that the intermolecular forces in the brine were enhanced by addition of calcium, which resulted in a higher IFT. Despite the differences in the properties of the crude oils, the percentage decrease in IFT when calcium was added was similar when both SDBS and AOT was the present surfactant.

The effect of change in pH was larger on the crude oils than on the alkanes. This was as expected as excess  $H^+$  or  $OH^-$  would react with the acidic and basic compounds in the oil. Due to the lack of acids and base, this reaction did not occur in the alkanes. Both crudes showed a decrease in IFT as pH was increased, with both SDBS and AOT as the respective surfactant. This indicates that both the crudes are more acidic than basic, as a basic crude would have had a decrease in IFT at a low pH. In addition, the effects of change in pH increased with increasing salinity. The greater change in pH at higher salinities is likely to be attributed to that a higher salinity lowers the solubility of both commercial and in-situ surfactant in the bulk, inducing higher accumulation at the interface. At low salinities, the in-situ surfactants created by a change in pH, are more soluble in the bulk, and are thus not as active at the interface.

Each SCOB and SOB systems behaved as expected as the temperature was changed. The IFT of each system increased with increasing temperature, which is an effect of the surfactant solubility in each phase increasing as temperature is increased. A higher solubility in the bulk-phases for the surfactants, gives a lower surfactant accumulation at the interface, and thus a higher IFT. AOT was the most effective surfactant with changes in temperature, like the in salt-scans and in the measurements regarding surfactant concentration.

## **7 Further work**

### **Multivariate data analysis**

A multivariate data analysis of the results obtained could prove useful to identify which factors that have the greater influence on the SCOB system, in addition to correlate the effect of different variables (e.g. temperature, surfactant concentration) to each other.

### **Minimum $\text{Ca}^{2+}/\text{Na}^+$ ratio**

Optimal  $\text{Ca}^{2+}/\text{Na}^+$  ratios were identified only for the systems containing AOT, against heptane and Crude A. A further investigation over a wider range of ratios could identify a minimum in IFT and  $\text{Ca}^{2+}/\text{Na}^+$  ratio for the other SOB and SCOB systems. This would give further understanding of each respective behaviour of the surfactants with regards to the crude oils.

### **Different divalent ions**

Calcium is consistently used as divalent ions to investigate trends and surfactant behaviour when divalent ions are added to the system. It would be interesting to investigate the effect, if one exists, of exchanging the  $\text{Ca}^{2+}$  ions with e.g.  $\text{Mg}^{2+}$  ions. Also, systematic study trends of IFT with varying ratios of  $\text{Na}^+$ ,  $\text{Ca}^{2+}$  and  $\text{Mg}^{2+}$  with all three ions present, to further mimic the properties of sea water would be interesting, as seawater often is injected during a EOR process.

### **Identification of types of acids present in the crude**

Throughout this thesis, only the TAN's of the crudes have been known. However, which types of acids that are present in the crude will largely influence how the crudes will react to both addition of divalent ions and changes in pH. An identification of which classes, and respective amounts, of acids in the crude would prove useful for understanding the results obtained with regards to variations in pH and divalent ion addition in particular.

### **Correlation of surfactants EACN and alkanes ACN to optimal salinity**

The results obtained in this thesis indicate that the more the ratio between the EACN of the surfactant and the ACN of the alkane are unity, the lower the optimal salinity is. This is, however, only investigated here for two alkanes. A study of the correspondence across a larger number of alkanes would reveal if this is the case in general.

### **TBN**

Only the TAN for the crudes in this thesis are known. Measurements of the crudes TBN would prove useful for further understanding of the crude systems, as well as further interpreting the effects of change in pH on the systems.

## 8 Bibliography

1. *Short-Term Energy Outlook*, U.S.E.I. Administration, Editor. 2017: EIA Energy Conference June 26-27.
2. Sheng, J., *Modern Chemical Enhanced Oil Recovery : Theory and Practice*. 2010: Burlington: Gulf Professional Publishing.
3. Speight, J.G., *Enhanced Recovery Methods for Heavy Oil and Tar Sands : A Guide to Heavy Oil*. 2013: Gulf Publishing Company.
4. Green, D.W., *Enhanced Oil Recovery*. 1997: Society of Petroleum Engineers.
5. Fingas, M., *Hanbook of Oil Spill Science and Techology*. 2014: John Wiley & Sons Inc. .
6. Schobert, H.H., *Chemistry of Fossil Fuels and Biofuels*. 2013: Cambridge University Press.
7. Sjöblom, J., et al., *Our current understanding of water-in-crude oil emulsions: Recent characterization techniques and high pressure performance*. *Advances in Colloid and Interface Science*, 2003. **100-102**: p. 399-473.
8. Saad, O.M., G.A. Gasmelseed, and A.H.M. Hamid, *Separation of Naphthenic Acid from Sudanese Crude Oil Using Local Activated Clays*. *Journal of Applied and Industrial Science*, 2014. **2**(1): p. 14-18.
9. Berry, J.D., et al., *Measurement of surface and interfacial tension using pendant drop tensiometry*. *Journal of Colloid and Interface Science*, 2015. **454**: p. 226-237.
10. Zolotukhin, A.B. and J.-R. Ursin, *Introduction to Reservoir Engineering*. 2000: Høyskoleforlaget.
11. Berg, J.C., *An Introduction to Interfaces & Colloids - The Bridge to Nanoscience*. 2009: World Scientific Publishin Co. Pte. Ltd. . 804.
12. Arriola, A., G.P. Willhite, and D.W. Green, *Trapping of Oil Drops in a Noncircular Pore Throat and Mobilization Upon Contact With a Surfactant*. *Society of Petroleum Engineers Journal*, 1983. **23**(01).
13. Rouquerol, J., et al., *Adsorption by Powders and Porous Solids*. 2013, Oxford, UNKNOWN: Elsevier Science.
14. Parashar, K., *Adsorption*. 2015, Power Point slides, University of Johannesburg, Department of Applied Chemistry, URL: <https://www.slideshare.net/Kamyaparashar/adsorption-presentation-44669901> Accessed: 27.04.2017.
15. Kronberg, B., K. Holmberg, and B. Lindman, *Surface Chemistry of Surfactants and Polymers (1)*. 2014: Wiley. 499.
16. Myers, D., *Surfactant science and technology*. 3rd ed. ed. 2006, Hoboken, N.J: Wiley.
17. Rahman, A. and C.W. Brown, *Effect of pH on the critical micelle concentration of sodium dodecyl sulphate*. *Journal of Applied Polymer Science*, 1983. **28**(4): p. 1331-1334.

18. Rosen, J.M. and J.T. Kunjappu, *Surfactants and Interfacial Phenomena*. 2004, New Jersey: John Wiley & Sons Inc.
19. Tichelkamp, T., et al., *Systematic study of the effect of electrolyte composition on interfacial tensions between surfactant solutions and crude oils*. Chemical Engineering Science 2015. **132**: p. 244-249.
20. Wan, L.S.C. and P.K.C. Poon, *Effect of salts on the surface/interfacial tension and critical micelle concentration of surfactants*. Journal of Pharmaceutical Sciences, 1969. **58**(12): p. 1562-1567.
21. Brandal, Ø. and J. Sjöblom, *Interfacial Behavior of Naphthenic Acids and Multivalent Cations in Systems with Oil and Water. II: Formation and Stability of Metal Naphthenate Films at Oil-Water Interfaces*. Journal of Dispersion Science and Technology, 2005. **26**(1): p. 53-58.
22. Hosseini, S., et al., *The Role of Salinity and Brine Ions in Interfacial Tension Reduction While Using Surfactant for Enhanced Oil Recovery 1*. Research Journal of Applied Sciences, Engineering and Technology, 2015. **9**(9): p. 722-726.
23. Maibaum, L.D., Aaron R. and D. Chandler, *Micelle Formation and the Hydrophobic effect*. Journal of Physical Chemistry, 2004(108): p. 6778-6781.
24. Sheng, J.J., *Status of surfactant EOR technology*. Petroleum, 2015. **1**(2): p. 97-105.
25. Solairaj, S., et al., *Measurement and Analysis of Surfactant Retention*. Society of Petroleum Engineers, 2012.
26. Baloch, M., G. Hameed, and A. Bano, *Effect of electrolyte concentration and temperature on CMC of surfactants*. J. Chem. Soc. Pak., 2002. **24**(2): p. 77-86.
27. Karnanda, W., et al., *Effect of temperature, pressure, salinity, and surfactant concentration on IFT for surfactant flooding optimization*. Arabian Journal of Geosciences, 2013. **6**(9): p. 3535-3544.
28. Mohajeri, E. and G.D. Noudeh, *Effect of Temperature on the Critical Micelle Concentration and Micellization Thermodynamic of Nonionic Surfactants: Polyoxyethylene Sorbitan Fatty Acid Esters*. E-Journal of Chemistry, 2012. **9**(4).
29. Khan, A. and S.S. Shah, *Determination of critical micelle concentration (Cmc) of sodium dodecyl sulfate (SDS) and the effect of low concentration of pyrene on its Cmc using ORIGIN software*. J. Chem. Soc. Pak., 2008. **30**(2): p. 186-191.
30. Kumar, S. and A. Mandal, *Studies on interfacial behavior and wettability change phenomena by ionic and nonionic surfactants in presence of alkalis and salt forenhanced oil recovery*. Applied Surface Science, 2016(372): p. 42-51.
31. Umlong, I.M. and K. Ismail, *Micellization of AOT in aqueous sodium chloride, sodium acetate, sodium propionate, and sodium butyrate media: A case of two different concentration regions of counterion binding*. Journal of Colloid and Interface Science, 2005. **291**(2): p. 529-536.
32. Hutin, A., J.-F. Argillier, and D. Langevin, *Mass transfer between Crude Oil and Water. Part 1: Effect of Oil Components*. Energy&fuels, 2014(28): p. 7331-7336.



33. Varadaraj, R. and C. Brons, *Molecular origins of heavy crude oil interfacial activity part 2: Fundamental interfacial properties of model naphthenic acids and naphthenic acids separated from heavy crude oils*. Energy Fuels, 2007. **21**(1): p. 199-204.
34. Varadaraj, R. and C. Brons, *Molecular origins of heavy oil interfacial activity part 1: Fundamental interfacial properties of asphaltenes derived from heavy crude oils and their correlation to chemical composition*. Energy Fuels, 2007. **21**(1): p. 195-198.
35. Al-Sahhaf, T., et al., *The Influence of Temperature, Pressure, Salinity, and Surfactant Concentration on the Interfacial Tension of the N-Octane-Water System*. Chemical Engineering Communications, 2005. **192**(5): p. 667-684.
36. Santos, F.K.G., et al., *Molecular behavior of ionic and nonionic surfactants in saline medium*. Colloids and Surfaces A: Physicochemical and Engineering Aspects, 2009. **333**(1-3): p. 156-162.
37. Xu, W., S.C. Ayirala, and D.N. Rao, *Measurement of Surfactant-Induced Interfacial Interactions at Reservoir Conditions*, in *SPE Annual Technical Conference and Exhibition, 9-12 October, 2005*, Society of Petroleum Engineers: Dallas, Texas.
38. Ruckenstein, E. and I.V. Rao, *Interfacial tension of oil-brine systems in the presence of surfactant and cosurfactant*. Journal of Colloid and Interface Science, 1987. **117**(1): p. 104-119.
39. Aveyard, R., B.P. Binks, and J. Mead, *Interfacial tension minima in oil + water + surfactant systems. Effects of salt, temperature and alkane in systems containing ionic surfactants*. Journal of the Chemical Society, Faraday Transactions 1: Physical Chemistry in Condensed Phases, 1985. **81**(9): p. 2169-2177.
40. Aveyard, R., et al., *Interfacial tension minima in oil-surfactant systems: behaviour of alkane-aqueous NaCl systems containing Aerosol OT*. Journal of the Chemical Society. Faraday Transactions I, 1986. **82**(1): p. 125-142.
41. Griffin, W.C., *Classification of Surface-Active Agents by HLB*. Journal of the Society of Cosmetics Chemists, 1949. **1**(5): p. 311-326.
42. Housaindokht, M.R. and A. Nakhaei Pour, *Study the effect of HLB of surfactant on particle size distribution of hematite nanoparticles prepared via the reverse microemulsion*. Solid State Sciences, 2012. **14**(5): p. 622-625.
43. Mittal, K.L. and P. Kumar, *Handbook of microemulsion science and technology*. 1999, New York: CRC Press.
44. Matsaridou, I., et al., *The Influence of Surfactant HLB and Oil/Surfactant Ratio on the Formation and Properties of Self-emulsifying Pellets and Microemulsion Reconstitution*. AAPS PharmSciTech, 2012. **13**(4): p. 1319-1330.
45. Granet, R., R.D. Khadirian, and S. Piekarski, *Interfacial Tension and Surfactant Distribution in Water-Oil-NaCl Systems Containing Double Tailles Sulfonates*. Journal of Colloids and Surfaces, 1989(49): p. 199-09.
46. Kim, I.B. and G.L. Allee, *Effect of Carbohydrate Sources in Phase I and Phase II Pig Starter Diets*. Asian-Australas J Anim Sci, 2001. **14**(10): p. 1419-1424.

47. Kuhlreshtha, A.K., O.N. Singh, and G.M. Wall, *Pharmaceutical Suspensions: From Formulation Development to Manufacturing*. From Formulation Development to Manufacturing. 2010, New York, NY: Springer New York: New York, NY.
48. Marszall, L., *Bancroft's Rule and emulsion inversion*. Journal of Colloids and Interface Science, 1977. **61**(1): p. 202-203.
49. Alagic, E. and A. Skauge, *A Combined Low Salinity Brine Injection and Surfactant Flooding in Mixed-Wet Sandstone Cores*. Energy&fuels, 2010. **24**: p. 3551-3559.
50. Nagarajan, R., *Molecular Packing Parameter and Surfactant Self-Assembly: The Neglected Role of the Surfactant Tail*. Langmuir, 2002. **18**(1): p. 31-38.
51. Tichelkamp, T., et al., *Interfacial Tension between Low Salinity Solutions of Sulfonate Surfactants and Crude and Model Oils*. Energy&fuels, 2014. **28**: p. 2408-2414.
52. Wang, Z., *Interactions Between an Anionic Fluorosurfactant and a PEO-PPO-PEO Triblock Copolymer in Aqueous Solutions*. Journal of Surfactants and Detergents, 2009. **13**(1): p. 97-102.
53. Hunter, R.J., *Chapter 2 - Charge and Potential Distribution at Interfaces*, in *Zeta Potential in Colloid Science*. 1981, Academic Press. p. 11-58.
54. Shukla, A. and H. Rehage, *Zeta Potentials and Debye Screening Lengths of Aqueous, Viscoelastic Surfactant Solutions (Cetyltrimethylammonium Bromide/Sodium Salicylate System)*. Langmuir, 2008. **24**(16): p. 8507-8513.
55. Brown, M.A., A. Goel, and Z. Abbas, *Effect of Electrolyte Concentration on the Stern Layer Thickness at a Charged Interface*. Angewandte Chemie International Edition, 2016. **55**(11): p. 3790-3794.
56. Rosen, M.J., *Surfactants and Interfacial Phenomena (3)*. 2004, Hoboken, US: Wiley-Interscience.
57. Reed, R. and L.N. Healy, *Some Physicochemical Aspects of Microemulsion Flooding: A review*. In, 1977. **Improved Oil Recovery by Surfactant and Polymer Flooding**(Shah, D.O., Shechteter R. S. ): p. 383-347.
58. Ramirez, W.F., *Application of optimal control theory to enhanced oil recovery*. Developments in petroleum science. Vol. 21. 1987, Amsterdam: Elsevier.
59. Ahsan, T., R. Aveyard, and B.P. Binks, *Winsor transitions and interfacial film compositions in systems containing sodium dodecylbenzene sulphonate and alkanols*. Colloids and Surfaces, 1991. **52**: p. 339-352.
60. AVEYARD, R., B. BINKS, and J. MEAD, *Interfacial tension minima in oil- water- surfactant systems*. Journal of the Chemical Society. Faraday Transactions I, 1987. **83**(8): p. 2347-2357.
61. Spildo, K., et al., *A strategy for low cost, effective surfactant injection*. Journal of Petroleum Science and Engineering, 2014. **117**: p. 8-14.
62. Bera, A., et al., *Screening of microemulsion properties for application in enhanced oil recovery*. Fuel, 2014(121): p. 198-207.

63. Aarra, M.G., H. Høiland, and A. Skauge, *Phase Behavior and Salt Partitioning in Two- and Three-Phase Anionic Surfactant Microemulsion Systems: Part I, Phase Behavior as a Function of Temperature*. Journal of Colloid and Interface Science, 1999. **215**(2): p. 201-215.
64. Puerto, M.C. and W.W. Gale, *Estimation of Optimal Salinity and Solubilization Parameters for Alkyl Orthoxylene Sulfonates Mixtures*. Society of Petroleum Engineers Journal 1977. **17**(3): p. 193-200.
65. Buckley, J.S. and Y. Liu, *Some mechanisms of crude oil/brine/solid interactions*. Journal of Petroleum Science and Engineering, 1998. **20**(3-4): p. 155-160.
66. Farooq, U., et al., *Interfacial Tension Measurements Between Oil Fractions of a Crude Oil and Aqueous Solutions with Different Ionic Composition and pH*. Journal of Dispersion Science and Technology, 2013. **34**(5): p. 701-708.
67. Kunieda, H. and K. Shinoda, *Solution behavior and hydrophile-lipophile balance temperature in the aerosol OT-isooctane-brine system: Correlation between microemulsions and ultralow interfacial tensions*. Journal of Colloid and Interface Science, 1980. **75**(2): p. 601-606.
68. Sherman, P. and C. Parkinson, *Mechanism of temperature induced phase inversion in O/W emulsions stabilised by O/W and W/O emulsifier blends*, in *Emulsions*. 1978, Steinkopff: Heidelberg. p. 10-14.
69. Ye, Z., et al., *The effect of temperature on the interfacial tension between crude oil and gemini surfactant solution*. Colloids and Surfaces A: Physicochemical and Engineering Aspects, 2008. **322**(1-3): p. 138-141.
70. Healy, R.N., R.L. Reed, and D.G. Stenmark, *Multiphase Microemulsion Systems*. Society of Petroleum Engineers Journal, 1976. **16**(03).
71. Miquilena, A., et al., *Influence of Drop Growth Rate and Size on the Interfacial Tension of Triton X-100 Solutions as a Function of Pressure and Temperature*. International Journal of Thermophysics, 2010. **31**(11): p. 2416-2424.
72. Bayrak, Y., *Micelle Formation in Sodium Dodecyl Sulfate and Dodecyltrimethylammonium Bromide at Different Temperatures*. Turkish Journal of Chemistry, 2003. **27**(4): p. 487-492.
73. Hussain, A., P. Luckham, and T. Tadros, *Phase behaviour of pH dependent microemulsions at high temperatures and high salinities*. Rev. Inst. Fr. Pet., 1997. **52**(2): p. 228-231.
74. Strassner, J.E., *Effect of pH on Interfacial Films and Stability of Crude Oil-Water Emulsions*. Society of Petroleum Engineers Journal. **20**(03).
75. Hemmingsen, P.V., et al., *Structural Characterization and Interfacial Behavior of Acidic Compounds Extracted from a North Sea Oil*. Energy & Fuels, 2006. **20**(5): p. 1980-1987.
76. Høiland, S., et al., *The effect of crude oil acid fractions on wettability as studied by interfacial tension and contact angles*. Journal of Petroleum Science and Engineering, 2001. **30**(2): p. 91-103.
77. Farooq, U., J. Sjöblom, and G. Øye, *Desorption of Asphaltenes from Silica-Coated Quartz Crystal Surfaces in Low Saline Aqueous Solutions*. Journal of Dispersion Science and Technology, 2011. **32**(10): p. 1388-1395.

78. Poteau, S., et al., *Influence of pH on Stability and Dynamic Properties of Asphaltenes and Other Amphiphilic Molecules at the Oil–Water Interface*. Energy & Fuels, 2005. **19**(4): p. 1337-1341.
79. Liu, Q., M.Z. Dong, and H.J.R. Yue, *Synergy of alkali and surfactant in emulsification of heavy oil in brine*. Colloids and Surfaces A: Physicochemical and Engineering Aspects, 2006. **273**(1-3): p. 219-228.
80. Santanna, V.C., et al., *Microemulsion flooding for enhanced oil recovery*. Journal of Petroleum Science and Engineering, 2009. **66**(3): p. 117-120.
81. Bera, A., A. Mandal, and B.B. Guha, *Synergistic Effect of Surfactant and Salt Mixture on Interfacial Tension Reduction between Crude Oil and Water in Enhanced Oil Recovery*. Journal of Chemical & Engineering Data, 2014. **59**(1): p. 89-96.
82. Schulman, J.H., W. Stoeckenius, and L.M. Prince, *Mechanism of Formation and Structure of Micro Emulsions by Electron Microscopy*. The Journal of Physical Chemistry, 1959. **63**(10): p. 1677-1680.
83. Winsor, P.A., *Hydrotropy, solubilisation and related emulsification processes*. Transactions of the Faraday Society, 1948. **44**(0): p. 376-398.
84. NAKAMAE, M., A. Masahiko, and K. OGINO, *Effects of Hydrophobic Groups in Surfactants and Alkanes on the Phase Equilibrium Rate of Middle Phase Microemulsion*. Journal of The Japan Petroleum Institute, 1990. **33**(4): p. 247-249.
85. Bera, A. and A. Mandal, *Microemulsions: a novel approach to enhanced oil recovery: a review*. Journal of Petroleum Exploration and Production Technology, 2015. **5**(3): p. 255-268.
86. Stoeckenius, W., J.H. Schulman, and L.M. Prince, *The structure of myelin figures and microemulsions as observed with the electron microscope*. Kolloid-Z, 1960. **169**: p. 170-178.
87. Salager, J., et al., *Mixing Rules for Optimum Phase-Behavior Formulations of Surfactant/Oil/Water Systems*. Old SPE Journal, 1979. **19**(5): p. 271-278.
88. Gurgel, A., et al., *A review on chemical flooding methods applied in enhanced oil recovery*. Brazilian journal of petroleum and gas, 2008. **2**(2).
89. Huh, C., *Interfacial tensions and solubilizing ability of a microemulsion phase that coexists with oil and brine*. Journal of Colloid and Interface Science, 1979. **71**(2): p. 408-426.
90. Salager, J.-L., et al., *How to Attain an Ultralow Interfacial Tension and a Three-Phase Behavior with a Surfactant Formulation for Enhanced Oil Recovery: A Review. Part 2. Performance Improvement Trends from Winsor's Premise to Currently Proposed Inter- and Intra-Molecular Mixtures*. Journal of Surfactants and Detergents, 2013. **16**(5): p. 631-663.
91. Fotland, P. and A. Skauge, *ULTRALOW INTERFACIAL TENSION AS A FUNCTION OF PRESSURE*. Journal of Dispersion Science and Technology, 1986. **7**(5): p. 563-579.
92. Skauge, A. and P. Fotland, *Effect of Pressure and Temperature on the Phase Behavior of Microemulsions*. Society of Petroleum Engineers Journal. **5**(4).
93. Broze, G., *Handbook of Detergents, Part A: Properties*. 1999, CRC Press.

94. Bera, A., et al., *Interfacial tension and phase behavior of surfactant-brine–oil system*. Colloids and Surfaces A: Physicochemical and Engineering Aspects, 2011. **383**(1–3): p. 114-119.
95. Eastoe, J. and J.S. Dalton, *Dynamic surface tension and adsorption mechanisms of surfactants at the air–water interface*. Advances in Colloid and Interface Science, 2000. **85**(2–3): p. 103-144.
96. Melrose, J.C., *Role of Capillary Forces In Detennining Microscopic Displacement Efficiency For Oil Recovery By Waterflooding*. Journal of Canadian Petroluem Technology, 1974. **13**(04).
97. Marle, C.M., *Oil Entrapment and mobilisation*. Basic Concepts in Enhanced Oil Recovery Processes, ed. M. Bavière. 1991, Barking, Essex, England: Elsevier Science Publishers LTD. 3-39.
98. Butt, H.-J., K. Graf, and M. Kappl, *Physics and chemistry of interfaces*. 2nd, rev. and enlarged ed. ed. 2006: Wiley-VCH.
99. Chatzis, I. and N.R. Morrow, *Correlation of Capillary Number Relationships for Sandstone*. Society of Petroleum Engineers Journal. **24**(05).
100. Lake, L.W., *Enhanced oil recovery*. 2010, Richardson, Tex: Society of Petroleum Engineers.
101. Wan, W., et al., *Characterization of Crude Oil Equivalent Alkane Carbon Number (EACN) for Surfactant Flooding Design*. Journal of Dispersion Science and Technology, 2014.
102. Wade, W.H., et al., *Low Interfacial Tensions Involving Mixtures of Surfactants*. Society of Petroleum Engineers Journal, 1977. **17**(02).
103. Ysambertt, F., R. Anton, and J.-L. Salager, *Retrograde transition in the phase behaviour of surfactant-oil-water systems produced by an oil equivalent alkane carbon number scan*. Colloids and Surfaces A: Physicochemical and Engineering Aspects, 1997. **125**(2): p. 131-136.
104. Cayias, J.L., R.S. Schechter, and W.H. Wade, *Modeling Crude Oils for Low Interfacial Tension*. Society of Petroleum Engieneers Journal, 1976: p. 351-357.
105. Butt, H.-J., K. Graf, and M. Kappl, *Physics and chemistry of interfaces*. 2nd, rev. and enlarged ed. ed. Physics textbook. 2006, Weinheim: Wiley-VCH.
106. du Noüy, P.L., *A NEW APPARATUS FOR MEASURING SURFACE TENSION*. The Journal of General Physiology, 1919. **1**(5): p. 521-524.
107. Viades-Trejo, J. and J. Gracia-Fadrique, *Spinning drop method: From Young–Laplace to Vonnegut*. Colloids and Surfaces A: Physicochemical and Engineering Aspects, 2007. **302**(1–3): p. 549-552.
108. Rønsberg, T.T., *An investigation of the correlation between interfacial properties and phase composition in the crude oil/water system*. 2015, MSc thesis, University of Bergen: Faculty of Mathematics and Natural Science - Department of Chemistry.
109. Sørnbø, G., *Polar Components in Crude Oils and their Correlations to Physiochemical Properties*. 2016, MSc Thesis, University of Bergen Faculty for Matemathics and Natural Science - Chemical institute.

110. Maier, G., *Operating Manual DataPhysics OCA, version 2.05.*, in *DataPhysics Instruments GmbH*. 2002, Filderstadt.
111. McMurry, J., *Fundamentals of organic chemistry*. 7th ed. ed. 2011, Belmont, Calif: Brooks/Cole. 672.
112. School, N.S.H. *Chapter 11: Molecular Geometry, Polarity of Molecules, and Advanced Bonding Theory*. Andover's Chem 550/580: Advanced Chemistry Table of Contents [cited 2017 02.05.2017]; Available from: <http://nonsibihighschool.org/advancedch11.php#advancedch11sec4>.
113. Shapley, P. *Absorbing Light with Organic Molecules*. 2012 [cited 2017 14.02]; Available from: <http://butane.chem.uiuc.edu/pshapley/GenChem2/B2/1.html>.
114. Becchi, C.M. and M. D'Elia, *Introduction to Quantum Physics*, in *Introduction to the Basic Concepts of Modern Physics: Special Relativity, Quantum and Statistical Physics*, C.M. Becchi and M. D'Elia, Editors. 2007, Springer Milan: Milano. p. 29-91.
115. Larkin, P., *Chapter 2 - Basic Principles*, in *Infrared and Raman Spectroscopy*. 2011, Elsevier: Oxford. p. 7-25.
116. Rüdiger, W. and F. Thümmel, *The phytochrome chromophore*, in *Photomorphogenesis in Plants*, R.E. Kendrick and G.H.M. Kronenberg, Editors. 1994, Springer Netherlands: Dordrecht. p. 51-69.
117. Geng, J., et al., *Spectroscopic route to monitoring individual surfactant ions and micelles in aqueous solution: A case study*. Central European Journal of Chemistry, 2014. **12**(3): p. 307-311.
118. Workman Jr, J., *9 - Functional Groupings and Band Locations For UV-VIS Spectroscopy in Nanometers (NM)*, in *The Handbook of Organic Compounds*. 2001, Academic Press: Burlington. p. 69-70.
119. Workman Jr, J., *10 - UV-VIS Spectra Correlation Charts*, in *The Handbook of Organic Compounds*. 2001, Academic Press: Burlington. p. 71-74.
120. Kelter, P.B., M.D. Mosher, and A. Scott, *Chrmistry: The Practical Science*. Vol. 10. 2009: Houghton Mifflin Company. 1088.
121. Leccese, F., et al., *Analysis and Measurements of Artificial Optical Radiation (AOR) Emitted by Lighting Sources Found in Offices*. Sustainability, 2014. **6**(9): p. 5941.
122. Ball, D.W., *FG08 : Field Guide to Spectroscopy (1)*. 2006, Bellingham, US: SPIE Press.
123. Naskar, B., A. Dey, and S.P. Moulik, *Counter-ion Effect on Micellization of Ionic Surfactants: A Comprehensive Understanding with Two Representatives, Sodium Dodecyl Sulfate (SDS) and Dodecyltrimethylammonium Bromide (DTAB)*. Journal of Surfactants and Detergents, 2013. **16**(5): p. 785-794.
124. Tu, Z.D., L. , M. Frappart, and M.Y. Jaffrin, *Studies on Treatment of Sodium Dodecyl Benzen Sulfonate Solution by High Shear Ultrafiltration System*. Desalination, 2009. **240**: p. 251-256.
125. Johannessen, A.M. and K. Spildo, *Can Lowering the Injection Brine Salinity Further Increase Oil Recovery by Surfactant Injection under Otherwise Similar Conditions?* Energy & Fuels, 2014. **28**(11): p. 6723-6734.

126. Isaacs, E.E. and K.F. Smolek, *Interfacial tension behavior of athabasca bitumen/aqueous surfactant systems*. The Canadian Journal of Chemical Engineering, 1983. **61**(2): p. 233-240.
127. Bai, J.-M., et al., *Influence of interaction between heavy oil components and petroleum sulfonate on the oil–water interfacial tension*. Journal of Dispersion Science and Technology, 2010. **31**(4): p. 551-556.
128. Price, L.C., *Aqueous solubility of petroleum as applied to its origin and primary migration*. AAPG Bulletin, 1976. **60**(2): p. 213-244.
129. Varadaraj, R. and C. Brons, *Molecular Origins of Heavy Oil Interfacial Activity Part 1: Fundamental Interfacial Properties of Asphaltenes Derived from Heavy Crude Oils and Their Correlation To Chemical Composition*. Energy & Fuels, 2007. **21**(1): p. 195-198.
130. Acevedo, S., et al., *Isolation and Characterization of Low and High Molecular Weight Acidic Compounds from Cerro Negro Extraheavy Crude Oil. Role of These Acids in the Interfacial Properties of the Crude Oil Emulsions*. Energy & Fuels, 1999. **13**(2): p. 333-335.
131. Kolltveit, Y., *Relationship Between Crude Oil Composition and Physical-Chemical Properties.*, in *Department of Chemistry - Faculty of Mathematics and Natural Science*. 2016, University of Bergen. p. 88.
132. Alagic, E. and A. Skauge, *Combined Low Salinity Brine Injection and Surfactant Flooding in Mixed–Wet Sandstone Cores*. Energy & Fuels, 2010. **24**(6): p. 3551-3559.
133. Hosseinzade Khanamiri, H., et al., *EOR by Low Salinity Water and Surfactant at Low Concentration: Impact of Injection and in Situ Brine Composition*. Energy & Fuels, 2016. **30**(4): p. 2705-2713.
134. Trabelsi, S., et al., *Effect of Added Surfactants on the Dynamic Interfacial Tension Behaviour of Alkaline/Diluted Heavy Crude Oil System*. Oil Gas Sci. Technol. – Rev. IFP Energies nouvelles, 2012. **67**(6): p. 963-968.
135. Touhami, Y., et al., *Effects of Added Surfactant on the Dynamic Interfacial Tension Behavior of Acidic Oil/Alkaline Systems*. Journal of Colloid and Interface Science, 2001. **239**(1): p. 226-229.
136. Chu, Y.-P., et al., *Studies of synergism for lowering dynamic interfacial tension in sodium  $\alpha$ -(n-alkyl) naphthalene sulfonate/alkali/acidic oil systems*. Journal of Colloid and Interface Science, 2004. **276**(1): p. 182-187.
137. Smit, B., et al., *Effects of chain length of surfactants on the interfacial tension: molecular dynamics simulations and experiments*. The Journal of Physical Chemistry, 1990. **94**(18): p. 6933-6935.
138. Kellay, H., et al., *Local properties of an AOT monolayer at the oil-water interface : neutron scattering experiments*. Journal de Physique II, 1993. **3**(12): p. 1747-1757.
139. Bastidas, Y., et al., *Phase Behavior and Emulsion Stability of the Aot/Decane/ Water/NaCl System at Very Low Volume Fractions of Oil*. RCEIF, 2014. **03**.
140. Fukumoto, A., et al., *Investigation on Physical Properties and Morphologies of Microemulsions formed with Sodium Dodecyl Benzenesulfonate, Isobutanol, Brine, and Decane, Using Several Experimental Techniques*. Energy & Fuels, 2016. **30**(6): p. 4690-4698.

141. Tien, T.H., et al., *Correlation of Optimal Salinity as Function of Water/Oil Ratio in Brine/Surfactant/Alcohol/Oil System*, in *Groundwater Updates*, K. Sato and Y. Iwasa, Editors. 2000, Springer Japan: Tokyo. p. 105-110.
142. Rout, D.K., et al., *Predicative Modeling of Microemulsion Phase Behaviour and Microstructure Characterisation in the 1-Phase Region*. *Microemulsions - An Introduction to Properties and Applications*, ed. D.R. Najjar. 2012, InTech.
143. Pearson, J.R.A., *Interfacial Phenomena - Equilibrium and Dynamic Effects (2nd Edition) By Clarence A Miller and P Neogi*. *AIChE Journal*, 2008. **54**(11): p. 3032-3032.
144. Teigen, E., *Partitioning of surfactants between the water and oil phases and relations to enhanced oil recovery methods*, in *Department of Chemical Engineering*. 2014, MSc Thesis, Norwegian University of Science and Technology. p. 95.
145. Standal, S.H., *Wettability of solid surfaces induced by adsorption of polar organic components in crude oil*. 1999, Department of Chemistry, University of Bergen: Bergen.
146. Weissenborn, P.K. and R.J. Pugh, *Surface tension of aqueous solutions of electrolytes : Relationship with ion hydration, oxygen solubility, and bubble coalescence*. *Journal Of Colloid And Interface Science*, 1996. **184**: p. 550-563.
147. Hey, M.J., et al., *Surface tensions of aqueous solutions of some 1:1 electrolytes*. *Journal of the Chemical Society, Faraday Transactions 1: Physical Chemistry in Condensed Phases*, 1981. **77**(1): p. 123-128.
148. Slavchov, R.I., et al., *Surface tension and surface  $\Delta\chi$ -potential of concentrated  $Z^+ : Z^-$  electrolyte solutions*. *Journal of Colloid and Interface Science*, 2013. **403**: p. 113-126.
149. Bhuyan, D., L.W. Lake, and G.A. Pope, *Mathematical Modeling of High-pH Chemical Flooding*. *Society of Petroleum Engineers Journal*, 1990. **5**(02): p. 213-220.
150. Powney, J. and C.C. Addison, *The properties of detergent solutions*. *Transactions of the Faraday Society*, 1937. **33**(0): p. 1243-1260.
151. Lin, S.-Y., et al., *A Study of the Equilibrium Surface Tension and the Critical Micelle Concentration of Mixed Surfactant Solutions*. *Langmuir*, 1999. **15**(13): p. 4370-4376.



## A. Appendix A – Calculations

### A.1 Uncertainties

For calculating uncertainties during the thesis, the following equation is used:

$$S = \sqrt{\frac{\sum_{i=1}^n (x_i - \bar{x})^2}{n}} \quad (\text{Equation A.1})$$

S is the standard deviation,  $x_i$  the result of a given parallel,  $\bar{x}$  average value of all parallels, and n the number of parallels.

### A.2 Ionic strength

Throughout the thesis ionic strength, I, is calculated using the following equation:

$$I = \frac{1}{2} \sum_{i=1}^n c_i z_i^2 \quad (\text{Equation A.2})$$

c is the electrolyte concentration and z the valance of the ions.

## B. Appendix B – Additional results

### B.1 Identification of CMC

As 0.02M NaCl brine are used as a base-solution in all measurements, CMC for each of the three surfactants was identified in a 0.02M NaCl brine. CMC for SDS, SDBS and AOT was found by measuring ST with variations in surfactant concentration. Measurements are done at room temperature ( $\approx 23\pm 2^\circ\text{C}$ ). Trendlines to identify CMC are created with the use of Microsoft Excel.

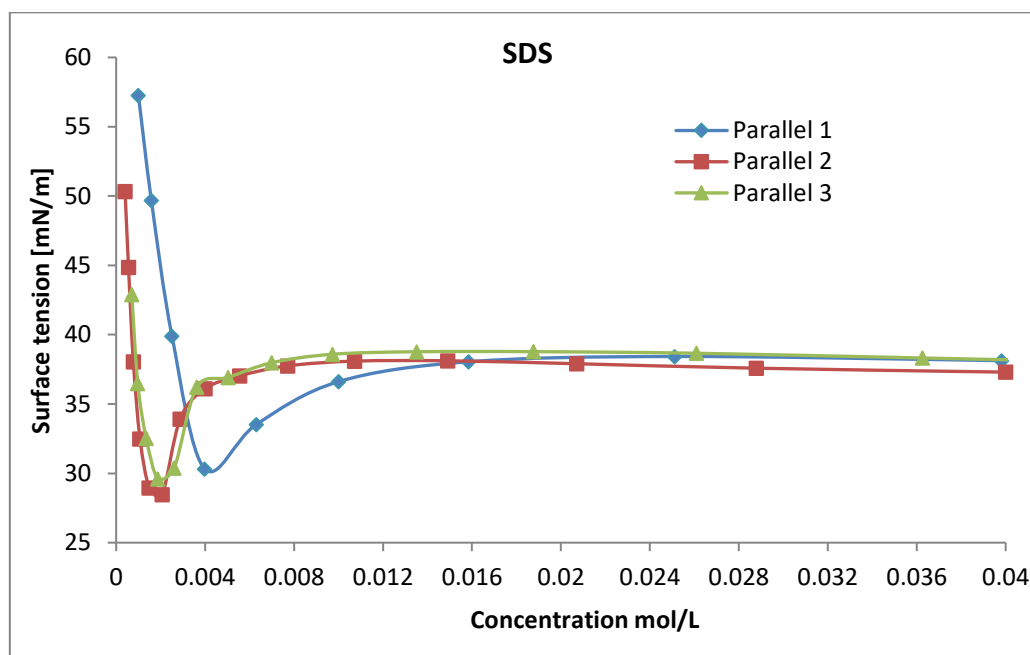


**Figure B-1** Identification of CMC for SDS by plotting surface tension against surfactant concentration.

#### SDS

Two parallel solutions were made and measured, parallel 1 and parallel 2 respectively. The two parallels showed two different CMC's. Based on the two parallels giving two different values for CMC, a third solution was made. This third parallel's surface minimum agreed with the second parallel, but was, however, in disagreement with the first parallel. Based on the similarity of the third and second parallel, CMC was determined from the second and third parallel, and the result from the first parallel neglected. The CMC are taken at the lowest ST measured, as done by Powney & Addison [150].

The cause for the unregularly V-shape, contrary to the L-shape explained in section 2.3.2, is the presence of lauryl alcohol created when SDS is dispersed in water. Lauryl alcohol is a highly surface active compound. The surface active lauryl alcohol decrease the ST below what is possible for pure SDS. As concentration is increased and micelles begin to form, the lauryl alcohol is solubilised in the

micelles. As this happens, the concentration of the alcohol at the surface lowers, and the ST increase back to that of a pure SDS solution [151].

The measured value of  $2.0 \times 10^{-3} \text{M}$  does agree with Naskar et.al. [123] who found the CMC for SDS in  $0.025 \text{M}$  brine to be  $3.4 \times 10^{-3} \text{M}$ , the difference between them are not significant. The first parallel measured from figure B-1 are more in agreement with the value found by Naskar et.al. [123], with a CMC at approximately  $4.0 \times 10^{-4} \text{M}$ .

The literature value [123] is found by use of conductivity, whilst the results obtained are found by measuring ST. This should in theory not affect the CMC value, but might be the basis of why the measured value deviate some from the one found by Naskar et,al [123].

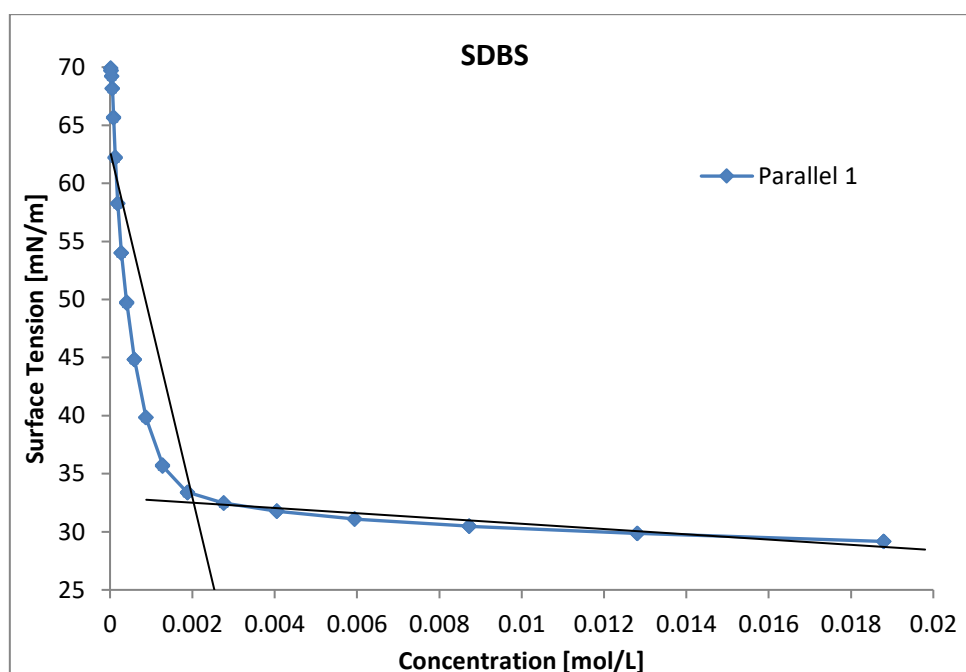


**Figure B-2** Identification of CMC for SDBS by plotting surface tension against surfactant concentration. Linear trendlines are used to determine CMC.

### SDBS

The SDBS curve behaved as expected, and a reasonable CMC was found by the use of trendlines. The first parallel showed a curve as expected, with a reasonable value for CMC. A CMC for SDBS at  $2.0 \times 10^{-3} \text{M}$  are in agreement to  $1.9 \times 10^{-3} \text{M}$  found by Tu et.al [124]. Due to the agreement between measured value and literature value, no further parallels were measured.

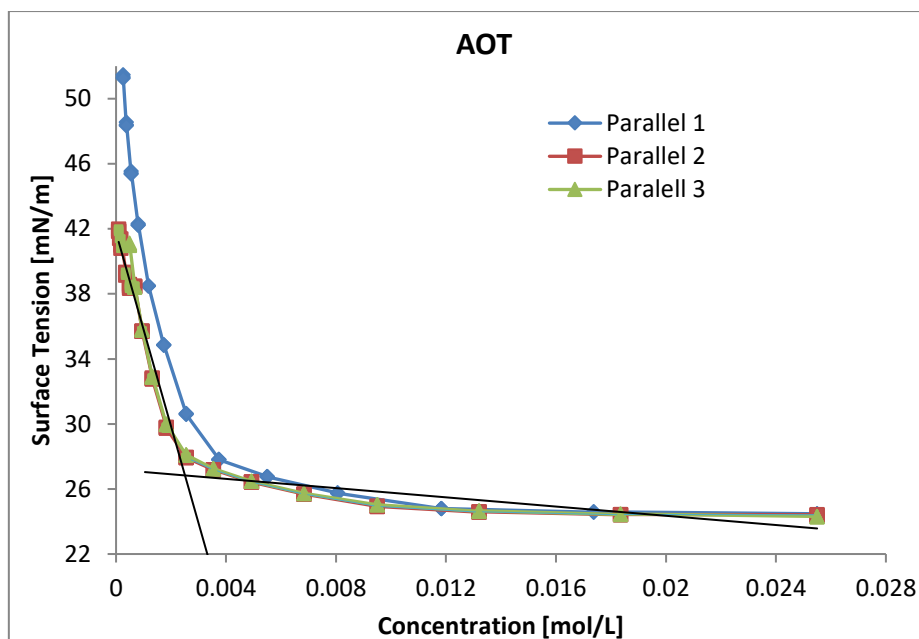


**Figure B-3** Identification of CMC for AOT by plotting surface tension against surfactant concentration. Linear trendlines are used to determine CMC.

### *AOT*

To eliminate possible sources of error in both preparing solution and measuring CMC, two parallel AOT solutions were prepared and measured at same start-concentration. The two parallels (1 and 2 respectively) showed different CMC`s. Due to the difference in CMC, a third solution at the same concentration was prepared and measured. The second and third run gave the same values in terms of CMC. The result in the first parallel were therefore chosen to be neglected.

Umlong & Ismail [31] found the CMC for AOT to be 1.1E-03M by measuring ST. This is not in complete agreement with the measured value of 2.6E-03M, without significant difference. As there is an off-set in the parallels measured on AOT, some of the set-up prior to the measurements could have been the origin of the deviation between the literature value [31] and the measured value.

## B.2 Standard absorption curves for SDBS

Figure B-4 shows the standard curves created for SDBS for correlating absorbance to surfactant concentration.

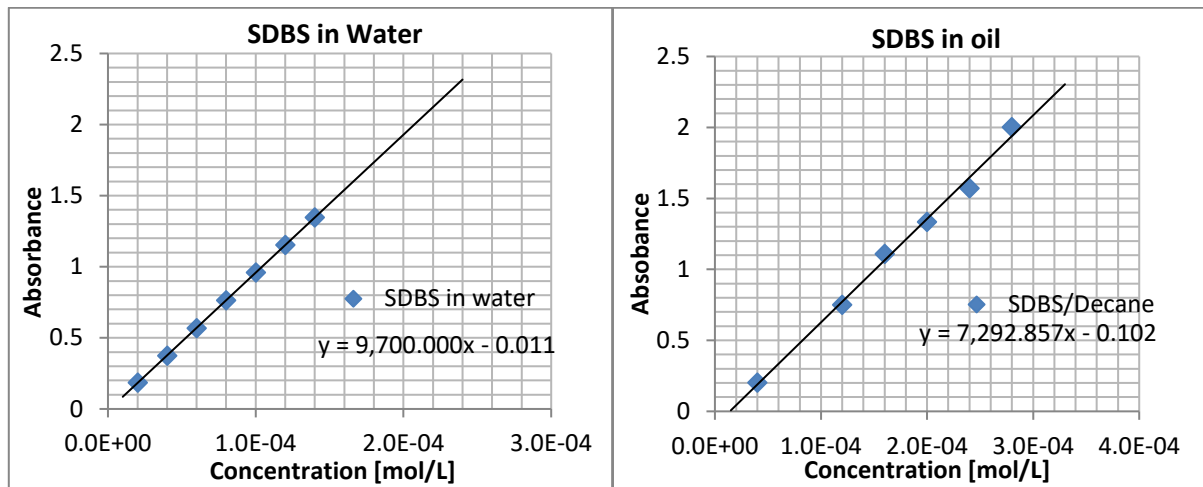


Figure B-4 Standard curves correlating surfactant concentration and absorbance for SDBS in water and oil.

## C. Appendix C – Tables of data

### C.1 Additive- free variation in salinity

**Table C-1.** Measured IFT's between the two crudes and brines at different salinities.

<i>Crude C</i>		<i>Crude A</i>	
Brine NaCl Concentration [M]	IFT [mN/m]	Brine NaCl Concentration [M]	IFT [mN/m]
0.00	26.88	0.00	36.89
0.01	26.99	0.01	36.78
0.10	21.75	0.10	28.83
0.25	21.64	0.25	26.25
0.50	16.83	0.50	22.83
1.00	17.46	1.00	19.33
1.50	14.22	1.50	15.48
2.00	11.58	2.00	14.12
2.50	8.90	2.50	10.81
3.00	7.43	3.00	7.75
4.00	5.12	4.00	5.28
5.00	4.65	5.00	4.53

**Table C-2** IFT's between additive-free brine at LS and LS-Ca and heptane and decane. Measurements of IFT between LS-Ca brine and decane were not done.

	IFT [mN/m]	
	LS (0.02M NaCl)	LS-Ca (I = 0.02)
<b>Heptane</b>	51±1	56.9±0.7
<b>Decane</b>	52.9±0.5	-

## C.2 Variation in surfactant concentration

**Table C-3** Measured IFT's with variations in surfactant concentration for a) Crude C systems b) Crude A systems and c) Heptane systems.

a)	SDS/Crude C [mN/m]	SDBS/Crude C [mN/m]	AOT/Crude C [mN/m]
[1/10*CMC]	15.0±0.9	5.7±0.4	10.24±0.08
[CMC]	3.3±0.1	0.95±0.01	0.43±0.03
[10*CMC]	2.67±0.04	0.87±0.01	0.418±0.005

b)	SDS/Crude A [mN/m]	SDBS/Crude A [mN/m]	AOT/Crude A [mN/m]
[1/10*CMC]	18.9±1.5	11.8±0.3	12.9±0.5
[CMC]	6.20±0.07	1.70±0.09	0.49±0.01
[10*CMC]	4.55±0.03	1.08±0.03	0.47±0.02

c)	SDS/Heptane [mN/m]	SDBS/Heptane [mN/m]	AOT/Heptane [mN/m]
[1/10*CMC]	23.8±0.5	8.3±0.5	12.0±0.2
[CMC]	10.8±0.2	5.6±0.3	0.40±0.02
[10*CMC]	10.7±0.2	5.3±0.2	0.24±0.01

### C.3 Variation in salinity

**Table C-4** Variations in IFT with change in salinity for all AOT systems.

AOT/Heptane	
NaCl Concentration [M]	IFT [mN/m]
0.02	0.25
0.03	0.15
0.04	0.09
0.045	0.06
0.047	0.03
0.049	0.04
0.05	0.02
0.051	0.03
0.053	0.05
0.055	0.04
0.06	0.06
0.07	0.07
0.08	0.08
0.09	0.19
0.1	0.18

AOT/Decane	
NaCl concentration [M]	IFT [mN/m]
0.010	0.45
0.020	0.43
0.030	0.29
0.040	0.19
0.050	0.12
0.060	0.08
0.070	0.03
0.075	0.02
0.080	0.04
0.090	0.05
0.100	0.07
0.120	0.07
0.140	0.11

AOT/Crude A	
NaCl concentration [M]	IFT [mN/m]
0.020	0.35
0.030	0.33
0.040	0.21
0.050	0.16
0.060	0.14
0.065	0.12
0.070	0.10
0.075	0.07
0.080	0.06
0.085	0.08
0.090	0.05
0.095	0.12
0.100	0.12
0.110	0.21
0.120	0.32
0.130	0.37
0.140	0.41

AOT/Crude C	
NaCl concentration [M]	IFT [mN/m]
0.020	0.58
0.030	0.36
0.040	0.29
0.050	0.19
0.060	0.12
0.070	0.10
0.080	0.09
0.085	0.09
0.090	0.07
0.095	0.13
0.100	0.15
0.105	0.18
0.110	0.25
0.120	0.32
0.130	0.38
0.140	0.41
0.150	0.46



**Table C-5** Variation in IFT with change in salinity for all SDBS systems.

<b>SDBS/Heptane</b>	
<b>NaCl Concentration [M]</b>	<b>IFT [mN/m]</b>
0.01	5.11
0.02	4.58
0.10	3.82
0.30	1.57
0.50	1.21
0.60	1.02
0.70	0.86
0.80	0.67
0.90	0.53
1.00	0.63
1.10	0.74
1.20	1.05
1.30	1.11
1.40	1.19
1.70	1.33
2.00	1.36

<b>SDBS/Decane</b>	
<b>NaCl concentration [M]</b>	<b>IFT [mN/m]</b>
0.02	3.19
0.1	0.86
0.2	0.62
0.25	0.57
0.3	0.52
0.35	0.57
0.4	0.64
0.5	0.69
0.7	0.84
0.9	0.92
1.1	0.78
1.3	0.65

<b>SDBS/Crude A</b>	
<b>NaCl concentration [M]</b>	<b>IFT [mN/m]</b>
0.02	1.14
0.10	0.62
0.20	0.35
0.30	0.29
0.40	0.26
0.50	0.19
0.60	0.13
0.65	0.10
0.70	0.10
0.75	0.09
0.80	0.11
0.90	0.15
1.00	0.26
1.10	0.33
1.20	0.38
1.30	0.46

<b>SDBS/Crude C</b>	
<b>NaCl concentration [M]</b>	<b>IFT [mN/m]</b>
0.1	0.92
0.2	0.62
0.3	0.46
0.4	0.36
0.5	0.27
0.6	0.18
0.7	0.14
0.8	0.01
0.9	0.21
1.0	0.38
1.1	0.55
1.2	0.54
1.3	0.57
1.4	0.63

**Table C-6** Variation in IFT with change in salinity for all SDS systems.

SDS/Heptane	
NaCl concentration [M]	IFT [mN/m]
0.20	7.3
0.40	6.5
0.60	6.3
0.80	5.4
1.00	4.3
1.20	3.5
1.40	2.9
1.60	2.4
1.80	1.7
2.00	1.2

SDS/Crude A	
NaCl concentration [M]	IFT [mN/m]
0.02	4.55
0.2	1.32
0.8	0.55
1.0	0.50
1.1	0.42
1.2	0.46
1.3	0.52
1.4	0.47
1.6	0.58
1.8	0.62
1.9	0.68
2.1	0.82

SDS/Crude C	
NaCl concentration [M]	IFT [mN/m]
0.2	1.35
0.4	0.97
0.6	0.78
0.8	0.67
1.0	0.59
1.1	0.52
1.2	0.42
1.3	0.44
1.4	0.38
1.5	0.43
1.6	0.45
1.8	0.52
2.1	0.64

## C.4 Variation in pH

### AOT

Table C-7. a) lower- b) optimal- and c) upper salinity pH measurements for AOT.

a)		IFT [mN/m]		
LS NaCl [M]	Compound	pH 3	pH 6	pH 9
0.02	<b>C7</b>	0.201	0.206	0.195
0.02	<b>C10</b>	0.373	0.416	0.387
0.02	<b>Crude A</b>	0.406	0.449	0.437
0.02	<b>Crude C</b>	0.368	0.397	0.404

b)		IFT [mN/m]		
OS NaCl [M]	Compound	pH 3	pH 6	pH 9
0.050	<b>C7</b>	0.027	0.027	0.027
0.075	<b>C10</b>	0.026	0.026	0.027
0.090	<b>Crude A</b>	0.181	0.055	0.045
0.090	<b>Crude C</b>	0.219	0.081	0.031

c)		IFT [mN/m]		
HS NaCl [M]	Compound	pH 3	pH 6	pH 9
0.14	<b>C7</b>	0.325	0.327	0.326
0.14	<b>C10</b>	0.093	0.101	0.119
0.14	<b>Crude A</b>	0.492	0.385	0.321
0.14	<b>Crude C</b>	0.443	0.363	0.061

**SDBS****Table C-8** a) lower- b) optimal- and c) upper salinity pH measurements for SDBS.

<b>a)</b>		<b>IFT [mN/m]</b>		
<b>LS NaCl [M]</b>	<b>Compound</b>	<b>pH 3</b>	<b>pH 6</b>	<b>pH 9</b>
0.02	<b>C7</b>	4.47	5.11	5.29
0.02	<b>C10</b>	4.15	4.23	4.43
0.02	<b>Crude A</b>	0.70	1.26	1.07
0.02	<b>Crude C</b>	0.47	0.81	0.65

<b>b)</b>		<b>IFT [mN/m]</b>		
<b>OS NaCl [M]</b>	<b>Compound</b>	<b>pH 3</b>	<b>pH 6</b>	<b>pH 9</b>
0.90	<b>C7</b>	0.42	0.41	0.43
0.30	<b>C10</b>	0.49	0.51	0.50
0.75	<b>Crude A</b>	0.95	0.26	0.06
0.80	<b>Crude C</b>	3.27	0.12	0.07

<b>c)</b>		<b>IFT [mN/m]</b>		
<b>HS NaCl [M]</b>	<b>Compound</b>	<b>pH 3</b>	<b>pH 6</b>	<b>pH 9</b>
1.30	<b>C7</b>	0.76	0.77	0.80
1.30	<b>C10</b>	0.59	0.61	0.62
1.30	<b>Crude A</b>	4.03	0.62	0.12
1.30	<b>Crude C</b>	3.05	0.47	0.23

## C.5 Variation in temperature

**Table C-9** Measured IFT's with variation in temperature. Measurements done at a) 28°C b) 40°C (only AOT was measured at this temperature) and c) 50°C.

28° [mN/m]				
a)	Heptane	Decane	Crude A	Crude C
SDS	7.0±0.2	11.2±0.3	4.8±0.1	2.94±0.09
SDBS	4.5±0.2	4.2±0.2	1.1±0.5	0.92±0.01
AOT	0.16±0.02	0.40±0.01	0.471±0.004	0.43±0.01

40° [mN/m]				
b)	Heptane	Decane	Crude A	Crude C
AOT	0.37±0.02	0.64±0.01	0.64±0.01	0.53±0.01

50° [mN/m]				
c)	Heptane	Decane	Crude A	Crude C
SDS	8.6±0.2	12.6±0.3	6.88±0.05	4.5±0.3
SDBS	5.3±0.2	5.1±0.3	1.51±0.04	1.17±0.01
AOT	0.46±0.03	0.69±0.02	0.70±0.02	0.71±0.01

## C.6 Absorption of UV-light

**Table C-10** Absorbance and corresponding calculated surfactant concentration in each phase at different salinities.

NaCl concentration [M]	Water phase		Oil phase	
	Measured absorbance	Calculated surfactant concentration in phase [M]	Measured absorbance	Calculated surfactant concentration in phase [M]
0.40	0.194	2.1E-02	1.137	1.70E-04
0.45	0.194	2.1E-02	1.496	2.19E-04
0.50	0.204	2.2E-02	1.432	2.10E-04
0.60	0.060	7.4E-03	2.003	2.89E-04
0.65	0.060	7.4E-04	2.292	3.28E-04
0.70	0.034	4.7E-04	2.466	3.52E-04
0.80	0.030	4.3E-04	1.398	4.11E-04
0.90	0.326	3.5E-04	1.300	3.85E-04
1.00	0.271	2.9E-04	1.306	3.86E-04
1.20	0.270	2.9E-04	1.337	3.95E-04
1.30	0.423	4.5E-04	1.358	4.00E-04